



<https://theses.gla.ac.uk/>

Theses Digitisation:

<https://www.gla.ac.uk/myglasgow/research/enlighten/theses/digitisation/>

This is a digitised version of the original print thesis.

Copyright and moral rights for this work are retained by the author

A copy can be downloaded for personal non-commercial research or study, without prior permission or charge

This work cannot be reproduced or quoted extensively from without first obtaining permission in writing from the author

The content must not be changed in any way or sold commercially in any format or medium without the formal permission of the author

When referring to this work, full bibliographic details including the author, title, awarding institution and date of the thesis must be given

Enlighten: Theses

<https://theses.gla.ac.uk/>
research-enlighten@glasgow.ac.uk

Interactions of Cells with Nanotopography

John Ogilvie Gallagher BSc (Hons)

Centre for Cell Engineering

Division of Infection and Immunity

Institute of Biomedical and Life Sciences

University of Glasgow

A Thesis Submitted to the Faculty of Biological and Life Sciences

of the

University of Glasgow for the Degree of Doctor of Philosophy.

January 2003

©John Gallagher

ProQuest Number: 10390802

All rights reserved

INFORMATION TO ALL USERS

The quality of this reproduction is dependent upon the quality of the copy submitted.

In the unlikely event that the author did not send a complete manuscript and there are missing pages, these will be noted. Also, if material had to be removed, a note will indicate the deletion.



ProQuest 10390802

Published by ProQuest LLC (2017). Copyright of the Dissertation is held by the Author.

All rights reserved.

This work is protected against unauthorized copying under Title 17, United States Code
Microform Edition © ProQuest LLC.

ProQuest LLC.
789 East Eisenhower Parkway
P.O. Box 1346
Ann Arbor, MI 48106 – 1346

GLASGOW
UNIVERSITY
LIBRARY

13071

copy-1

From Langside to La Jolla.....

This thesis is dedicated to the memory of Michael and Kevin McNulty.

Acknowledgements

I would firstly like to genuinely thank my supervisor Professor Adam Curtis for his

support, encouragement and his good humour over the past 3 years. I would also like to thank him for sending me to some spectacular conferences in some far out places

(Milport aside). I would also like to extend these thanks to his wife whom was the hostess with the mostess at many a party at Kirklee circus.

I would like to offer a very special thank you to Dr Mathis Riehle who was instrumental in helping guide a lot of the work contained in this thesis, also for making me buy a bike (only fell off twice in 3 years), and for waking me up for work on several occasions. It should also not go unmentioned the very rare occasions we socialised together with Christianne his very quite and reserved wife.

Thanks should also go to Professor Chris Wilkinson for helpful discussions and quite a few smokes that we managed to squeeze in along the way. Also a big Thank you to the accident prone Keiran McGhee who fabricated many nanostructures for me and also for a few working lunches we had in the GUU. There are few people in my life that are quite like the genius Dr Bob Hartely (OBE)

whom I had the pleasure of spending a few years doing time with, in the CCE. With Bob being such a quiet chap it was a bit of drag sharing a office with him, but nonetheless I couldn't get enough of your silence because at the end of the day we all know "you're a great guy!"

There are of course other members of the lab old and new that I would like to thank for putting up with my bad breath and right wing opinions. I would like to thank Mairead for showing me how to behave in social situations, Elena for the had chat and the occasional trip to the Far East. A special note of thanks should go to Toby for the odd wise word of wisdom and having to endure several league titles, a treble and a six-two humiliation.

Lucia (for tales of Leningrad), George (sorry about the biscuits) and Ajay for being my answering machine. I would also like to thank Angus and Kenny for letting me get a word in edgeways. And thank the rest; Thomas Brolin, Van der Hogg, Jeanty, Dinger, Tony, Colin Wee Martin and the tax payer, for keeping up the façade.

I would like to thank my Father for some very sound career advice and the rest of my family for little or no encouragement, and for even less in the way of financial support (Thanks a bunch), Daniel is however excused from this on grounds of him only being three years old. Kate's family Judy, Ann, Jane, Greg and little lady Caitlin for many a good time and encouragement.

Last but not least I would like to thank my 'significant other' Kate, for putting up with the occasional tantrum, helping me through my fear of dentistry, a few nursed hangovers, six happy years together and hopefully there will be another sixty of the same to come.

Table of Contents

TITLE PAGE.....	I
DEDICATION.....	II
ACKNOLWEDGEMENTS.....	III
TABLE OF CONTENTS.....	V
FIGURES AND TABLES.....	XI
ABBREVEATIONS.....	XVII
ABSTRACT.....	XVIII
CHAPTER1.....	1
INTRODUCTION.....	1
CONSTRUCTS FOR TISSUE ENGINEERING.....	5
SPATIAL CONTROL OF CELLS.....	8
NANOSCALE TOPOGRAPHY.....	13
ORDEREDNANOTOPOGRAPHY.....	20
SURFACE ROUGHNESS.....	24
CELL ADHESION.....	25
MOLECULAR COMPLEXITY OF FOCALADHESIONS.....	26
CELL ADHESION AND THE ROLE OF FORCE.....	27
TENSION GENERATED BY THE CYTOSKELETON.....	37

POSSIBLE MECHANISMS OF FORCE TRANSMISSION BETWEEN THE ECM AND INTRACELLULAR STRUCTURES.	28
CHLORIDE CHANNELS AND THEIR ROLE IN MECHANICAL TENSION RECEPTION.....	28
CELL CRAWLING.....	29
AIMS OF PROJECT.....	32
CHAPTER2.....	33
MATERIALS AND METHODS.....	33
CELL LINES.....	33
ISOLATION AND PRIMARY CULTURE OF EPITENON CELLS.....	33
CELL CULTURE SOLUTIONS AND FINAL MEDIA	34
MEDIA RECIPES	37
MDCK CELL MEDIA (MEM).....	41
METHODS OF ROUTINE CULTURE	38
HGTFNCELLCULTURE.....	38
MDCK CELL CULTURE	38
p388D1.....	39
CRYOPRESERVATION OF STOCK CELLS.	39
CELL COUNTING.....	40
CELL COUNTING.....	40
CELL SEEDING ON STRUCTURES.....	40
CELL STAINING.....	41
VIDEO CAPTURE AND ANALYSIS.....	41

FLUORESCENT STAINING REAGENTS AND PROTOCOL.....	42
IMMUNOFLUORESCENCE AND CYTOSKELETAL OBSERVATION...	44
IMAGE ACQUISITION.....	44
POLYMER CASTING OF MASTER SURFACES.	45
MICROSCOPY	45
ATOMIC FORCE MICROSCOPY.....	45
FABRICATION OF QUARTZ MASTER SURFACE.....	49
POLY-L-LYSINE COATING OF POLYMER SURFACES	52
SEM FREEZE-DRYING.....	52
CHAPTER 3.....	53
FABRICATION AND INITIAL INVESTIGATION OF THE CELLULAR REACTION TO DEFINED NANOTOPOGRAPHY	53
INTRODUCTION.....	53
RESULTS	57
FABRICATING NANOTOPOGRAPHICAL STRUCTURES IN POLYCAPROLACTONE.....	57
DETAILED METHOD FOR PRODUCING SUPER COOLED PCL EMBOSSED NANOSTRUCTURES.....	58
EPITENON CELL ADHESION TO NANOTOPOGRAPHY AT VARIOUS TIMES	63
BHK 21, B10D2, AND HGTFN ADHESION TO NANOPITTED TOPOGRAPHY AFTER 4, 20, AND 96 HOURS.....	68
CELL ADHESION TO POLYSTYRENE, POLYURETHANE AND POLYCARBONATE FABRICATED STRUCTURES.....	79

CELL ADHESION TO NANOTOPOGRAPHY IN SERUM -FREE CULTURE CONDITIONS.....	84
DISCUSSION.....	87
FABRICATING NANOTOPOGRAPHICAL STRUCTURES IN POLYCAPROLACTONE.....	87
EPITENON CELL ADHESION TO NANOTOPOGRAPHY AFTER VARYING TIME POINTS.....	88
BHK 21, B10D2, AND HGTFN ADHESION TO NANOPITTED TOPOGRAPHY AFTER 4, 20, AND 96 HOURS	88
CELL ADHESION TO POLYSTYRENE, POLYURETHANE AND POLYCARBONATE FABRICATED STRUCTURES	89
CELL ADHESION TO NANOTOPOGRAPHY IN SERUM-FREE CULTURE CONDITIONS	91
CHAPTER 4.....	91
SPATIAL CONTROL OVER CELLS	91
INTRODUCTION.....	91
RESULTS	94
DISCUSSION.....	100
CHAPTER 5.....	102
CELL MIGRATION	102
INTRODUCTION.....	102
RESULTS.....	105
TIME LAPSE VIDEO MICROSCOPY.....	105
SINGLE CELL ATTACHMENT	105

CELL CLUSTERING.....	106
THE PLANAR/ PIT BOUNDARY.....	106
CELL MOTILITY SPEEDS.....	106
SCANNING ELECTRON MICROSCOPY INVESTIGATION OF CELLULAR REACTION TO	
NANOTOPOGRAPHY	112
FILOPODIA POSITIONING OF EPITHELIAL CELLS ON NANOTEXTURED PCL.....	115
AFM INVESTIGATION OF CELL INTERACTION.....	117
CELL MIGRATION RATES OF CELLS ON PLANAR AND NANOTOPOGRAPHY....	119
DISCUSSION.....	121
TIME LAPSE VIDEO MICROSCOPY	121
SEM INVESTIGATION.....	122
ATOMIC FORCE MICROSCOPY INVESTIGATION OF CELL INTERACTION.	123
CHAPTER 6.....	124
THE CYTOSKELETON AND ITS RESPONSE TO NANOTOPOGRAPHY	124
INTRODUCTION.....	124
RESULTS	128
F-ACTIN	128
VINCULIN CONTAINING FOCAL CONTACTS.....	131
FOCAL ADHESION SIZES ON NANO AND PLANAR TOPOGRAPHY.....	133
AMOUNT OF FOCAL ADHESIONS PER CELL.....	136
B-TUBULIN DISTRIBUTION.....	137

DISCUSSION.....	140
F-ACTIN CYTOSKELETON.....	140
VINCULIN CONTAINING FOCAL ADHESIONS.....	141
B-TUBULIN DISTRIBUTION	141
CHAPTER 7.....	143
TOPOGRAPHY OR CHEMISTRY?	143
INTRODUCTION.....	143
RESULTS	146
DISCUSSION.....	155
CHAPTER 8.....	184
GENERAL DISCUSSION	157
REDUCTION OF CELL ADHESION AS A RESULT OF ORDERED NANOTOPOGRAPHY.....	159
CELLULAR RESPONSE TO NANOTOPOGRAPHY.....	160
THE ROLE OF THE CYTOSKELETON	164
FOCAL ADHESION SPACING	165
CELL MIGRATION	167
CHEMISTRY VERSUS TOPOGRAPHY.....	167
SPATIAL CONTROL	168
FUTURE WORK.....	169
DIFFERENT NANOMETRIC SURFACE TOPOGRAPHIES	169
IDEAS FOR FUTURE STRUCTURE FABRICATION.....	170

PROTEIN ADSORPTION.....	171
CONTACT ANGLE MEASUREMENTS.....	171
SURFACE TREATMENTS	171
REFERENCES.....	171

Figures and Tables

Chapter 1: Introduction

Figure 1.1 60° tilt SEM of a typical region of silicon grass.

Figure 1.2 Scanning confocal micrograph of LRM55 cells adhering preferentially to the wet-etch modified regions of the silicon substrate.

Figure 1.3 An SEM of rat hippocampal neurons cultured for 24 hours on silicon pillars coated with poly-L-lysine.

Figure 1.4 Primary cortical astrocytes immunocytochemically stained for vinculin and actin filaments.

Chapter 2: Materials and methods

Figure 2.1 contact mode operation

Figure 2.2 Fabrication of topography

Chapter 3: Fabrication and initial investigation of the cellular reaction to defined nanotopography

Figure 3.1 Quartz nanostructure fabricated by Electron beam lithography.

Figure 3.2 An array of pits at a 300-nm centre to centre spacing, with an average depth of 80 nm in polycaprolactone.

Figure 3.3 Apparatus used for melt moulding of polycaprolactone nanostructures.

Figure 3.4 Cell adhesion of rat epitenon fibroblasts to nanopitted and planar polycaprolactone after 4 hours.

Figure 3.5 Cell adhesion of rat epitenon fibroblasts to nanopitted and planar

polycaprolactone after 20 hours.

Figure 3.6 Cell adhesion of rat epitenon fibroblasts to nanopitted and planar polycaprolactone after 96 hours.

Figure 3.7 Coomassie blue stained cells after 21 Days

Figure 3.8 Cell adhesion of BHK 21 cells to nanopitted and planar polycaprolactone after 4 hours.

Figure 3.9 Cell adhesion of BHK 21 cells to nanopitted and planar polycaprolactone after 20 hours.

Figure 3.10 Cell adhesion of BHK 21 cells to nanopitted and planar polycaprolactone after 96 hours.

Figure 3.9 Cell adhesion of HGTFN cells to nanopitted and planar polycaprolactone after 4 hours.

Figure 3.10 Cell adhesion of HGTFN cells to nanopitted and planar polycaprolactone after 20 hours.

Figure 3.11 Cell adhesion of HGTFN cells to nanopitted and planar polycaprolactone after 96 hours.

Figure 3.12 Cell adhesion of B10D2 cells to nanopitted and planar polycaprolactone after 4 hours.

Figure 3.13 Cell adhesion of B10D2 cells to nanopitted and planar polycaprolactone after 20 hours.

Figure 3.14 Cell adhesion of B10D2 cells to nanopitted and planar polycaprolactone after 96 hours.

Figure 3.15 Epitenon cell adhesion to polystyrene nanopitted and planar topographies for 48 hours.

Figure 3.16 Epitenon cell adhesion to polyurethane nanopitted and planar topographies for 48 hours.

Figure 3.17 Epitenon cell adhesion to polycarbonate nanopitted and planar topographies for 48 hours.

Figure 3.18 Cell adhesion to nano and planar topography in serum-free media conditions after 4 hours in culture.

Figure 3.19 Cell adhesion to nano and planar topography in serum-free media conditions after 20 hours in culture

Chapter 4: Spatial control over cells

Figure 4.1 Atomic force microscopy scan of Pit planar interface.

Figure 4.2 PCL sample of spatial arranged topography

Figure 4.3 Enlarged image of epitenon cells stained with Coommasie blue after a culture period of 48 hours.

Figure 4.4 Embossed PCL sample cultured with epitenon cells

Chapter 5: Cell Migration

Figure 5.1 Time lapse footage of epitenon cells adhering to nanopitted topography.

Figure 5.2 Time lapse footage of epitenon cells adhering to nanopitted topography.

Figure 5.3 A large cluster of approximately 10 cells

Figure 5.4 Time lapse footage of epitenon cells adhering to nanopitted topography.

Figure 5.5 SEM micrograph of an epitenon cell cultured on a nano topography for 48 hours.

Figure 5.6 Epitenon cells probing the nanotopography with their filopodia.

Figure 5.7 Graphical representation of filopodia behaviour.

Figure 5.8 micrograph of epitenon cells cultures on planar a nanopitted topography.

Figure 5.9 AFM scans in tissue culture media, of epitenon cells upon nanopitted topography cultured for 40 Days.

Figure 5.10 AFM san of a nanopitted surface kept in culture conditions without cells for 40 days.

Figure 5.11 Average migration rates for cell cultured on nanopitted and planar embossed polycarbonate surfaces.

Chapter 6: The cytoskeleton and its response to nanotopography

Figure 6.1 F-actin staining illuminating the cytoskeleton of epitenon cells cultured on a planar topography for 48 hours.

Figure 6.2 F-actin cytoskeleton of epitenon cells cultured on nanopitted topography for 48 hours.

Figure 6.3 Vinculin containing focal contacts of epitenon cells cultured on a planar PCL topography.

Figure 6.4 Vinculin containing focal contacts of epitenon cells cultured on nanopitted PCL topography.

Figure 6.5 Cell means for size of individual size of vinculin containing focal adhesions.

Figure 6.6 Means for amount of focal adhesions present per cell

Figure 6.7 b tubulin staining of HGTFN cells cultured on a control planar topography for 48 hours.

Figure 6.8 b tubulin staining of HGTFN cells cultured on nanopitted topography for 48 hours.

Chapter 7: Topography or chemistry?

Figure 7.1 Morphology of epitenon cells cultured on planar topography for 48 hours.

Figure 7.2 Morphology of epitenon cells cultured on nanopitted PCL topography for 48 hours.

Figure 7.3 Direct comparison of cell morphology of cell cultured upon 2 types of topography.

Figure 7.4 Graphical representation of epitenon cell spreading area.

Figure 7.5 Graphical representation of epitenon cell adhesion.

TABLE 1: P-values of statistical comparisons of cell spreading on 4 different surface types

TABLE 2: P-values of statistical comparisons of numbers of cells on 4 different surface types

Chapter 8: General Discussion

Figure 8.1 Attachment of fluorescent carboxylate 20mm diameter beads to a nanopitted surface in polycaprolactone.

Figure 8.2 Influence of symmetry on cellular reaction and orientation pattern to test the hypothesis.

Abbreviations

AFM	Atomic Force Microscopy
BHK	Baby Hamster Kidney Cells
DMEM	Dulbecco Modified Eagles Medium
EBL	Electron Beam Lithography
EC	Endothelial Cells
ECM	Extra Cellular Matrix
EDA	Ethylenediamine
FAK	Focal Adhesion Kinase
FC	Focal Contacts
FCS	Fetal Calf Serum
GTP	Guanosine Triphosphate
HGTEN	Human Granuloma Tissue Frank Niblock
HMDS	Hexamethyldisilazane
ITO	Indium Tin Oxide
MDCK	Madin-Darby Canine Kidney
MSC 80	Mouse Schwann Cell
PBS	Phosphate Buffered Saline
PC12	Pheochromocytoma
PCL	Polycaprolactone
PI[4,5]P₂	Phosphatidylinositol
PLL	Poly-L-lysine
pp60^{src}	Phosphoprotein 60 KD Sarcoma
PVA	Poly Vinyl Alcohol
RIE	Reactive ion Etching
RPMI	Roswell Park Memorial Institute
SAM	Self Assembled Monolayer
SEM	Scanning Electron Microscopy
SPARC	Secreted Protein, Acidic, Cysteine-Rich
SVHS	Super Vertical Helix Scan
VASP	Vasodilator Stimulated
μCP	Micro Contact Printing

Abstract

During the last 30 years, the semiconductor industry has had a significant influence on our society through advances in computers, communications, energy, and transportation. Semiconductor technology exploded following the development of exquisitely precise and versatile miniaturisation techniques that allowed features on computer chips to be reduced to submicron dimensions. In addition, microfabrication tools developed for the microelectronics industry have also entered the basic science arena and are beginning to serve as a driving force for discovery in cell biology, and tissue engineering in the utilisation of this technology for fabricating precisely defined cell devices. Recent advances in semiconductor technology have enabled scientists to fabricate devices in the nanometer range. In this thesis electron beam lithography was employed to fabricate nanometric pillars in quartz, which were then reversed embossed into a range of biocompatible polymers generating a relief pattern of nanopits. The effects of this type of topography on cell behaviour was then investigated using a combination of light, fluorescence, video scanning electron and atomic force microscopies. The results of using this type of topography revealed a marked decrease in cell adhesion, this was due to the super-hydrophobicity generated by fabricating ordered nanotopography. This reduction in cell adhesion had subsequent effects on cell behaviour, namely increased motility, a reduction in cell and focal adhesion size coupled with a disruption in cytoskeletal development. The work carried out in this thesis have possible implications for the future design of biomaterial implant surfaces as well as possible uses in the design of future in-vitro tissue engineering devices where the lack of cell adhesion in specific regions is a desirable outcome.

Chapter 1

Introduction

It has long been known that cells are greatly influenced by their environment. One of the first pioneers of cell biology was Ross Harrison. Observations he made in early cell culture experiments, lead him to recognised that this technique was valuable in being able to guide the extending nerve fibre. His experiments with cultured neural tissue (Harrison, 1910) led him to conclude that the nerve tip was positively stereotropic, in that it requires a solid support in order to extend through the medium. This was developed upon in experiments with cells from cold and warm blooded animals (Harrison, 1911; Carrel and Burrows, 1911; Burrows, 1911) and the general rule became clear that all tissue cells require a solid support in order to translocate. Stereotropism had already been mooted as necessary for cell movement *in vivo* 12 years earlier, (Leob, 1898) however it was Harrison (1912) who carried his investigations further and pinpointed many of the features which we now describe collectively as contact guidance. Harrison cultured various tissues on drawn out spider webs, and concluded that 'The behaviour of cells with reference to the surface of the cover slip and the spider webs shows not only that the surface of a solid is not only necessary condition, but also that when the latter has a specific linear arrangement, as in the spider web, it has an action in influencing the direction of movement as well as upon the form and arrangement of cells'.

Weiss (1945) was the first scientist in the field to postulate how and why cells react to the topography of their surroundings, work which stemmed from the guidance of cells on fibrillar matrices. Weiss hypothesised that cells reacted to the molecular orientation of their environment. Weiss extended this hypothesis showing cell orientation on glass fibres by fibrillar colloidal exudate produced by explants. He claimed that the colloidal exudate was oriented to the glass fibres via capillary forces and this in turn caused cells migrating from the explants to become oriented. However, when single cells were put on the fibres in the absence of colloidal exudate, they became aligned, contradicting Weiss's previous observations.

Curtis and Varde (1964) later proposed that cells responded to the topography of their environment, and were influenced by discontinuities of angle or radii of curvature. Dunn and Heath (1976) added further to these findings by studying the behaviours of fibroblasts on cylindrical substrata of varying diameters. They suggested that substrate shape and morphology exact restrictions on the formation of linear bundles of microfilaments located between the focal adhesions of the leading lamella and within the nuclear region. These microfillaments are comparatively inflexible, so any attempt by the cell to conform to an angled topography would result in a shortening of the leading lamella. The lamella is key in terms of spreading due to the furthestmost part of a cell during locomotion as suggested by its more descriptive name "the leading edge". Dunn and Heath concluded that as the radii of curvature shortened below 50 μm or prism angles increased 16° over that of the plane, the lamella would become too undersized and unable to exert sufficient traction to allow cell spreading and migration in that direction. This

work was echoed to great acclaim 20 years later when Chen et al., (1997a) altered the size of polystyrene beads (and hence angle) and produced an abatement in cell spreading to the point of apoptosis in mammalian cells.

An early example of this work was carried out by Maroudas (1972), who grew cells on glass beads of ranges of 20 to 60 μm . He found that BHK cells failed to grow and proliferate upon beads in bellow 20 μm in diameter, and on larger diameter beads the cells tend toward multilayers of a thickness found on a culture dish, indicating that the shape of a cell seems to govern the required dimension of substrate.

Dunn and Heath's theory certainly appeared to give an explanation of cell reaction to a single topography, however O'Hara and Buck (1979) suggested that it did not explain cell reaction to substrates with multiple features like grooved surfaces. Using multiple grooved substrata with features smaller than cell size, they showed that cells were agile enough to bridge the grooves, in that cell substrate contact was restricted to the ridges at the top the grooves. This implied that the substrate was constraining the pattern of the focal adhesions to confines of the grooves, in turn controlling the freedom of the cytoskeleton to determine where contact upon the substrate would be. This had the knock-on effect of influencing direction of cell movement. In an expansion of this work Meyle et al., (1993, 1995) suggested that cells align to their substratum to avoid distortion of their cytoskeleton. They observed that intracellular F-actin fibres must be straight and not bent if they are to exert forces upon the topography.

Constructs for tissue engineering

At the heart of the tissue-engineered replacement is the biomaterial construct or scaffold, in which a given cell population is seeded. One of the challenges in tissue engineering is to find a more suitable method for the fabrication of scaffolds of defined architecture to guide cell growth and development (Desai 2000a). Ideally, a biomaterial scaffold should have well-controlled microarchitectures, including well-defined pore sizes and porosity, reproducibility, biocompatibility, thermal and biochemical stability. These physical factors should allow nutrient supply and vascularisation of the cells in the implant and permit development of a fibrous tissue layer.

Basement membranes comprise a complex mixture of pores, ridges, and fibres, which have sizes in the nanometer range. Abrams and coworkers (Abrams et al., 1997) used scanning electron microscopy, transmission electron microscopy, and atomic force microscopy to measure the sizes of features on the surface of the corneal epithelial basement membrane of the Macaque monkey. The average feature heights were between 147 and 191 nm and the average fiber width was 77 nm (Abrams et al., 1997; Abrams and Presser, 1997). They found that pores made up 15% of the total surface area of the membrane and had an average diameter of 72 nm . Similar features were observed on the human corneal epithelial basement membrane and on MatrigelTM, a commercially available basement membrane matrix (Abrams et al., 1997).

Shirato et al., (1991) studied the glomerular basement membrane of the rat kidney and observed a meshwork of fibrils 5-9 nm thick and pores 11-30 nm wide on the lamina *rara interna* and 6-11 nm fibrils and 10-24 nm pores on the lamina *rara externa* (Shirato et al., 1991). Yamasaki and coworkers examined the pores and fibers present in bovine glomerular and tubular basement membranes (Yamasaki et al., 1994). They found pore diameters near 10 nm in the glomerular membranes and pores near 12 nm in diameter in the tubular membranes. Fibrous strands were seen to have widths of 3-15 nm. Another study by Hironaka et al., (1993) found that the glomerular, tubular, and Bowman's capsule basement membranes of the rat kidney all had mean fiber diameters of 6-7 nm while having mean pore diameters of 9.7, 14.1, and 13.1 nm, respectively (Hironaka et al., 1993).

Many tissue engineering constructs use porous or mesh-like polymeric matrices, these matrices should also allow for cell in-growth and structural maintenance for tissue regeneration. It is also prudent to acknowledge that a tissue engineered surface may also prevent cell integration. e.g. the blood interface of a vascular graft.

Several polymer-processing procedures are currently used, including solvent casting, fiber bonding, and membrane lamination (Thompson et al., 1997; Mikos et al., 1993). The fiber bonding technique depends on choice of solvent, polymer immiscibility, and melting temperatures to achieve the desired shape. Solvent casting is employed in combination with particulate leaching to prepare porous scaffolds and can be applied to polymer systems that are soluble in a given solvent (Lo et al., 1995; Mooney et al., 1994). The handicap of this technique lies in the fact that porosity is achieved by varying

the amount and size of salt particles during evaporation. Moreover, in several of these techniques, microarchitecture is achieved by altering solute or solvent concentration, thus making it difficult to attain precise reproducible features in the micro- and nanometer range (Desai, 2000b).

A tissue engineered construct that has a well defined microstructure will better maintain cell morphology, differentiation, and functionality over long periods of time (Desai, 2000b). A key feature of these constructs will be the replication of *in vivo* geometry and dimensional size scale that will aid in the maintenance of an *in vivo*-like cell phenotype. The development of microfabricated constructs using established natural and polymeric biomaterials might permit us to engineer highly controlled interfaces, which are more physiologically relevant and hierarchically arranged. This would result in a reliable biologically, mechanically and optically compliant material. Indeed using microtechnology, we may create tissue-engineering implants with precise microarchitectures for immunoisolation, cellular ingrowth, and drug delivery.

Silicon microfabrication techniques make it relatively easy to generate the complex geometries on the nanometer and micron scale. This is required to model physiological environments in living tissue. Although microfabrication has traditionally been applied to semiconductor materials due to their oxidation and etching properties, techniques to translate structures from inorganic to organic polymeric materials were introduced by Brunette (Brunette et al., 1983). Brunette used epon, a hard epoxy, to reproduce features by reverse embossing, in grooved silicon wafers. Since then, several different approaches have been employed to create microstructured polymer.

Polymer embossing from electron beam etched quartz (Curtis et al., 2002) microtextured membranes (Deutsch et al., 2000), molding of polydimethylsiloxane for micro fluidics and biological applications (Folch et al., 1999; Kapur et al., 1996) was another approach. These developments have opened up unique opportunities in substrate development for biological and tissue engineering applications.

One of the first studies using microfabricated substrates to study cellular behavior was performed by Brunette et al., (1983). His group established the use of a silicon mask etching technique to prepare grooved surfaces to control the direction of outgrowths of human gingival explants. They found enhanced osseointegration and induction of mineralized tissue using surface microtexture (Brunette et al., 1999). In their studies, titanium coated microgrooves varied the ingrowth of adjacent epithelium in percutaneous skull implants, yielding important implications for maxillofacial or dental reconstruction. In addition, Campbell and von Recum (1989) described how surface micropatterns could be used to reduce the inflammatory response at the implant tissue interface. In the ensuing period, there have been many studies showing topographical control of cells and tissues (reviewed by Singhvi et al., 1994) where the techniques of microfabrication and micromachining have been used to create more complex biomaterials with defined surfaces incorporating microchannels or micropores for cellular interfacial control (Matsuda et al., 1994; Desai et al., 2000b).

By culturing cells on novel surfaces with defined topography or surface chemistry, investigators have begun to address crucial issues such as cell migration, orientation and adhesion, as well as tissue integration, and

vascularisation (Ito, 1999). For example, microtexture has significant effects on cell proliferation and adhesion (Den Braber et al., 1995, 1996 and 1998). Surfaces with parallel grooved microtopography can augment fibroblast attachment and induce contact guidance of these cells (Clark et al., 1991, Meyle et al., 1995). Furthermore, van Kooten et al., (1998) showed that gene expression was influenced by microtexture (Chou et al., 1995) and that cells on 10 μm wide grooves proliferated less than cells on 2 μm and 5 μm grooves. The organization of cells in controlled two and three-dimensional arrangements has been shown to have beneficial effects on cell differentiation, maintenance, and functional longevity (Kapur et al., 1999).

Many researchers have demonstrated that topography can influence and direct cell migration. Moreover, the width and spacing of the lines can be used to control the speed of cell movement. For example, etched parallel grooves can control cell spreading and migration in the axis of the lines, even when the depth and spacing of the grooved features are as small as 500 nm, about ten times smaller than the typical length of a mammalian cell, (Flemming et al., 1999; Curtis and Clark, 1990; Curtis and Wilkinson, 1997).

Spatial control of cells

In this thesis, a novel method for the spatial control of cells using arrays of nanometrically arranged pitted structures, embossed into the biodegradable polymer polycaprolactone (PCL), will be detailed and discussed in the ensuing chapters. This work is novel in the respect that topography is the driving force behind the control. However, the spatial control of cells has been studied by the use of many different approaches.

Surface hydrophobicity or electric charge of polymer substrates strongly influences cell adhesion. This effect was visualised by using micropatterning methods, embracing both photolithography and chemical coupling with silane or transferring from a patterned stamp alkanethiol self-assembled monolayers (SAM).

Matsuda's group (Matsuda et al., 1990; Matsuda and Inoue, 1990; Matsuda and Sugawara, 1995) reported the development of micropatterning technology for cultured cells by defined surface regional modification via photochemical fixation of phenyl azido-derivatized polymers on polymer surfaces. The photoreactive polymers included poly (N, N-dimethylacrylamide-co-3-azidostyrene), bis-4-azobenzamide-polyethylene glycol, and poly (styrene-co-3-azidostyrene). The photochemical fixation of these photoreactive polymers consisted of three steps: (1) coating of a photoreactive polymer on a material surface; (2) ultraviolet irradiation through a photomask; and (3) removal of nonreacted polymer by a solvent. Two different types of regionally modified surfaces were prepared; one was a hydrophilic polymer regionally fixed on a tissue culture dish and the other was a hydrophobic polymer regionally fixed on poly (vinyl alcohol) (PVA). Photochemical surface microfabrication permitted micron-order-dimensional precision, which was verified by the micropatterned tissue formation of bovine aorta endothelial cells (ECs) when they were seeded on these surfaces. ECs adhered, spread, and confluenty proliferated only on uncoated tissue culture dish surfaces or hydrophobic regions on PVA. Thus, the regionally differentiated cell adhesion regions were created by photochemically driven surface microprocessing.

Other photolithographic techniques have been used to spatially control cell populations (Ranieri et al., 1993; Soekarno et al., 1993; Valentini et al., 1993 and Thomas et al., 1997). Dewez et al., (1998) reported the adhesion of some mammalian cells, such as human epithelial cells, PC12 pheochromocytoma, MSC80 schwannoma, Hep G2 hepatoblastoma, and rat hepatocytes, on patterned (produced by photolithography and oxygen plasma treatment) polystyrene surfaces having tracks (width in the range of a few tens of μm) of reduced hydrophobicity.

DeFife et al., (1999) examined the surface effect of electric charges of surface polymers. Poly (ethylene terephthalate) films were coated with poly(benzyl N, N-diethylthiocarbamate-co-styrene) and progressively exposed to monomer solutions for photoirradiation. A photomask was placed over different regions to generate micropatterned surfaces with graft polymer stripes of three distinct ionic characters. Nonionic polyacrylamide greatly inhibited adhesion and induced clumping of the few monocytes that did not adhere. Macrophage adhesion and spreading led to high degrees of interleukin-13-induced foreign body giant cell formation on both the anionic poly(acrylic acid), sodium salt, and benzyl N, N-diethylthiocarbamate portions of the culture surface. In spite of the highest observed levels of monocyte/macrophage adhesion on cationic poly (dimethylaminopropylacrylamide), the adherent cells did not undergo fusion to form foreign body giant cells. These investigators concluded that inflammatory cell responses may be spatially controlled in a manner that may be ultimately exploited to improve the biocompatibility of medical devices (De Fife et al., 1999). Lee et al., (1993a) used an Na^+ ion-

implantation technique for selective cell adhesion. They used an ion beam instead of ultraviolet light for the lithography.

On the other hand, self assembled monolayers (SAM) of alkanethiolates on gold have been employed by some researchers to control cell attachment to substrates. Stenger et al., (1992) and Spargo et al., (1994) used SAM formed from two materials, an amino-alkylsilane, $\text{NH}_2(\text{CH}_2)_2\text{NH}(\text{CH}_2)_3\text{Si}(\text{OCH}_3)_3$ (EDA) and a perfluorinated alkylsilane $\text{CF}_3(\text{CF}_2)_5(\text{CH}_2)_2\text{Si}(\text{CH}_3)_2\text{Cl}$ (^{13}F). Deep ultraviolet (193 nm) radiation was used to induce photochemical changes in the cell adhesive EDA monolayers. X-ray spectroscopy indicated that the amine groups of EDA were removed by this exposure, leaving only Si-OH or alkyl fragments having less than three carbons. The exposed substrates then reacted with ^{13}F to form mixed monolayers or hydrophobic monolayers that inhibited cell adhesion in the irradiated regions. These patterns were used to spatially control the adhesion of porcine aortic endothelial cells *in vitro* and direct outgrowth of rat hippocampal neurons.

The group of Ingber and Whitesides (Singhvi et al., 1994a; Chen et al., 1997b; Mrksich et al., 1996) demonstrated, by patterning the formation of SAMs using microcontact printing into regions that promote or resist adsorption of protein, attachment of cells to surfaces could be confined to rows 10-100 μm wide, or to islands whose size was equivalent to that of a single cell. Using this technique, it was possible to place cells in predetermined locations and arrays, distributed by defined ranges, and to dictate their shape. This limited the degree of spreading and granted control over cell growth and protein secretion.

Scotchford et al., (1998) cultured primary human osteoblasts on SAM of alkylthiols on gold with carboxylic acid and methyl termini, and ascertained the kinetics of cell attachment and proliferation on these substrates. After 24 hours, the number of cells attaching to carboxylic-acid-terminated monolayers was 10 times the number adherent to methyl-terminated monolayers. Cell morphology and cytoskeleton actin organization was also different. Cells attached almost exclusively to carboxylic-acid-functionalized sections of the patterned surfaces, leaving methyl-functionalized regions bare. The patterns influenced the morphology of the attached cells. After 24 h, cells with carboxylic-acid-terminated regions separated by 75 μm were observed to bridge, but not those separated by 150 μm methyl-terminated regions. After 6 days in culture, osteoblasts formed multilayers on the carboxylic-acid-terminated regions of the pattern.

Qiu et al., (1998) cultured rat bone marrow stromal cells on a conductive and transparent indium tin oxide (ITO) pattern-coated substrate. On positively charged ITO, cell attachment was enhanced in serum-supplemented and serum-free media. Furthermore, decreases in cell spreading, alkaline phosphatase activity, and osteopontin were detected in cells cultured on the positively charged ITO. This result established that positively charged surfaces enhance cell attachment but suppress cell spreading and differentiation of rat marrow stromal cells.

There is considerable interest in controlling neuron cell adhesion and neurite outgrowth for studies of the influence and development of cytoarchitecture in dissociated neuronal cell cultures and investigations of neurite polarity in response to molecular cues (Lochter and Schacher, 1999). Micro contact

printing (μ CP) has been exploited specifically to control neuron cell attachment and neurite morphology (Wheeler et al., 1999; James et al., 1998; Branch et al., 2000). Poly-L-lysine has been patterned onto silicon oxide, silicon nitride, and glass surfaces in order to design neuron cell networks for studying dissociated cell development and long term network architecture plasticity. Using a two-level technique similar to that used by Kleinfeld and other researchers (Kleinfeld et al., 1988, Stenger et al., 1992, Lom et al., 1993) have printed poly-l-lysine structures and modified the remaining surface area with a cell-repulsive molecule to enhance the stability and longevity of cell guidance for long term cultures (Wheeler et al., 1999; Branch et al., 2000). Recently, James et al., (1998) have printed poly-L-lysine structures onto the surface of microfabricated multielectrode arrays. This approach provides three advantages. Firstly, the yield of recorded cells is increased due to the guidance of cells to the recording sites. Secondly, the cell-electrode coupling can be enhanced by selectively placing proteins immediately adjacent to electrode sites and, thirdly, cell networks with specifically designed architecture can be studied on a long-term basis. Working in this regime, they have patterned surfaces with 2 to 20 μ m wide poly-l-lysine structures and recorded extracellular field potentials. This technology allows a wide range of possible network designs to be constructed in order to explore issues such as synaptogenesis and synapse refinement during development.

Nanoscale Topography

In the past twenty years, scientists have taken advantage of the tools made available by the semiconductor industry to fabricate well-defined surface

features in materials ranging from silicon and quartz to polystyrene and silicone elastomer. Such tools have enabled the design and patterning of features in the range of 100 of micrometers, down to the 10s of nanometers and led researchers to probe the effects of features comparable to the size of a single cell down to the nanometer range of sub-cellular processes.

The structural features that a cell might encounter when in its natural environment include features that fall within the size range of nanometers to micrometers. Most studies, such as those begun by Curtis and Wilkinson (1997), Curtis and Clarke (1990) von Recum and von Kooten (1995) and Oakley and Brunette (1986), have addressed the effects of 'microgrooves' on cell lines such as fibroblasts, epithelial cells, and endothelial cells (Clarke and Connolly, 1991; Den Braber et al., 1995, 1996; von Recum et al., 1998; Wojciak-Stothard et al., 1995a; Chou et al., 1995; Curtis and Wilkinson, 1998; Walboomers et al., 1998). The majority of these studies have shown that cells will align with the grooves and that groove depth and width play crucial roles in the degree of alignment. Fewer groups have looked at the effects of pillars or spikes on cell growth. Such studies have looked at cardiac myocytes and rat epitenon cells as well as fibroblasts and endothelial cells (van Kooten et al., 1998; Rovensky et al., 1991; Wilkinson et al., 1998; Casey et al., 1997; Deutsch et al., 2000.)

Turner's investigations (Turner et al., 1997) have focused on the growth of central nervous system cells on columnar structures. They have shown how a transformed astroglial cell line, LRM55 cells, as well as primary cortical astrocytes respond to nanometer-scale columnar silicon structures (Figure 1.1)

(Turner et al., 1997; Craighead et al., 2001). Glial cells were plated on substrates with two different forms of surface texture: one a rough 'silicon grass' surface and the other a silicon grass surface that had been smoothed with a wet chemical etch. Transformed astrocytes from a continuous cell line showed a preference for wet-etched regions over grassy regions. In contrast, primary cortical astrocytes from neonatal rats showed a preference for silicon grass over the wet-etched surface (Figure 1.2). For the transformed astrocytes cells, the degree of response was continuous with the degree of wet-etch modification. Wilkinson et al., (1998) looked at the attachment of rat epitenon cells after 1 h to nanometer-sized polystyrene pillars and found that there was a significant decrease in the number of cells that attached compared to the smooth control surfaces (Wilkinson et al., 1998).

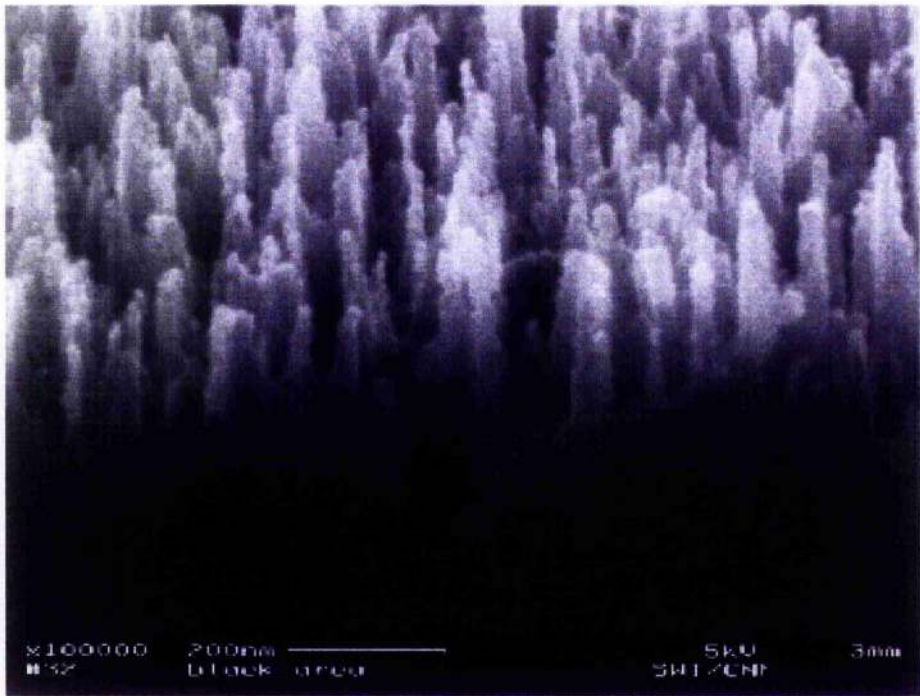


Figure 1.1 a 60° tilt SEM of a typical region of silicon grass; image taken from Turner et al., (1997).

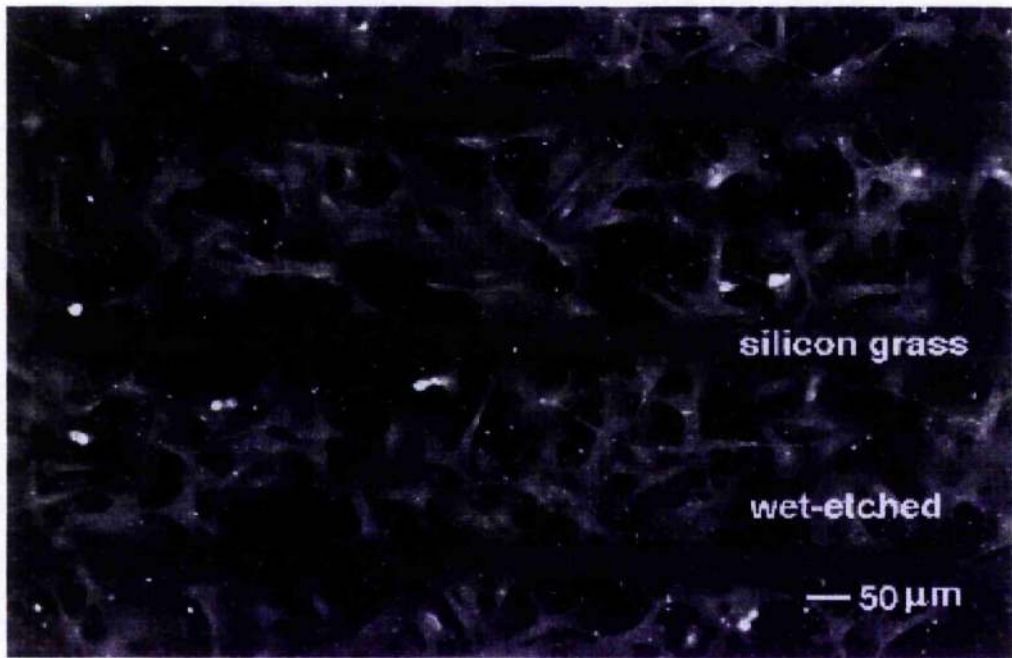


Figure 1.2 Scanning confocal micrograph of LRM55 cells adhering preferentially to the wet-etch modified regions of the silicon substrate. The lighter regions of the substrate are the silicon grass; the darker regions have been wet etched. (Image taken from Turner et al., 1997).

They propose that such nano patterned surfaces might be used as non-adhesive layers for implant devices. Based on these studies it is apparent that different cell lines respond differently to nanometer-sized surface features. The response of glial cells to more regular arrays of columnar structures has also been examined. In one study, the silicon pillars were 0.5 μm in width, 1.0 or 2.7 μm in height, and separated by 1.0 μm (Craighead et al., 2001). In this case, they found that both the LRM55 cells and the primary astrocytes demonstrated a preference for the pillars rather than the flat silicon surface and no discernable preference for either pillar height. To further this effort, they examined the growth of LRM55 cells on pillar arrays of different geometries (Turner et al., 1997). In this study, the features were wells and pillars ranging in size from 0.5 to 2.0 μm in diameter. Cells preferred to attach and grow on the pillars rather than the smooth silicon, regardless of the distance between pillars, and showed a lack of affinity for the surfaces with wells. Scanning electron micrographs and immunochemical staining revealed that the cells attached to the tops of the pillars with no contact being made with the silicon floor between the pillars. The attachment and growth of embryonic rat hippocampal neurons on these same pillar surfaces have been studied and have yielded very clear topographical effects. Other groups, such as Rajnicek et al., (1997), have also looked at the attachment and growth of central nervous system cells on surface structures (Clark et al., 1991; Rajnicek et al., 1997; Stepien et al., 1999; Bayliss et al., 1999). They have studied neuronal cells on materials such as porous silicon, scratched glass, ultra-fine quartz gratings and quartz microgrooves, where the primary focus has been

the degree of alignment brought about by the surface structures as well as the viability of the cells on these materials.

Nanostructures can also be formed by methods other than planar processes. In recent work, for example, Mattson et al., (2000) have cultured embryonic rat neurons on multi-walled carbon nanotubes. With the application of 4-hydroxynonenal, they were able to promote neurite outgrowth on these nanotubes. Based on the strength, electrical conductivity, and chemical functionality that carbon nanotubes can exhibit, they have proposed that such tubes may be used as nanometer scale neural probes. In the past few decades, researchers have discovered the remarkable electrical, mechanical and optical properties of yet another form of carbon, C-60 (bucky balls). A recent study by (Lin and Wu, 1999), looked at the adhesion of human platelets to polyurethane surfaces immobilized with these fullerenes and they observed an increase in platelet adhesion and activation on the surfaces modified with C-60.

At the nanoscale, chemistry and topography converge. An interesting approach to creating new biomaterials involves the creation of topographical features that mimic chemical species. Ratner et al. (1996) for example, have studied a method of nano-scale patterning of solid substrates using proteins as templates (Boeck, et al., 1998; Shi et al., 1999; Ratner et al., 1996; Shi and Ratner, 2000). Their work provides evidence that proteins will adsorb more readily to a surface if the surface is patterned with the 'imprint' of that protein. They have proposed that nano-imprinting of proteins can be used to make more biologically compatible implant devices

Ordered nanotopography

Only a handful of groups have fabricated a regular nanometric surface features such as those used in this thesis. The first to fabricate nanoscale features were Casey et al., (1997) who developed a process whereby nanometric features were uniformly transferred into a thermoplastic with the use of embossing. Master surfaces were made by using electron beam lithography, dry etching and electroplating and with these dies features as small as 60 nm were produced in the polymer cellulose acetate. (This work was the inspiration for the work carried out in this thesis).

Turner et al. (1997) have examined the response of glial cells to more regular arrays of columnar structures. In one study, the silicon pillars were 0.5 μm in width, 1.0 or 2.7 μm in height, and separated by 1.0 μm . In this case, they found that both the LRM55 cells and the primary astrocytes demonstrated a preference for the pillars rather than the flat silicon surface and no discernable preference for either pillar height. To further this effort, they also examined the growth of LRM55 cells on pillar arrays of different geometries. In this study, the features were wells and pillars ranging in size from 0.5 to 2.0 μm in diameter (Figure 1.3). Cells preferred to attach and grow on the pillars rather than the smooth silicon, regardless of the distance between pillars, and showed a lack of affinity for the surfaces with wells. Scanning electron micrographs and immunochemical staining revealed that the cells attached to the tops of the pillars with no contact being made with the silicon floor between the pillars (Figure 1.4). The attachment and growth of embryonic rat

hippocampal neurons on these same pillar surfaces has been studied and has yielded very clear topographical effects.

The most important feature of the above mentioned work is the emphasis on ordered nanometric features as opposed to disordered features. The role of symmetry is addressed in this thesis as well in Curtis et al., (2001) where the symmetry of the nano patterns appears to play a key role in the reaction of cells to nanotopography.

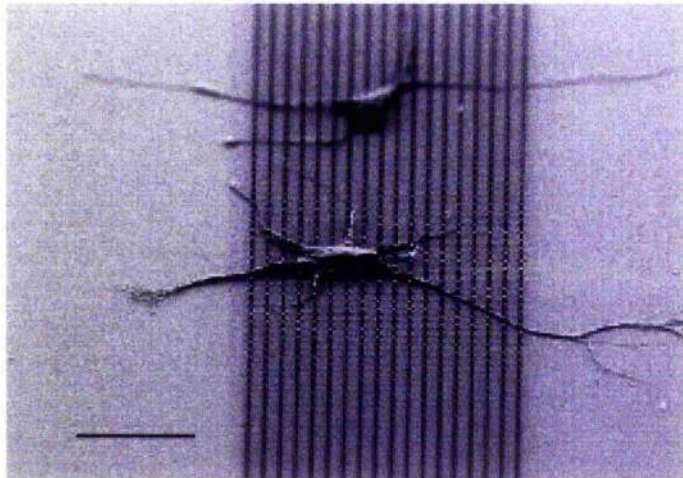


Figure 1.3 An SEM of rat hippocampal neurons cultured for 24 hours on silicon pillars coated with poly-L-lysine (scale bar 20 μm). (Image taken from Craighead et al., 2001)

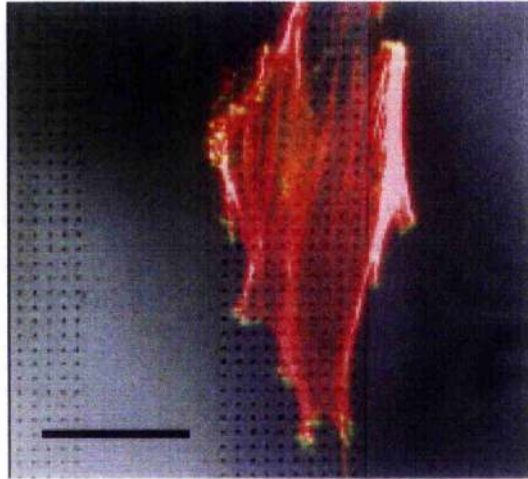


Figure 1.4 Primary cortical astrocytes immunocytochemically stained for vinculin (focal contacts) (shown in green) and actin filaments (shown in red) (scale bar 50 μm). (Image taken from Craighead et al., 2001)

Surface roughness

Surface roughness is a random type of surface topography. The degree of surface roughness is determined either by machine process during the preparation of a surface, or by the subsequent modification of the surface. The most common methods for obtaining general surface roughness, include turning surfaces; plasma spraying, coated surfaces, sandblasting, reactive ion etching, isotropic etching, acid etching and electro-polishing. These surfaces present an extremely varied topography that cells can encounter, when used to pattern implant material surfaces. There is substantial *in vitro* evidence that increasing surface roughness results in increased compressive, tensile and shear forces (Wilke et al., 1990; Feighan et al., 1995). In some studies an increase in the bone in contact with an implant surface was noted with increasing surface roughness (Bruser et al., 1991). *In vitro* studies have examined the attachment of fibroblasts (Inoue et al., 1987; Meyle et al., 1993; Cochran et al., 1994) epithelial cells (Chochran et al., 1994) macrophages (Salthouse, 1984) and osteoblast-like cells (Bowers et al., 1992; Keller and Spieth, 1994; Martin et al., 1995) to surfaces of differing roughness. Most of these studies relate to the ability of the cells studied to attach to the different surfaces, to proliferate and differentiate and to secrete extracellular matrix and proteins. Studies that have looked at macrophage attachment show an increase in cell attachment with increased surface roughness.

Cell adhesion

The association with cells and the extracellular matrix initiates the assembly of specific cell-matrix adhesion sites. These sites are implicated in the physical attachments of cells to outward surfaces, which is imperative for cell migration and tissue formation as well as for activation of adhesion-mediated signalling responses and their integrins, which are heterodimeric transmembrane receptors for ECM components (Hynes, 1992). Following association with their ligands, integrins induce reorganisation of the actin cytoskeleton and associated proteins, ensuing in the formation of cell-matrix adhesion sites.

The best known class of matrix adhesions in cultured cells are the focal contacts (FCs), which can be visualised by immunocytochemistry (Geiger and Bershadsky, 2001), electron microscopy and interference reflection microscopy (Abercrombie and Dunn, 1975; Jockusch et al., 1995). These sites contain a multitude of anchor and cytoskeletal molecules such as vinculin, paxillin and talin (Chrzanowska-Wodnicka and Burridge, 1996) as well as signal transduction molecules, such as focal adhesion kinase (FAK), C-terminus Src kinase, protein kinase C and others. Recent studies have shown that the assembly and tyrosine phosphorylation of FCs relies on actomyosin contractility, which in turn is regulated by cytoplasmic factors such as rho, caldesmon, or microtubule integrity (Jockusch et al., 1995; Bershadsky and Chausousky, 1996; Pelham and Wang, 1997).

Molecular complexity of Focal adhesions

Classical focal contacts are flat elongated structures associated with the ends of actin filament bundles (stress fibers) in a wide variety of cultured adherent cells and can be visualised by fluorescence, interference reflection or electron microscopy (Abercrombie and Dunn, 1975, Heath and Dunn, 1978). These structures appear to be extremely crowded with different molecules. To date over 30 distinct molecules have been reported to reside in them, and the list is rapidly expanding (for review, Petit and Thiery, 2000)

One of the characteristic properties of most focal contact proteins is their multi-domain structure. Interestingly vinculin, can interact (not simultaneously) with at least 10 other focal contact components, including actin, tensin, paxillin, hic-5, talin, α -actinin, vinexin, ponsin, vasodilator-stimulated phosphoprotein (VASP) and phosphatidylinositol 4,5-bisphosphate (PI[4,5]P₂), and many of these can further bind to multiple additional partners. Another noteworthy observation is that about half of the known molecular residents of focal contacts are established components of different signal transduction pathways, among them protein tyrosine kinases (e.g. focal adhesion kinase (FAK) and pp60^{src} (Parsons, et al., 2000) serine-threonine kinases, protein phosphatases and leukocyte common antigen related tyrosine phosphatase and adaptor proteins (Zamir and Geiger 2001a)

Cell adhesion and the role of force

Cells generate forces against the focal adhesion that they form with the ECM in order to heal wounds, maintain correct tissue shape and perform

physiological organ functions. Although it is extensively accepted that the biochemical composition of the ECM influences the signalling pathways, recent studies have shown that the cell also responds to the mechanical stiffness of the ECM (Chouquet et al., 1997 and Halliday, 1997) and the area the area of ECM available for binding (Chen et al., 1997b). As the cell spreads, it determines the size and the spatial distribution of the contacts that it can form with the ECM (Chen et al., 1997b). The cell then arranges its cytoskeleton to exert force against its adhesive contacts and to structurally support the cell interior (Sims et al., 1992). The cell sets an internal stress field (the distribution of intracellular forces at mechanical equilibrium) that results from the combination of the forces generated within the cytoskeleton.

Tension generated by the cytoskeleton

The organisation of the actin cytoskeleton allows the spreading cell to exert contractile forces against the ECM. Activated rhoA, a ras-related GTP binding protein, stimulates the appearance of stress fibres, focal adhesions and tyrosine phosphorylation in quiescent cells (Ridley, 1996). It has been stated that myosin light chain phosphorylation activates rho, which stimulates contractility and drives the formation of stress fibres as well as the aggregation of diffusely distributed integrins into focal adhesions (Chrzanowska-Wodnicka and Burridge, 1996). This Rho mediated contractility may also be important in promoting the assembly of fibronectin into a fibrillar matrix.

Possible mechanisms of force transmission between the ECM and intracellular structures.

Two types of model have been proposed to explain how a cell is able to sense the mechanical environment of the ECM: a tensegrity model (Ingber, 1997) and a cytoskeleton-ECM force transduction model (Sheetz et al., 1998). The tensegrity model suggests that the cell is rigidly coupled, or hard wired, to instantaneously respond to mechanical stress transmitted through integrins that are physically coupled the cytoskeleton and the ECM. Alternatively, the cytoskeleton-ECM force transduction model predicts that forces acting on particular cytoskeletal links produce biochemical signals that are sufficient to modify cell function without the need for a rigid mechanical transmission linkage.

Chloride channels and their role in mechanical tension reception

It has been reported (Tobasnick and Curtis, 2001) that stretch sensitive chloride channels may be involved in the earliest stages of the reaction of epitenon cells to substratum topography (such as groove-ridge structures) on the micrometric and nanometric scale. The reaction of cells to these structures includes cell extension, elongation and orientation to the grooved topography. They reported that rat epitenon-cells can develop appreciable lateral and mechanical tension that could stretch both the force generating cells themselves and those nearby. Tobasnick and Curtis showed that cells in medium in which more than 80% of the chloride has been replaced by nitrate

show little reaction to topography. Spreading of the cells takes place but is much reduced along the direction of the groove-ridge topography but is however, enhanced across the topography. Chloride channel inhibitors were also utilised in experiments and produced similar results, which are further accentuated when these inhibitors are present in low chloride medium.

The results of the chloride channel experiments are consistent with the hypothesis that an active chloride channel system is required for the reaction of cells with topography. The changes in tension shown in these experiments are consistent with the idea that the treatments used have reduced the reaction of cells to their own mechanical tensions.

Cell crawling

The crawling cell usually has a polarity, the most conspicuous feature of which are the leading lamella, thin veil-like structures that are free of organelles visible in the light microscope and that extend from the organelle-rich cell body in the direction of movement (Trinkhaus, 1992). The lamella, which may have smooth or serrated anterior edges, appear to glide forward, pulling the cell body passively behind them. As the lamella advance, they consolidate their progress by transient attachment to the underlying surface. Thus, the crawling machinery requires, in addition to the restructuring of the peripheral substance of cells, reversible adhesion of externally disposed plasma membrane molecules to the substrate along which the cell crawls (Hynes, 1992).

Cells put out variable numbers of lamella, but only the lamella that contact the substrate on which cells are crawling are capable of generating locomotion. Of these, usually one becomes dominant in an actively crawling cell. As the dominant lamella expand, the others withdraw coordinately. Contractions at the junction of the lamella and the cell body and also at the rear of the cell deform the cell body and propel its internal contents forward to the leading lamella. The flat anterior portion of the polarised cell and its narrow tail give it a shape that resembles a hand-held fan.

The advance of the leading lamella may proceed in different ways, depending on the cell type or the external environment. Cylindrical spikes, called filopodia, may protrude, and they sometimes coalesce to form extensions of the leading lamella. Alternatively, the protrusion takes place by the extension of small bubbles or blebs that subsequently flatten. A typical feature of an advancing lamella is a vertical thickening that begins at the leading edge and then moves back rearward. The most extreme version of this phenomenon is ruffling, in which the leading edge of the lamellar veil lifts upward from the substrate and, while continuing to protrude, bends backwards to a position perpendicular to the adherent portion of the lamella. The dorsally extended veil, called the ruffle, then migrates rearwards across the plane of the attached lamella toward the cell body. During its retrograde journey, the ruffle continues to fold over backwards as it simultaneously retracts and eventually dissipates near the cell body (Hynes, 1992).

As the lamella advances, selected external molecules on the lamellar surface diffuse randomly in the plane of the membrane. Others move forward toward the leading edge where they remain immobilized, and still others,

especially those crosslinked by antibodies or lectins, migrate rearwards, a phenomenon known as capping (Dembo and Harris, 1981). The term 'Cortical flow' encompasses ruffling, capping, and related centripetal movements of lamellar substance. The lamella of spreading cells exhibit circumferential cortical flow from the entire periphery to the cell body (Dembo and Harris, 1981). Although cortical flow always accompanies cell locomotion, this process can be slower than lamellar protrusion and is therefore probably not directly responsible for it (Theriot and Mitchison, 1992).

Aims of Project

The introduction of this thesis highlighted the importance of surface chemistry and topography in influencing a desired cellular response to materials. Constructs used for future cell devices may have defined chemical and topographical surface features. It will be a major advantage for us to understand how cells respond to surfaces with a defined chemistry and most relevant to the work in this thesis, the design and control of the surface topography and its effect upon cellular response.

The purpose of this thesis was to investigate the reaction of cells to a defined topography. This work was to take previous work upon cellular reaction to microtopography to a further level. This was to further scale the feature size down to the nanometer scale and to see what if any effect a predetermined topography would have on cell behaviour. This work was novel in the respect that the nanotopography was precisely controlled on a nanometer scale and any effect that was elicited by the topography, could be reproduced exactly.

The major aim of this project was to examine the effects of nanotopography on cell behavior and also what specific aspects of the fabricated topography are influencing cell behavior. Different microcopies were utilised to analyse the cellular response comprising atomic force, light, fluorescence, confocal, scanning electron, and video microcopies.

Chapter 2

Materials and methods

Cell lines

p388D1 Macrophage like cells

p388D1 mouse macrophage were routinely cultured in the Centre for Cell Engineering laboratory, University of Glasgow, but were originally a gift from Prof. P Bongrand, Marseilles.

MDCK cells

Maden Darby Canine Kidney (MDCK) cells for initial experiments were from departmental stock. However, fresh cells were later bought from the European Collection of Cell Cultures catalogue number 84121903 (passage 12) as a growing culture for experimental work. These were expanded at passage 13, then frozen in liquid nitrogen following the manufacturers instructions. For experiments, cells were used at passage 16-30.

Isolation and primary culture of epitenon cells

One male Sprague Dawley rat was anaesthetised using halothane. A small transverse incision was made at the base of the middle digit of the hind paw under tourniquet control. The tendons were then removed for transfer into polystyrene culture dish. Tendons free of attachments to bone and muscle were washed in Ham's serum-free media (Gibco BRL, life technologies, Paisely, UK), then treated with 0.5% collagenase (Clostidiopetidase A; EC

3.4.24.3; Sigma chemical Co., Poole, UK) for 10 minutes at 37°C. The freed cell population was centrifuged at 200g for 6 minutes and plated into Petri culture dishes at a cell density of 1×10^5 cells/ml. Then cells were incubated in culture medium containing a 3:1 (v/w) mixture of DMEM (Gibco) supplemented with 10% tryptose-phosphate broth (Gibco) and Hams F-12 nutrient mixture with 10% calf serum (Gibco-biocult, Paisley, UK) and antibiotics. For experiments, cells were used at passage 5-20.

Cell culture solutions and final media

All solutions, except MDCK cell antibiotic mix, cryopreservant solution and final media, were prepared by Graham Tobasnick and Gordon Campbell, Division of Infection and Immunity, University of Glasgow.

Eagles water

MilliporeTM reverse osmosis (MilliQ RO) purified water that was subsequently autoclaved and stored at 4°C.

Hepes water

1 litre Milli Q RO water plus 5.25 g HEPES (N-2 hydroxyethyl piperazine-N' 2 ethane sulphonic acid) (Sigma) pH adjusted to pH 7.5 and stored at 4°C.

7.5% Bicarbonate

7.5 g Sodium bicarbonate/100 ml distilled water then filter sterilised.

HEPES saline buffer

Sodium Chloride	8 g
Potassium Chloride	0.4 g
D-Glucose	1 g
HEPES	2.38 g
Phenol-Red Sodium Salt	0.1 g

Made to 1 litre with RO water and pH to 7.5

Versene buffer

Sodium Chloride	8 g
Potassium Chloride	0.4 g
D-Glucose Sigma	1 g
HEPES Sigma	2.38 g
Phenol-Red	0.1 g
EDTA (Di Sodium Salt)	0.2 g

Made to 1 litre with RO water and pH to pH7.5

General antibiotics mixture

Glutamine	Gibco	144 mM
Amphotericin	Gibco	11.9 μ M
Penicillin	Gibco	100 μ g/ml
Streptomycin	Gibco	100 U/ml
Bicarbonate	Gibco	7.5% w/v.

PBS

5 Sigma PBS tablets added to 1 litre RO water and pH adjusted to 7.3

ITS (Insulin, Transferrin, Selenite solution)

5 μ g/ml of transferrin (iron saturated), Insulin and 5 ng/ml selenite. Lyophilised transferrin was dissolved in water (pH adjusted to pH3 with acetic acid). The solution was filter sterilised and stored at -20°C.

Trypsin

Sterile trypsin (Gibco) 0.25% w/v was dissolved in HEPES Saline (stored at -20°C). For cell dissociation; 0.5 ml trypsin solution was added to 20 ml versene.

Media recipes

MDCK cell media (MEM)

MEM (Sigma)

Glutamine	Gibco	200 mM final concentration
Streptomycin	Gibco	100 µg/ml final concentration
Penicillin	Gibco	100 U/ml final concentration

Hepes Water		180 ml
HamsF10 10x	Gibco	16 ml
Antibiotics mix		5 ml
Foetal Calf Serum	Gibco	6 ml
ITS		2 ml
Bicarbonate mix		1 ml

(RPMI) for culturing mouse macrophages

HEPES Water		180 ml
RPMI 10x	Gibco	16 ml
Antibiotics mix		5 ml
Calf Serum		20 ml
Bicarbonate mix		5 ml

Methods of routine culture

HGTFN cell culture

HGTFN endothelial cells were cultured at 37°C in 25cm² Falcon tissue culture flasks with Ham's F10 media and were opened on the third day for 10-15 minutes to allow re-oxygenation of the media unless passaged. For subculture, the cells were washed twice with hepes saline (37°C) to remove serum (a trypsin inhibitor) then 5ml trypsin-versene (37°C) was added for 30 seconds to 1 minute (or until cells began to round up) and excess trypsin-versene poured off. The cells were returned to a 37°C hot-room and observed using phase contrast microscopy until detached. Immediately upon detachment, 15ml of Ham F10 + serum (pre-warmed to 37°C) was added to neutralise the trypsin. The cells were then pelleted by centrifugation for 4 minutes at 600g and 4°C. Once pelleted, the supernatant was removed and the cells resuspended in 10ml of Ham F10 then plated in 25cm² tissue culture flasks.

MDCK cell culture

MDCK cells were cultured at 37°C, passaged every three to four days and re-seeded at medium density (approximately 20% flask coverage). Initially, the cells were washed with hepes saline at 37°C. If the cells were nearly confluent, they were incubated in Versene (37°C) for 5 minutes to "loosen" the Ca²⁺ dependent adherens junctions. They were then subcultured by adding 5ml trypsin versene (37°C) (most of which was removed after 10 seconds

leaving a thin film) until detached from each other's sides. They were further incubated for up to 5 minutes or until released from basal adhesion by gently tapping the flask. Following detachment, they were centrifuged, re-suspended in MEM + 10% FCS (37°C) and plated at approximately 10-15% confluence. An additional 5ml of 100% CO₂ was sterile filtered into the flask for buffering.

p388D1

p388D1 macrophage were cultured at (37°C), passaged every 3 days and seeded at approximately 10% confluence. Due to the low adherence of these cells, they were detached from the flask by tapping by hand. The cell suspension was centrifuged at 600g for 4 minutes to pellet the cells, which were resuspended in RPMI media (37°C) and plated into 25cm² tissue culture flasks.

Cryopreservation of stock cells

Cells were detached, centrifuged and resuspended as previously described. Where trypsin was used, the cells were given an additional resuspension. They were then centrifuged and re-suspended in 90% FCS + 10% dimethyl sulfoxide. To reduce the cooling rate, cell suspensions were incubated for four hours at -20°C in a foam surround within a sealed polystyrene box then overnight at -70°C. This method was used as a temporary storage situation

for three-month working stock. Additional vials were transferred to liquid nitrogen for long term storage.

Cell counting

Cell counts were performed using a haemocytometer (Fuchs-Rosenthal ruling). The eight squares volume was 10^{-4} ml. Therefore 32 squares were counted, for better averaging.

Cell seeding on structures

Epitenon cells were seeded directly onto structures in a media droplet (approximately 300 μ l of media with the required cell density) and allowed to attach for 30 minutes (to prevent selective adhesion of a subset of cells). Once the cells had adhered the remaining media was added and the cells incubated for a total of 3 hours and 18 hours (HGTFN cells) or until the diversity of cell morphologies could be assessed (MDCK cells). HGTFN cells were then formalin fixed and stained with Coomassie blue. MDCK cells were video taped for movement analysis. The cell parameters measured are described later.

Cell staining

Coomassie Brilliant Blue

Methanol	225ml
Glacial Acetic Acid	50ml
Water	added to 500ml
Coomassie Brilliant Blue R-250	1.25g

Stirred for 30 minutes and filtered through Whatman number 1 filter paper.

Cells were washed in 1xPBS (pre-warmed to 37°C) and fixed in 4% buffered formalin (37°C) for 5 minutes. They were then washed with 1xPBS and stained with Coomassie Brilliant Blue for 1-2 minutes or until the required stain density was achieved.

Video capture and analysis

Images for MDCK cell movement video were captured at 4x and 10x magnification (Zeiss Axiovert 20 microscope) by CCD camera in SVHS format on a Panasonic time-lapse video recorder. The individual frames were captured on a Macintosh PowerPC Computer fitted with digitising card using NIH Image software. Images were converted to tiff stacks and subsequently, QuickTime movies.

Fluorescent staining reagents and protocol

Formaldehyde Solution (Calcium 1% w/v)

Phosphate Buffered Saline	200 ml
37% formaldehyde	4.32 ml
Sucrose	4 g

Detergent wash

Phosphate Buffered Saline	100 ml
Tween 20	0.5 ml

Blocking agent (For reducing non-specific binding)

Phosphate Buffered Saline	100 ml
Bovine Serum Albumin	1 g

Permeabilising buffer

Water	100 ml
Sucrose	10.3 g
Sodium Chloride	0.292 g
Magnesium Chloride.6H ₂ O	0.06 g
HEPES	0.476 g

pH adjusted to 7.2 Then added

Triton x100 0.5 ml

Antibodies and actin stain

	(Dilution)
Mouse Anti β -Tubulin (Sigma)	1/100
Mouse Anti vinculin (Sigma)	1/100
Anti Vimentin (Sigma)	1/100
Rhodamine Phalloidin (Molecular Probes)	1/100
Biotin Anti-mouse IgG (Vector Laboratories)	1/50
FITC-Streptavidin (Vector Laboratories)	1/50

All antibodies were diluted in "Blocking Agent"

Fixation

Cells were washed in 1x PBS for 3x 5 minutes at 37⁰C. They were then fixed with pre-warmed 4% buffered formaldehyde for 10 minutes at 37⁰C.

The fixative was removed by washing 2x for 5 minutes with 1x PBS.

Cell permeabilising

The PBS was removed and the cells incubated in "Permeabilising Buffer" for 5 minutes at 4⁰C.

The permeabilising buffer was removed and the cells incubated in blocking buffer.

Immunofluorescence and cytoskeletal observation

After 2 and 3 days of culture, the cells on the test materials were fixed in 4% formaldehyde/PBS, with 1% sucrose at 37°C for 15 minutes. When fixed, the samples were washed with PBS, and a permeabilising buffer (10.3 g sucrose, 0.292 g NaCl, 0.06 g MgCl₂, 0.476 g Hepes buffer, 0.5ml Triton X, in 100 ml water, pH 7.2) was added at 4°C for 5 min. The samples were then incubated at 37°C for 5 min in 1% BSA/PBS, followed by the addition of primary antibody (1:100 in 1% BSA/PBS, Sigma, Poole, UK) for 1 h (37°C).

Simultaneously, rhodamine conjugated phalloidin was added for the duration of this incubation (1:100 in 1% BSA/PBS, Molecular Probes, Oregon, USA).

The samples were next washed in 0.5% Tween 20/PBS (5 minutes x 3). A secondary, biotin conjugated antibody, (1:50 in 1% BSA/PBS, monoclonal horse anti-mouse (IgG), Vector Laboratories, Peterborough, UK) was added for 1 h (37°C) followed by washing. A FITC conjugated streptavidin third layer was added (1:50 in 1% BSA/PBS, Vector Laboratories, Peterborough, UK) at 4°C for 30 min, and given a final wash. Samples were then viewed by scanning confocal fluorescence microscope (Noran).

Image acquisition

Images were captured on a NORAN confocal microscope with Metamorph 3 imaging application software. Post capture image analysis and 3D construction was performed using Metamorph 4.5 Windows 98 SE PC and NIH Image on a Macintosh computer.

Polymer casting of master surfaces

Polycaprolactone beads were melted on glass slides heated to 60°C with a temperature controlled hotplate. Once the beads had merged to form one droplet, the surface to be cast was inverted onto the polymer. Following this, another glass slide was put on top and the two slides pressed together. The composite was removed and allowed to cool. The cast surface was then removed by water immersion.

Microscopy

Confocal microscopy

Cytoskeletal images were captured on a NORAN confocal laser-scanning microscope (Middleton, WI) using Metamorph 3 image acquisition software.

Atomic force microscopy sample preparation

All samples imaged were cut with a scalpel blade to a diameter of 13 mm or less, then they were attached to a 13 mm stainless steel puck with an adhesive tab, touching the edges gently with the point of a scalpel to secure to the adhesive. The samples were then transferred using tweezers into the AFM holding bay ready for scanning. The principles of Contact mode operation are contained in figure 2.1.

AFM operation

The machine was set to contact mode for standard operation. A contact mode tip (Digital instruments, Santa Barbara, CA) was then introduced to the sample holder placed approximately 1 to 5 mm above the sample.

The laser contained in the AFM holding bay was aligned to the centre of the tip using x and y control knobs, and then was precisely aligned via the tilt mirror lever located at the back of the holding chamber.

The tip was lowered down to within touching distance of the sample. The tip is was checked visually to assure horizontal positioning to the sample, to position the tip horizontally the front and back height controls were adjusted to facilitate repositioning of the tip.

The tip was engaged automatically using the nanoscope IIIa software command of engage.

The nanoscope IIIa controls were then set as follows:

Feedback controls

Integral gain: 1
Proportional gain: 2
Lookahead gain: 0.00
Deflection set point: 0.00v

Other controls

Microscope mode: Contact
Z limit: 2.00 μm
Units: Metric
Colour table: 9

Channel 1

Data type: Height
Data scale: 100 nm
Line direction: Trace
Realtime plane fit: Line
Offline plane fit: Full
Highpass filter: Off
Lowpass filter: Off

(For an even more detailed operation of this equipment please refer to the Multimode SPM instruction manual Version 4.31ce)

Contact mode operation

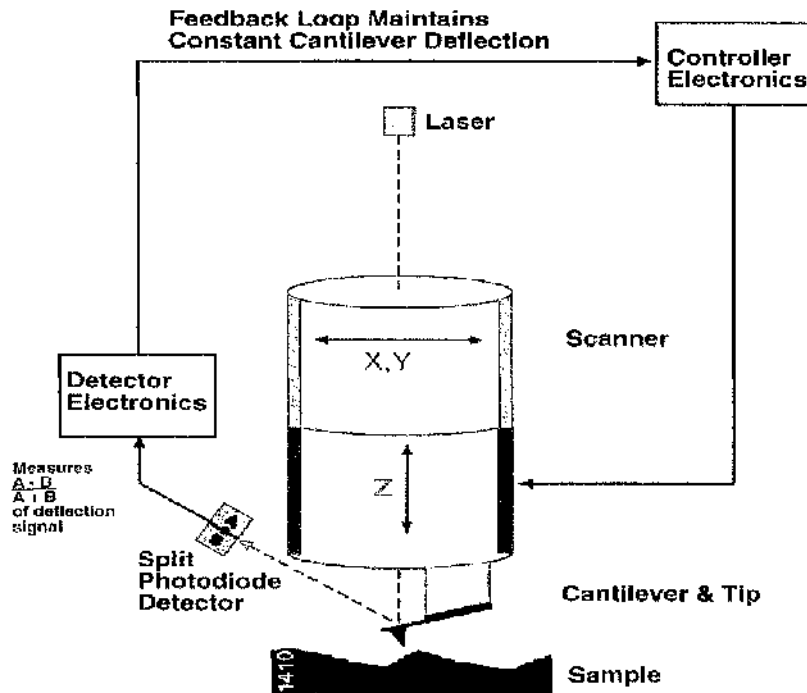


Figure 2.1 Contact mode AFM operates by scanning a tip attached to the end of a cantilever across the sample surface while monitoring the change in cantilever deflection with a split photodiode detector. The tip contacts the surface through the adsorbed fluid layer on the sample surface. A feedback loop maintains a constant deflection between the cantilever and the sample by vertically moving the scanner at each (x,y) data point to maintain a "setpoint" deflection. By maintaining a constant cantilever deflection, the force between the tip and the sample remains constant. (Image taken from Multimode SPM instruction manual Version 4.31ce)

The force is calculated from Hooke's Law: $F = -kx$

- F = Force
- k = spring constant
- x = cantilever deflection.

Force constants usually range from 0.01 to 1.0 N/m, resulting in forces ranging from nN to μ N in an ambient atmosphere. The distance the scanner moves vertically at each (x,y) data point is stored by the computer to form the topographic image of the sample surface.

Fabrication of quartz master surface

Electron beam lithography

The fused silica masters for the embossing process were produced using electron beam lithography and reactive ion etching. The fused silica substrates were 25 x 25 mm and consisted of 5 x 5 mm² areas of nanometre-scale pillars. Electron beam lithography was carried out using a Leica Micro- Systems Lithography EBPG 5HR beamwriter (Bannockburn, IL) on fused silica samples, 1 mm thick. The substrates were cleaned before use by refluxing in Opticlear (Kimble, Vineland, NJ) 30 minutes prior to successive ultrasonic rinses in acetone, methanol and reverse osmosis (RO) water. A 50 nm thick titanium layer was then deposited using an electron beam evaporator. This titanium film acts as a charge conduction layer during lithography and also as an intermediate etch layer during reactive ion etching (Elvenspoek et al., 1998). Prior to application of the resist, hexamethyldisilazane primer was spun onto the samples at 3000 rev. / min for 1 min before baking at 80°C. The pattern was specified using Shipley WIII DUV resist (Delmar, MD) which was applied to the substrates by spin coating at the same speed for 1 minute. The samples were then soft-baked on a hotplate at 135 °C for 1 minute. The electron beam lithography patterns needed to form the pillars were arrays of nanometre-scale circles. This was necessary in order to ensure that metallisation and lift-off resulted in arrays of metal pillars. The patterns were written using the beamwriter to write a large square area using a small beam spot size and a large pixel step size. For example, if a 15 nm spot is used to

write a square of side 150 nm, then the square is written using a raster scan method with the distance that the spot moves between exposures being set by the pixel step size. Therefore, if the pixel step size is set to 300 nm, then the 15 nm spot exposes the resist every 300 nm, producing arrays of dots on a 300 nm pitch. The actual dot size obtained depends on the dose and the beam spot size used. Using this method, the patterns were written using doses ranging from 2 to 30 $\mu\text{C}/\text{cm}^2$ and spot sizes from 15 to 56 nm. This produced dot sizes ranging from 60 to 150 nm. Development was carried out using Shipley CD26 developer at room temperature for 1 minute followed by rinsing in RO water. A 30 nm-thick layer of NiCr (60:40) was then evaporated onto the substrates and lifted off in acetone to define the nickel-chromium pillars on the titanium-coated fused silica. After lifting off the nickel-chromium film, the samples were dry etched to define the pillars in titanium and then in silica. The intermediate titanium layer was etched away using chlorine chemistry in an Oxford Instruments Plasmalab System 100 reactive ion etcher (Oxford, UK). SiCl_4 was used with a flow rate of 18 sccm at a pressure of 10 mTorr, 200 W RF power and a DC bias of -325 V. The removal of the titanium etch took 6 minutes at an etch rate of 8 nm/minute. The nickel-chromium pattern masks the titanium during this process, thus leaving a NiCr/Ti bi-layer mask for the quartz etching. The silica was etched in CHF_3 using a Plasma Technology BP80 RIE machine (Oxford, UK) with a flow rate of 30 sccm, a pressure of 23 mTorr, RF power and a DC bias of 310 V. The silica was etched for 3 minutes at an etch rate of 8 nm/minute and gave a final etch depth of approximately 100 nm (See figure 2.2 for diagrammatical representation of fabrication process).

Fabrication of topography

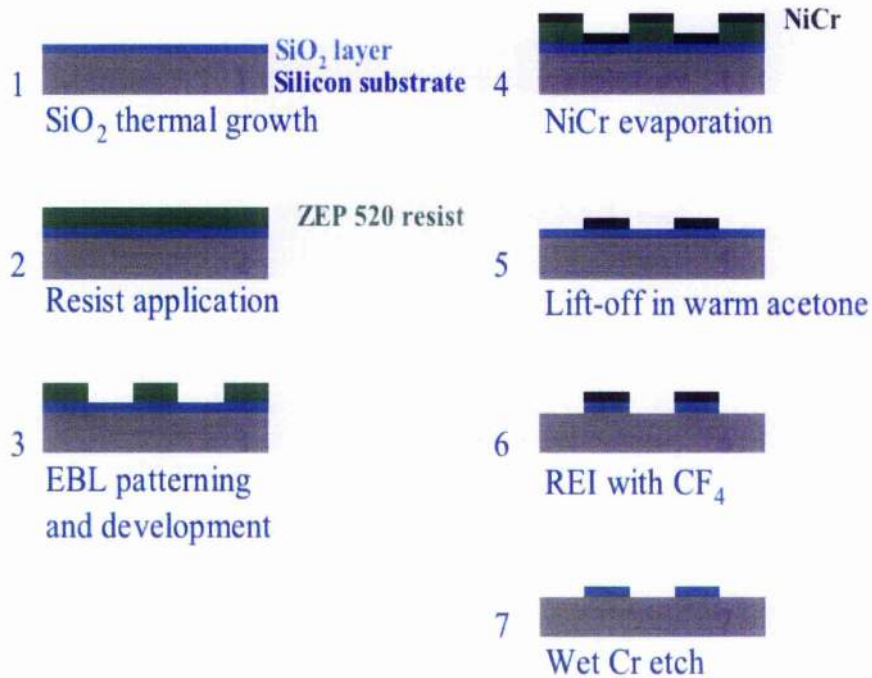


Figure 2.2 Diagram of electron beam lithography process for fabricating nanopillared master surfaces used in this thesis. This is the schematic representation of the lithographic process in detailed in full in the fabrication of quartz master surface section of Chapter2.

Poly-l-lysine coating of polymer surfaces

Surfaces with and without nanotopography were coated with poly-l-lysine, which was incubated at a concentration of 0.1% w/v, in water. 1 μ l of the poly-l-lysine solution was diluted with 1ml phosphate buffered saline. Then 5ml of the resulting solution was added to each sample and was then incubated for 15 minutes at 17°C.

SEM freeze-drying

Freeze-drying of the cryosections took place in a Baltec BAF 060 (Balzers, Liechtenstein) freeze-etch unit. The grids were transferred to the recipient at -160°C. The freeze-drying protocol was carried out at pressures around 6×10^{-8} mbar and proceeded as follows: -145°C (1 hour), -135°C (2 hours), -125°C (2 hours), -115°C (8-12 hours), -105°C (2 hours), -95°C (2 hours), -85°C (2 hours), -60°C (1 hour), -40°C (1 hour). The samples were then coated at -40°C with 8 nm carbon by an electron beam heated gun at an elevation angle of 60° and under rotation of the specimen stage (120 turns/min) to get a stable carbon coverage on all surface areas, then slowly warmed up to room temperature (0.5 hours). Samples that were not immediately transferred to the electron microscope were stored in a closed box containing drying beads until use on the same or the next day.

Chapter 3

Fabrication and initial investigation of the cellular reaction to defined nanotopography

Introduction

Topographical cues, independent of biochemistry, generated by the extracellular matrix (ECM) may have significant effects upon cellular behaviour. The topography of the basement membrane is a complex meshwork of pores, fibres, ridges and other features of nanometre sized dimensions (Flemming, et al., 1999). It is an established and well documented fact, that synthetic surfaces with topographical features have been shown to directly influence cell behaviour (as reviewed in Curtis and Clark, 1990; von Recum and van Kooten, 1995; Curtis and Wilkinson, 1997; Svinghi et al., 1994). Consideration of this fact leads to the hypothesis that the topography of the basement membrane plays an important role in regulating cell behaviour in a manner distinct from that of the chemistry of the basement membrane.

As early as 1962 and 1963 Rosenberg claimed (Rosenburg, 1962 and 1963), that nanometre sized features influenced cells. He used monolayers of stearic and behenic acids that were transferred to quartz slides by the Blodgett technique. Troughs of different depths were cut into these multilayers, and additional monolayers were superimposed. When embryonic cells were cultured on these substrata, the cells were entrapped within troughs whose depths were as small as 6 nm. The results demonstrate cell guidance by alterations in mono-molecular films. Despite such early work on features in the nanometre range, little work had been carried out at the nanometric scale

until the following decades (Flemming, et al., 1999). The reason for this was primarily due to the limitations of the fabrication methods that were available to bioengineers. Recently significant work in this field has moved from the study of cellular behaviour on micrometric grooves, to behaviour on nanometric grooved substrata.

However the emphasis of this thesis is on what effects regular pitted or pillared nanotopography has upon cell behaviour. The first credible adventure into the world of nanometric topography was an investigation into a microporous filter that was nylon dip-coated (Campbell and von Recum, 1989). The size of these pores ranged from 200 nm to 10 μ m in diameter (depth not listed). The experiments were conducted in an *in vivo* canine model. Results showed that the implants were non-adherent contracting capsules around implants with pore sizes below 500 nm. In terms of *in vitro* studies involving nanotopography, Konnonen (Kononen et al., 1992) used titanium substrates that were treated by electro-polishing, etching, and sandblasting to create a random surface roughness with peak to valley heights of 140 nm, 410 nm and 800 nm respectively. The random nanotopography made by sandblasting, prevented cells from spreading and from forming actin bundles and vinculin-containing focal adhesions.

It was not until 1997 that Turner (Turner et al., 1997) employed the use of reactive ion etching followed by photolithographic and isotropic wet etching in the fabrication process to modify silicon surfaces for biological ends. Transformed rat astrocytes and primary rat cortical astrocytes were used to study the cellular interaction with nanotopography and the underlying chemistry that was created by the fabrication process. Transformed cells

attached preferentially to wet etched regions rather than reactive ion etched silicon grass; transformed cells on the wet etched area, spread in an epithelial-like manner and were smooth; transformed cells on columnar regions were loosely attached, and exhibited complex surface projections. Transformed cells preferred areas exposed to increasing amounts of wet etching; primary rat cortical astrocytes preferred silicon grass of the reactive ion etched areas and did not spread on wet etched area.

Previous studies on the interactions of cells to nanotopography were taken to another level employing electron beam lithography to define the substratum topography (Casey et al., 1997). This work was pioneered by Casey et al. (1997) who made substrates that had a new feature missing from previous studies, in having precise control of surface roughness. This method of fabrication made it possible to define surfaces with a high degree of accuracy so that these topographies could give a defined assessment of cell adhesion and motion on nanotopographic surfaces. The reaction of two different cell types: 'macrophage like' (P388D1) and fibroblasts (tendon epitenon) were assessed on 15 nm and 60 nm diameter pillars. The results of the cell adhesion experiments demonstrated that the presence of these pillar arrays of either size seriously hinder cell adhesion to the surface.

This seminal work on precisely defined and controlled nanotopography was the driving force behind the initial experiments in this chapter. The aim of these preliminary studies was to investigate how to fabricate nanostructures into a polymer reliably and overcome fabrication problems with the previous method. The problems previously encountered were related to the microcracking of the polystyrene surfaces during the fabrication process,

which added an unwanted topography. Several surfaces were accurately manufactured. Epitenon cell adhesion at various time points was investigated, and whether general cell adhesion to nanotopography was cell specific. Also addressed in this chapter were the effects of topographies manufactured with varying polymers. Polycaprolactone (PCL) polyurethane and polystyrene were used to investigate this question.

Nanostructures used in all of these experiments had nanopits of a dimension of approximately 80 nm deep with a centre to centre spacing of 300 nm.

Results

Fabricating nanotopographical structures in polycaprolactone.

The motivation behind this work was to produce ordered well-defined nanostructures in a suitable biocompatible polymer. The goal of this work was to develop suitable surface modifications to control the long-term behaviour of cells on the surface of an implanted device.

The fabrication of the quartz master surface (Fig 3.1) was detailed in Materials and Methods (Chapter 2). The quartz surface used in the initial experiments had pillar features with a centre to centre spacing of 300 nm and an overall height of 80 nm. This surface was used as a template to replicate in reverse the nanofeatures into a suitable polymer substrate. Polycaprolactone was chosen due to its favourable attributes. It has FDA approval, has a low melting point of around 68°C, is biocompatible, and biodegradable.

Initial experiments were carried out by dissolving polycaprolactone pellets in chloroform (5% w/v). This allowed the polymer to be solvent cast at room temperature. The AFM scan (Fig 3.2) shows the replication of the nanostructure in the polymer to be accurate and true down to a few nanometres.

This method for fabricating nanostructures was adequate for producing reliable structures. However this method did have its drawbacks for use in cell biology experiments; the time taken of 40 minutes per structure was impinging on production of large amounts of nanostructure, and also the optical properties of the polymer were not suitable for viewing live cells. This was due to the opaque nature of the polymer due to crystallite formation,

furthermore the solvent cast films were very thin and had a tendency to roll up and float. It was necessary to formulate a novel method of structure fabrication to overcome these problems. Melt moulding was seen to be the answer to the constraints of the polymer casting method.

The melt moulding method is based on the premise that ordered polymer chains would result in a polymer with a transparent appearance, as opposed to the typical crystallite formation, which would scatter light and yield a translucent polymer. Crystallite formation needs mobility of the polymer chains, therefore cooling it fast enough would prohibit rearrangement, 'freezing' the polymer in its transparent state (Richle et al., 2002).

Detailed method for producing super cooled PCL embossed nanostructures

1. Polycaprolactone beads were washed in methanol for 21 days. (Washing in methanol removes residue that coats PCL beads).
2. Beads were then spaced on a grid 10 mm apart, in between two glass plates, clamped with bulldog clips and placed in an oven at 60°C overnight.
3. Glass plates were removed from the oven, left to cool at room temperature, and separated to leave an even sheet of PCL.
4. Sheet of polymer was then cut into 25 mm x 25 mm sections

5. The polymer section was placed on a standard microscope slide heated on a hot plate to a temperature of 60°C. When the polymer was molten the surface of the quartz master was pressed into the molten polymer with the thumb.
6. Two Copper discs were then placed in liquid N₂ until cooled.
7. The molten polymer, slide and master surface were sandwiched between the 2 copper discs. (The cooling of the polymer takes around 10 seconds to complete).
8. The polymer was then transferred to a beaker containing 100ml of RO water (the RO water is necessary due to its purity and is key as acting as a primitive but effective mould release agent).

The apparatus used in this method is detailed in figure 3.3. It can be quite clearly shown that there are some major benefits to this procedure. In figure 3.4 a comparison of the 2 surfaces is shown. The clear polymer has been supercooled by the copper discs.

To fabricate structures that are not required to be transparent *i.e.* for experiments that do not require cells to be imaged in their live state, steps 6 and 7 can be omitted from the protocol and the molten polymer construct can then be emmersed straight into the RO water for separation.

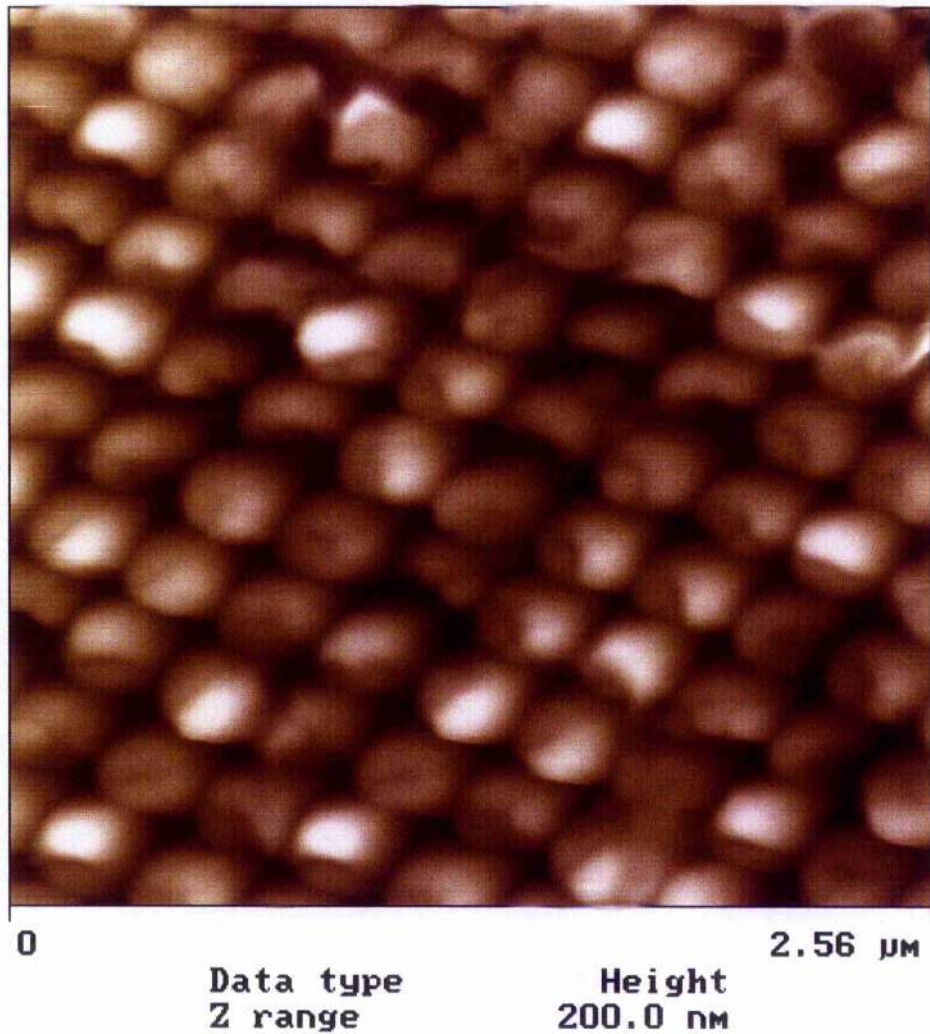


Figure 3.1 Quartz nanostructure fabricated by electron beam lithography (detailed in Chapter 2). It should be noted that the top of the nanostructure is not rounded and is slightly different from pillar to pillar. The spacing of 300 nm centre to centre is constant as is the 80 nm height of each pillar. Image obtained via atomic force microscopy in the contact mode. The tops of the pillars are uneven; this is thought to be due to a fabrication artefact coupled with wear caused by the embossing process.

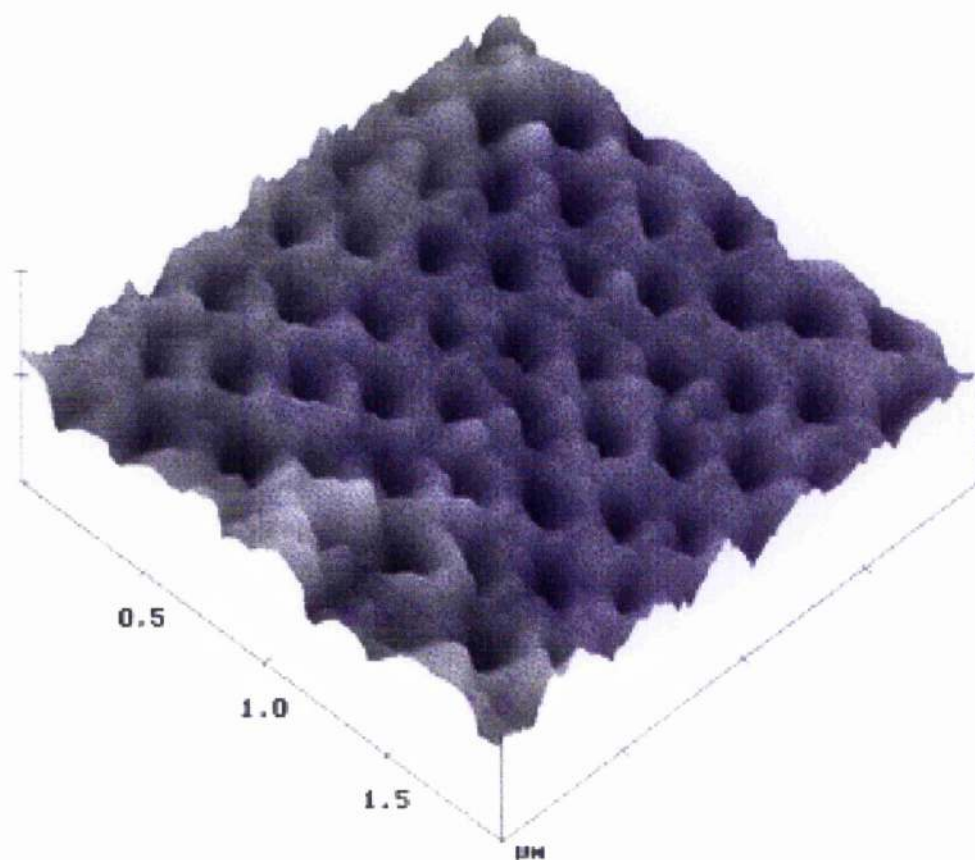


Fig 3.2. An array of pits at a 300 nm centre to centre spacing, with an average depth of 80 nm in polycaprolactone. This is a typical example of a polycaprolactone nanopitted topography revealed by atomic force microscopy (contact mode). This method of fabrication (polymer casting) was used for initial experiments detailed in this chapter. A quicker method of melt moulding was employed for the remainder of the work. All experiments where polymer casting was used are directly referred to. In all other cases, it will be assumed that melt moulding was used.

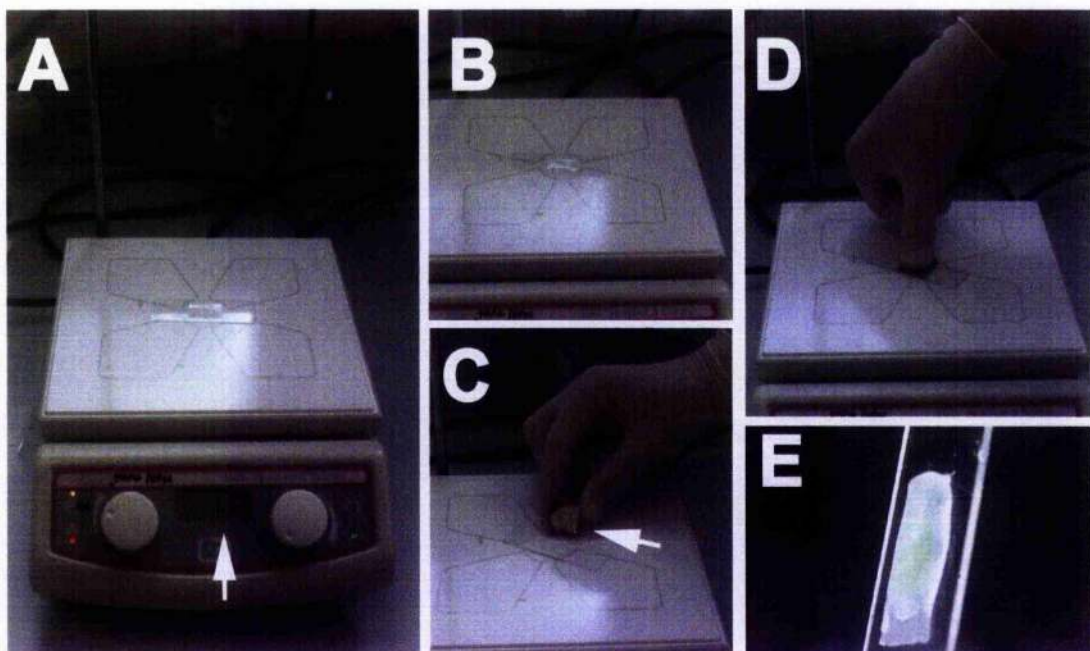


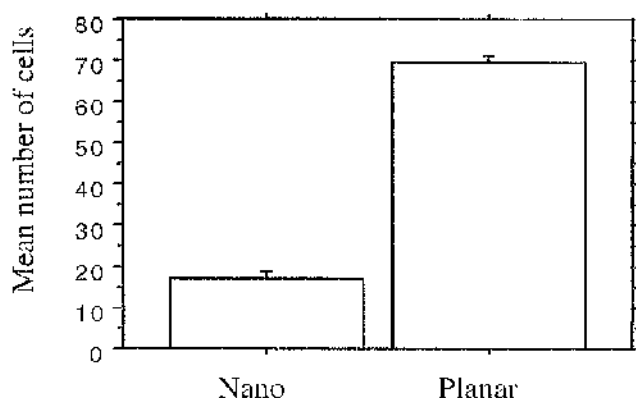
Figure 3.3 Apparatus used for melt moulding of polycaprolactone nanostructures. Panel A shows the hotplate used in the process. Part B shows the glass slide with PCL section at melting temperature. Panel C contains an image of the nickel shim with a nano-patterned surface. Panel D is the embossing process where pressure is applied to the nickel shim in a downward motion, exerting enough force to evacuate air bubbles between shim and polymer. Panel E shows the reversed embossed PCL replica. The Opalescent appearance of the nanostructured surface indicates successful replication of nanostructure due to refraction of light by the 80 nm layer of intermediate refractive index, formed by the ordered nanostructures which gives rise to interference.

Epitenon cell adhesion to nanotopography at various times

Epitenon cells were cultured upon polycaprolactone nanopitted surfaces with dimensions of 80 nm deep with a centre to centre spacing of 300 nm, made by reverse casting from PCL dissolved in chloroform (Fig 3.1). The primary hypothesis of how cells would react to the topography concerned how the cells would react to the regular topography of the nanopitted region, it was conceived that the cells extracellular matrix could possibly be influenced by the substrate and thus have an ordered pattern imparted upon it. This however was merely speculative and with hindsight appears fanciful.

The number of cells that adhered to the nanopitted areas was assayed via counts of cells adhering to the nanopitted region were directly compared to the numbers of cells cultured upon a planar topography. The following results show that adhesion of epitenon cells to the nanopitted topography was significantly reduced after 4, 20 and 96 hours (figures 3.4 to 3.6) and in some cases, almost non-existent after 21 days (figure 3.7) when compared to planar topographies. The conclusions that can be drawn from these experiments are manifest; cell adhesion is greatly reduced when cells encounter this type of ordered nanotopography with these specific dimensions. Therefore the topographic cue is directly influencing cell behaviour to the extent that, with time, epitenon cells find it almost impossible to adhere to this specific nanotopographic substrate.

Number of rat epitenon fibroblast cells adhering to planar and nanotopographic surfaces after 4 hours

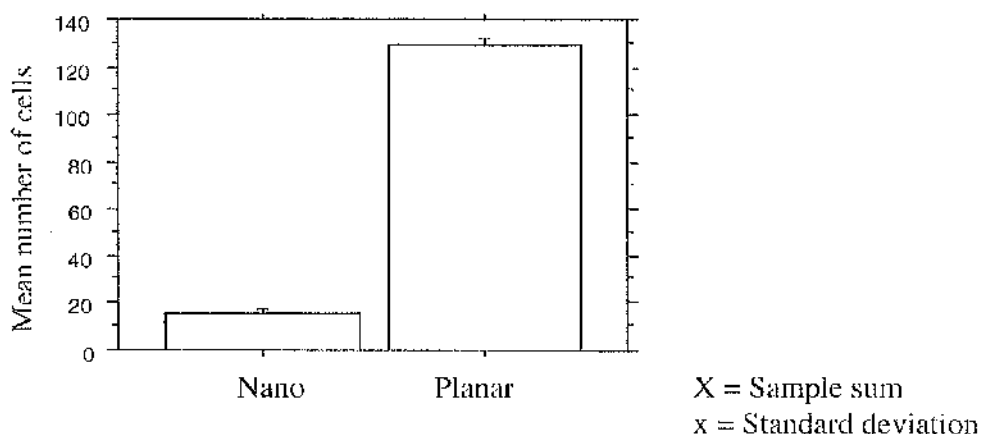


X = Sample sum
x = Standard deviation

	Nano	Planar		Nano	Planar
Mean	17	70	Max	25	81
Std Dev	4	4	Min	10	59
Std Error	1	1	ΣX^2	14031	218616
Count	45	45	Σx^2	754	1390

Figure 3.4 Cell adhesion of rat epitenon fibroblasts to nanopitted and planar polycaprolactone after 4 hours. Cell adhesion upon nanotopography was significantly different ($P < 0.0001$) when compared to adhesion of epitenon cells to a planar topography (Counting area 1.65 mm^2). Means of counts for 30 areas.

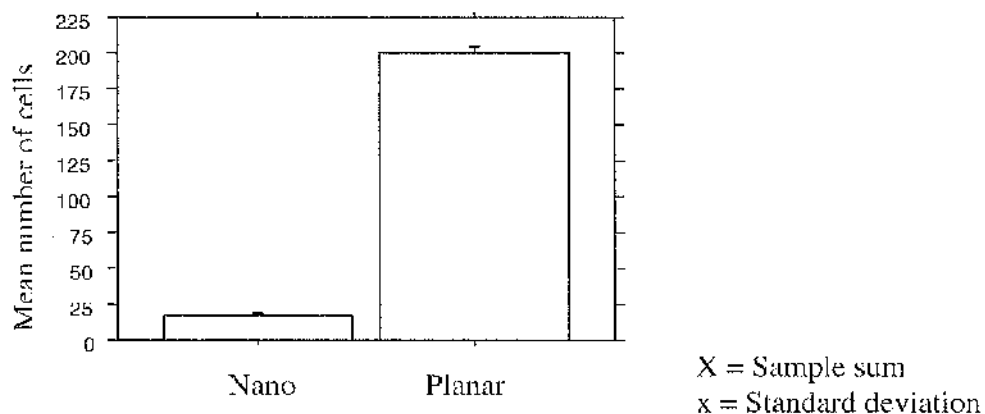
Number of rat epitenon fibroblast cells adhering to planar and nanotopographic surfaces after 20 hours



	Nano	Planar		Nano	Planar
Mean	16	129	Max	25	147
Std Dev	4	8	Min	10	115
Std Error	1	1	ΣX^2	12038	755270
Count	45	45	Σx^2	957	3071

Figure 3.5 Cell adhesion of rat epitenon fibroblasts to nanopitted and planar polycaprolactone after 20 hours. Cell adhesion upon nanotopography was significantly different ($P < 0.0001$) when compared to adhesion of epitenon cells to a planar topography (Counting area 1.65 mm^2). Means of counts for 30 areas.

Number of rat epitenon fibroblast cells adhering to planar and nanotopographic surfaces after 96 hours



	Nano	Planar		Nano	Planar
Mean	17	200	Max	23	222
Std Dev	4	11	Min	10	181
Std Error	1	2	ΣX^2	13386	1805096
Count	45	45	Σx^2	755	5096

Figure 3.6 Cell adhesion of rat epitenon fibroblasts to nanopitted and planar polycaprolactone after 96 hours. Cell adhesion upon nanotopography was significantly different ($P < 0.0001$) when compared to adhesion of epitenon cells to a planar topography (Counting area 1.65 mm^2). Means of counts for 30 areas.



Figure 3.7 Coomassie blue stained cells after 21 days on nanofeatured Polycaprolactone (solvent cast); 150 nm diameter, 300 nm centre to centre spacing, 80 nm deep pits, see fig 3.1 for AFM scan of surface. The broken line indicates the border of the nano-featured area. The planar region is to the righthand side of the vertical dotted line and the region above the horizontal dotted line. Scale bar = 200 μm

In this image the reaction of epitenon cells to the two opposing topographies is markedly different between the two opposing topographies. Epitenon cells cultured on the planar topography have formed a confluent layer, whereas the nanopitted region has very few cells attached to this type of ordered topography.

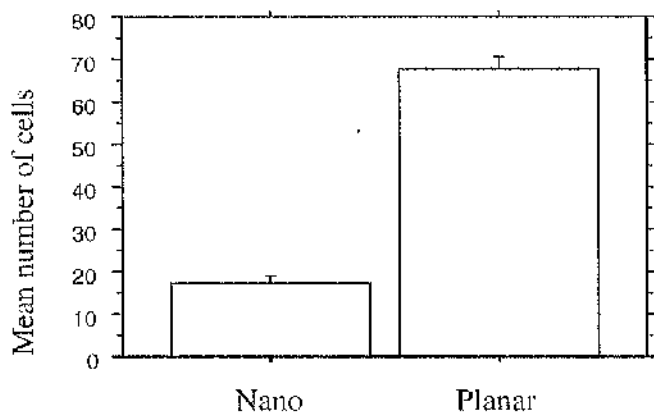
BHK 21, B10D2, and HGTFN adhesion to nanopitted topography after 4, 20, and 96 hours

It was necessary to establish that the reduced adhesion of cells to the nanopitted topography was not a cell type specific phenomenon. To address this question a selection of 'in house' cell types (BHK 21, B10D2, and HGTFN) were used and cultured for 4, 20 and 96 hours upon a polycaprolactone nano-patterned and planar substrate. The results detailed in Figure 3.8 to 3.14 clearly show that the observations of significantly reduced cell adhesion with epitenon cells were not cell specific. The endothelial, fibroblast and macrophage-like cell lines have significantly different patterns of cell adhesion to one another (by means of an ANOVA post-hoc testing), further increasing the scope of the nanotopography's potential use.

These experiments were crucial in showing that the non-adhesive behaviour of epitenon cells was not cell type specific and demonstrates the propensity of the nanopitted topography in being able to lower cell adhesion, in many other cell types. This was crucial in establishing whether the surface was interchangeable in a tissue engineering context, demonstrating its effect was widespread amongst these specific cell types. The different cell types that were cultured upon the nanopitted topography were by no means a comprehensive collection of different cell types but do go some way to suggest that this would provide a suitable surface for a tissue engineering construct that required low or no cell adhesion. These experiments highlight the possible use for this surface pattern, produced in PCL, being utilised upon

a cell engineering construct surface, as a means to reduce cell adhesion in a defined and controllable manner.

Number of BHK 21 Cells adhering to planar and nanopitted topography after 4 hours

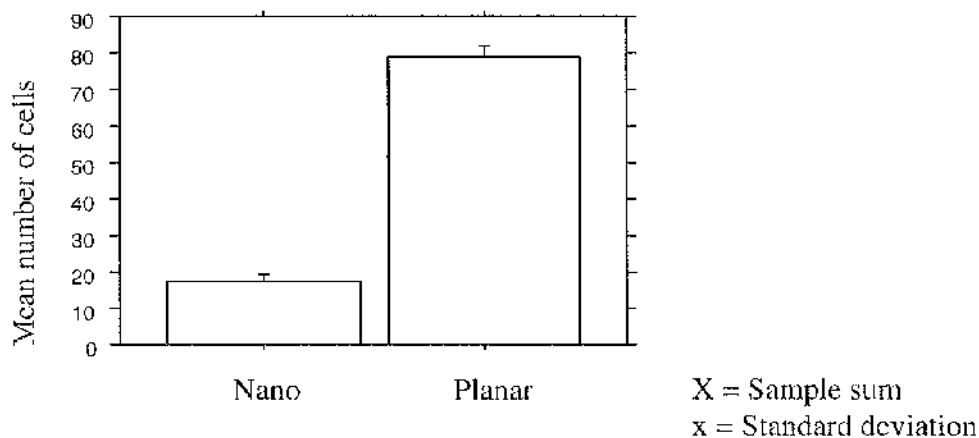


\bar{X} = Sample sum
 s = Standard deviation

	Nano	Planar		Nano	Planar
Mean	17	68	Max	29	82
Std Dev	5	6	Min	9	29
Std Error	1	1	ΣX^2	13882	204380
Count	44	44	Σx^2	962	1740

Figure 3.8 Cell adhesion of BHK 21 cells to nanopitted and planar polycaprolactone after 4 hours. Cell adhesion upon nanotopography was significantly different ($P < 0.0001$) when compared to adhesion of BHK 21 cells to a planar topography (Counting area 1.65 mm^2). Means of counts for 30 areas.

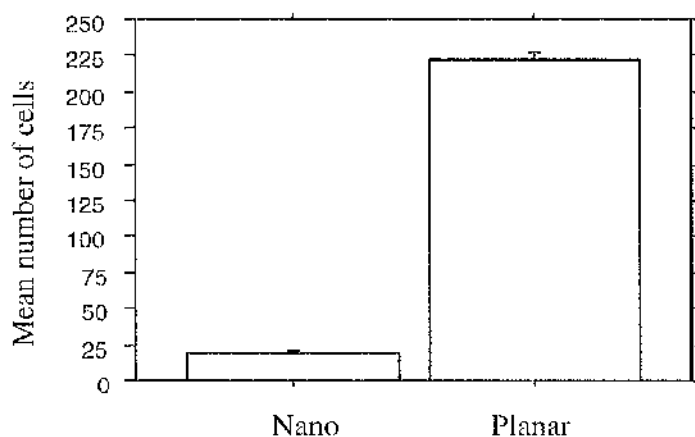
Number of BHK 21 Cells adhering to planar and nanopitted topography after 20 hours



	Nano	Planar		Nano	Planar
Mean	18	79	Max	26	93
Std Dev	4	8	Min	11	62
Std Error	1	1	ΣX^2	14440	274429
Count	44	44	ΣX^2	760	2511

Figure 3.9 Cell adhesion of BHK 21 cells to nanopitted and planar polycaprolactone after 20 hours. Cell adhesion upon nanotopography was significantly different ($P < 0.0001$) when compared to adhesion of BHK 21 cells to a planar topography (Counting area 1.65 mm^2). Means of counts for 30 areas.

Number of BHK 21 Cells adhering to planar and nanopitted topography after 96 hours

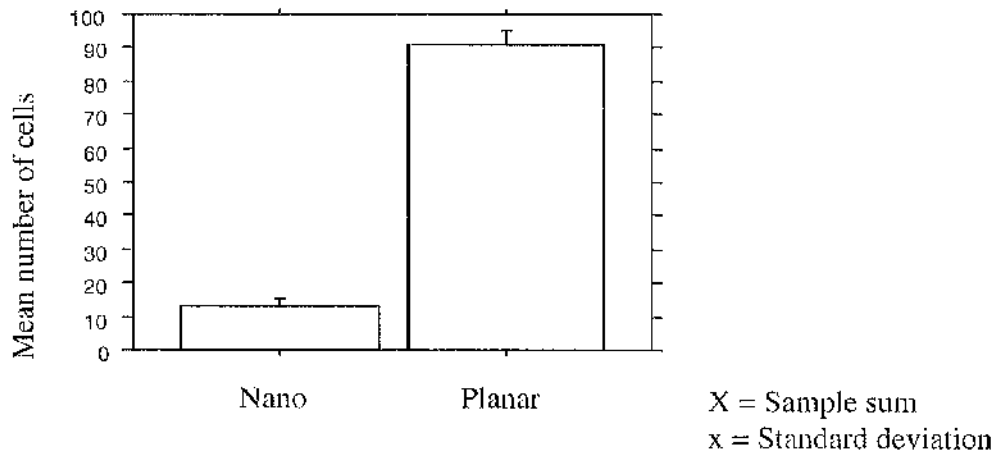


\bar{X} = Sample sum
 s = Standard deviation

	Nano	Planar		Nano	Planar
Mean	19	222	Max	29	245
Std Dev	4	15	Min	11	195
Std Error	1	2	ΣX^2	15796	2168393
Count	44	44	Σx^2	672	9221

Figure 3.10 Cell adhesion of BHK 21 cells to nanopitted and planar polycaprolactone after 96 hours. Cell adhesion upon nanotopography was significantly different ($P < 0.0001$) when compared to adhesion of BHK 21 cells to a planar topography (Counting area 1.65 mm^2). Means of counts for 30 areas.

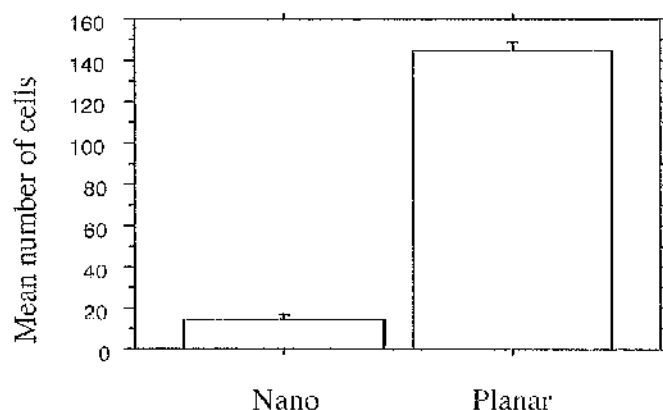
Number of HGTFN endothelial cells adhering to planar and nanopitted topography after 4 hours



	Nano	Planar		Nano	Planar
Mean	13	91	Max	22	116
Std Dev	5	10	Min	3	73
Std Error	1	2	ΣX^2	8672	367967
Count	44	44	Σx^2	1028	4513

Figure 3.9 Cell adhesion of HGTFN cells to nanopitted and planar polycaprolactone after 4 hours. Cell adhesion upon nanotopography was significantly different ($P < 0.0001$) when compared to adhesion of HGTFN cells to a planar topography (Counting area 1.65 mm^2). Means of counts for 30 areas.

Number of HGTFN endothelial cells adhering to planar and nanopitted topography after 20 hours

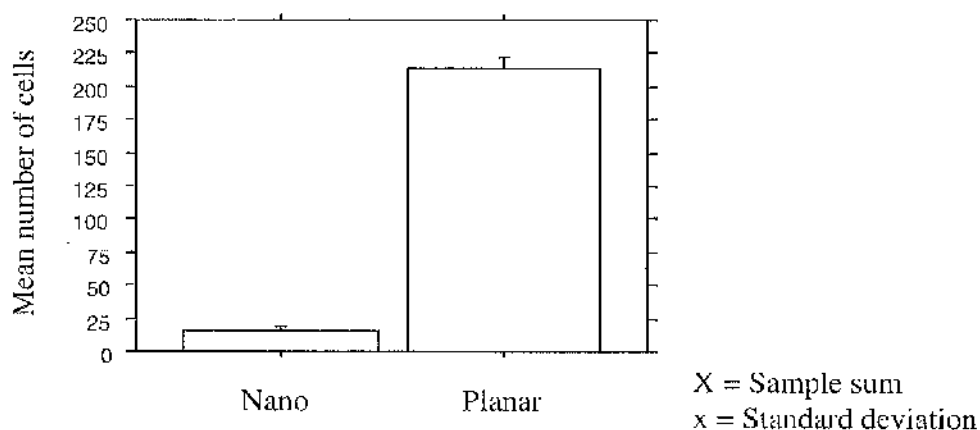


X = Sample sum
 x = Standard deviation

	Nano	Planar		Nano	Planar
Mean	15	145	Max	25	170
Std Dev	5	11	Min	2	127
Std Error	1	2	ΣX^2	10480	928979
Count	44	44	Σx^2	1180	4749

Figure 3.10 Cell adhesion of HGTFN cells to nanopitted and planar polycaprolactone after 20 hours. Cell adhesion upon nanotopography was significantly different ($P < 0.0001$) when compared to adhesion of HGTFN cells to a planar topography (Counting area 1.65 mm^2). Means of counts for 30 areas.

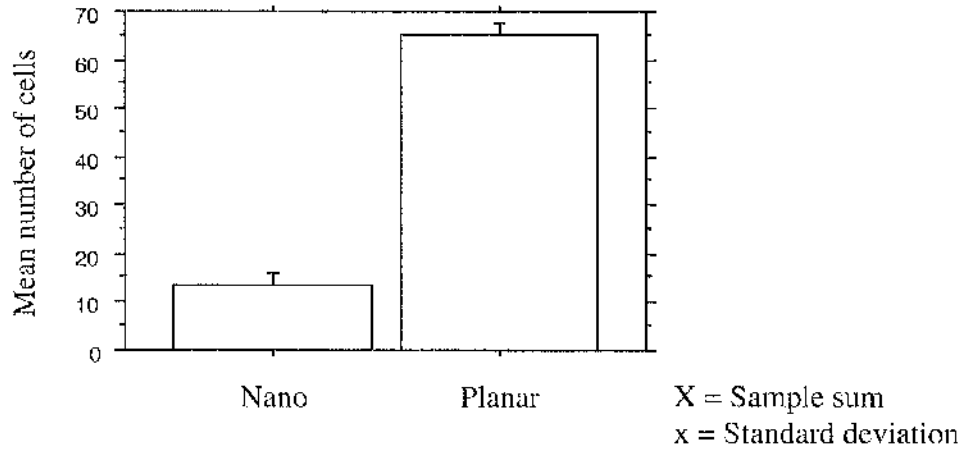
Number of HGTFN Cells adhering to planar and nanopitted topography after 96 hours



	Nano	Planar		Nano	Planar
Mean	16	213	Max	32	259
Std Dev	8	22	Min	3	179
Std Error	1	3	ΣX^2	15010	2012764
Count	44	44	Σx^2	3106	20812

Figure 3.11 Cell adhesion of HGTFN cells to nanopitted and planar polycaprolactone after 96 hours. Cell adhesion upon nanotopography was significantly different ($P < 0.0001$) when compared to adhesion of HGTFN cells to a planar topography (Counting area 1.65 mm^2). Means of counts for 30 areas.

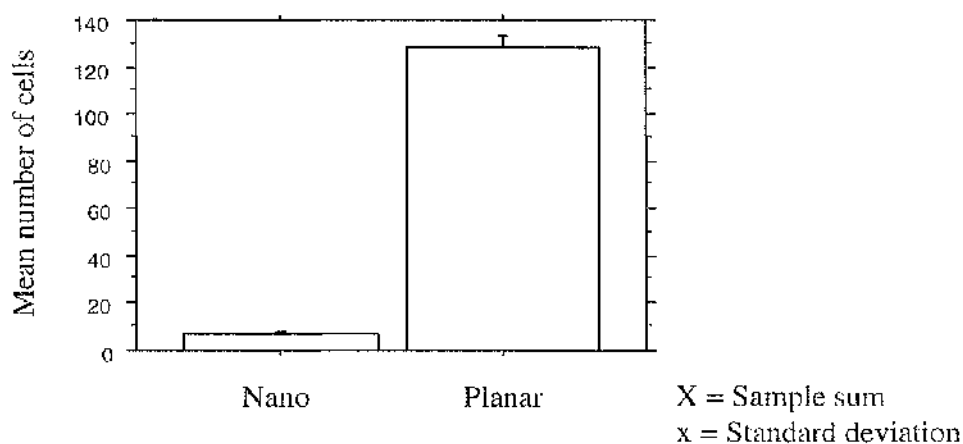
Number of B10D2 endothelial cells adhering to planar and nanopitted topography after 4 hours



	Nano	Planar		Nano	Planar
Mean	13	65	Max	29	79
Std Dev	7	6	Min	3	50
Std Error	1	1	ΣX^2	100013	187745
Count	44	44	Σx^2	2083	3832

Figure 3.12 Cell adhesion of B10D2 cells to nanopitted and planar polycaprolactone after 4 hours. Cell adhesion upon nanotopography was significantly different ($P < 0.0001$) when compared to adhesion of B10D2 cells to a planar topography (Counting area 1.65 mm^2). Means of counts for 30 areas.

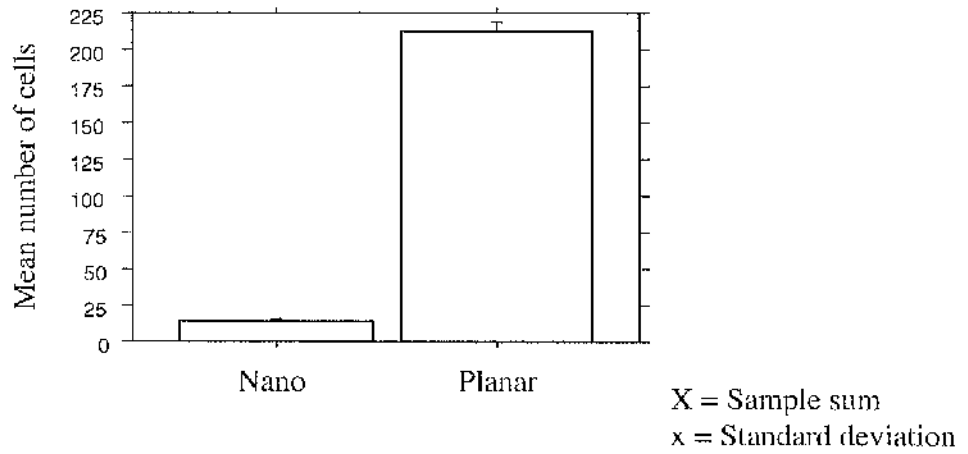
Number of B10D2 endothelial cells adhering to planar and nanopitted topography after 20 hours



	Nano	Planar		Nano	Planar
Mean	7	3	Max	14	148
Std Dev	3	12	Min	2	95
Std Error	1	2	ΣX^2	2265	728581
Count	44	44	Σx^2	319	6405

Figure 3.13 Cell adhesion of B10D2 cells to nanopitted and planar polycaprolactone after 20 hours. Cell adhesion upon nanotopography was significantly different ($P < 0.0001$) when compared to adhesion of B10D2 cells to a planar topography (Counting area 1.65 mm^2). Means of counts for 30 areas.

Number of B10D2 endothelial cells adhering to planar and nanopitted topography after 96 hours



	Nano	Planar		Nano	Planar
Mean	14	213	Max	24	237
Std Dev	6	15	Min	2	178
Std Error	1	2	ΣX^2	9675	1998714
Count	44	44	Σx^2	1527	10146

Figure 3.14 Cell adhesion of B10D2 cells to nanopitted and planar polycaprolactone after 96 hours. Cells adhesion upon nanotopography was significantly different ($P < 0.0001$) when compared to adhesion of B10D2 cells to a planar topography (Counting area 1.65 mm^2). Means of counts for 30 areas.

Cell adhesion to polystyrene, polyurethane and polycarbonate fabricated structures

It was hypothesised that the significantly reduced adhesion observed on the nanopitted region may be due to polymer specificity imparting an effect that was influencing cell behaviour, and indeed not the topography at all. To test this hypothesis I fabricated the nanotopography in a variety of polymers to test whether the effect that was observed was due to the topographical cue generated purely by surface shape or polymer type. As opposed to that of a cue generated by somehow changing the surface chemistry, to impart what would be a purely 'chemical cue' to reduce adhesion.

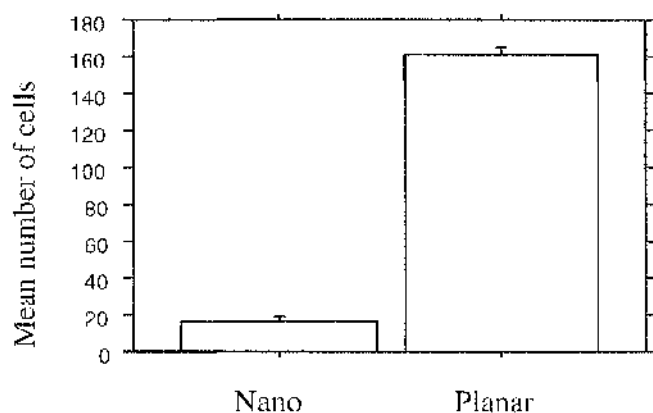
Polystyrene was the first polymer to be chosen, due to its universal use as the primary polymer for culturing tissue cells. The polymer was dissolved in chloroform, and the solution was then solvent cast onto the master surface. In a previous study polystyrene had been used by Casey et al., (1997) for cell adhesion studies. One drawback of polystyrene, for laboratory casting, was the tendency for the polystyrene to micro-crack, resulting in an intermittent topography. This was due to the manual separation of the polymer from the master. However, this could be avoided by leaving the polymer to free itself from the master overnight in RO water. The data in Figure 3.15 showed that cell adhesion of epitenon cells was significantly reduced after a 96-hour incubation period.

Polyurethane is an in-house polymer that is used for polymer casting, and has also been used in clinical trials by Aortec Ltd (personal communication),

Glasgow, UK. as a possible material for tri-leaflet heart valves. This made this polymer relevant for use due to its industrial applications.

Polycarbonate is a relatively new type of polymer to use *in vitro*. This was chosen for three principal reasons; firstly it has very good optical properties making it very desirable for use in a cell culture environment, secondly its widespread use in DVD production means that its properties for precise high level fabrication have already been established by the electronics industry. And thirdly, its relative cheapness of fabrication due to the scaling-up for mass production, which has already been implemented by many sectors of industry.

Number of Epitenon cells adhering to Polystyrene nanostructures after 48 hours

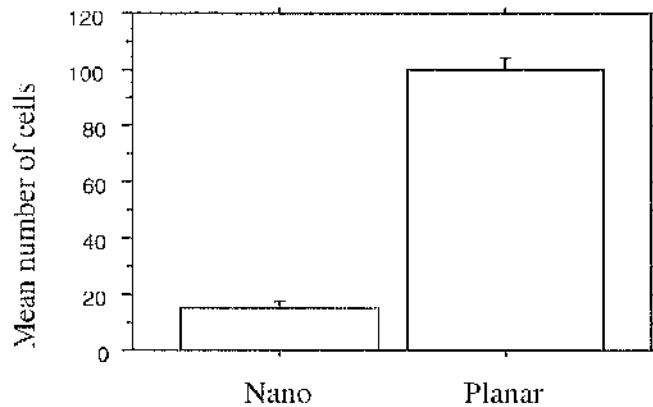


\bar{X} = Sample sum
 s = Standard deviation

	Nano	Planar		Nano	Planar
Mean	16	161	Max	35	179
Std Dev	7	8	Min	4	143
Std Error	1	1	ΣX^2	14873	1195917
Count	46	46	Σx^2	2425	3229

Figure 3.15 Epitenon cell adhesion to polystyrene nanopitted and planar topographies for 48 hours. It has been demonstrated via Post hoc Bonferroni/Dunn testing that the cell adhesion between the two types of topographies is statistically significant $P < 0.0001$. Counting area 1.65 mm^2 , means of counts for 30 areas.

Epitenon cell adhesion to Polyurethane nanostructures after 48 hours

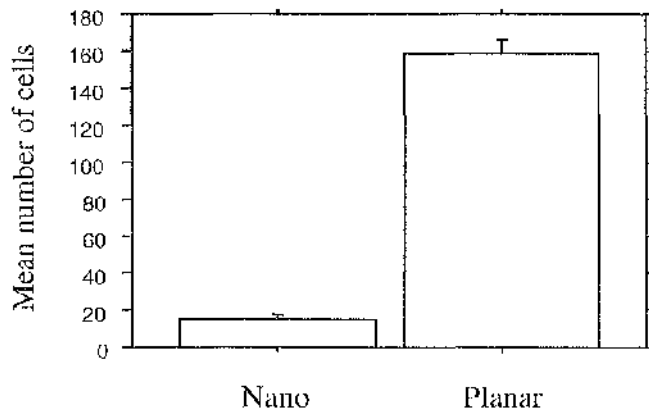


X = Sample sum
 x = Standard deviation

	Nano	Planar		Nano	Planar
Mean	15	100	Max	33	119
Std Dev	8	11	Min	3	80
Std Error	1	2	ΣX^2	12593	464577
Count	46	46	Σx^2	2633	5177

Figure 3.16 Epitenon cell adhesion to polyurethane nanopitted and planar topographies for 48 hours. It has been demonstrated via Post hoc Bonferroni/Dunn testing, that the cell adhesion between the two types of topographies is statistically significant. Counting area 1.65 mm², means of counts for 30 areas.

Epitenon cell adhesion to Polycarbonate nanostructures after 48 hours



\bar{X} = Sample sum
 s = Standard deviation

	Nano	Planar		Nano	Planar
Mean	15	159	Max	28	190
Std Dev	7	19	Min	2	110
Std Error	1	3	ΣX^2	12180	1183989
Count	46	46	ΣX	2310	15657

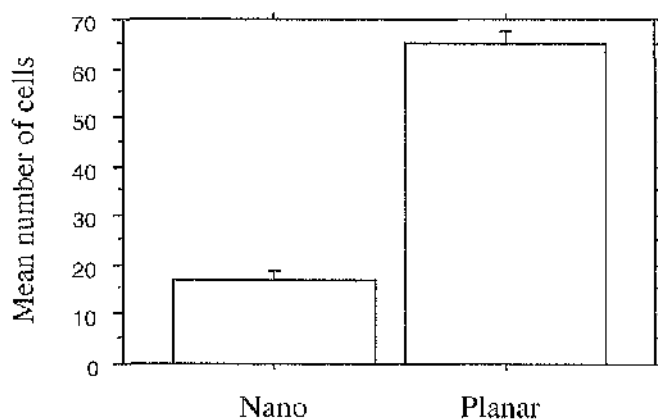
Figure 3.17 Epitenon cell adhesion to polycarbonate nanopitted and planar topographies for 48 hours. It has been demonstrated via Post hoc Bonferroni/Dunn testing, that the cell adhesion between the two types of topographies is statistically significant. Counting area 1.65 mm², means of counts for 30 areas.

Cell adhesion to nanotopography in serum -free culture conditions

It became clear from the experiments detailed in this chapter that cell adhesion was being significantly reduced on nano featured samples compared to flat. It was also clear that the effect was neither cell specific nor was it polymer specific. The question arose, whether there was differential protein adsorption on the different surfaces. This was an extremely relevant question due to the fact that the feature in question was within the same range of size as the protein typically found in the cell culture conditions. It was possible that the proteins encountering the nanotopography were in some way influenced by the topography imparting a conformation change and hence a functional change upon the protein. A simple answer to this question was to see what effect, if any, culturing cells in serum-free media had upon cell adhesion?

Epitenon cells were cultured upon nanopitted Polycaprolactone for 24 and 96 hour to test the possibility that the proteins contained within the serum containing culture media were having an effect upon cell adhesion. In figures 3.18 and 3.19, it was clear that from the statistical analysis of a post hoc Bonferroni/Dunn testing that the difference of adhesion, in serum-free culture conditions, was significantly reduced ($P < 0.0001$), upon the nanotopography, when directly compared to the adhesion of epitenon cells to the planar topography.

Cell adhesion to nano and planar topography in serum-free conditions after 4 hours

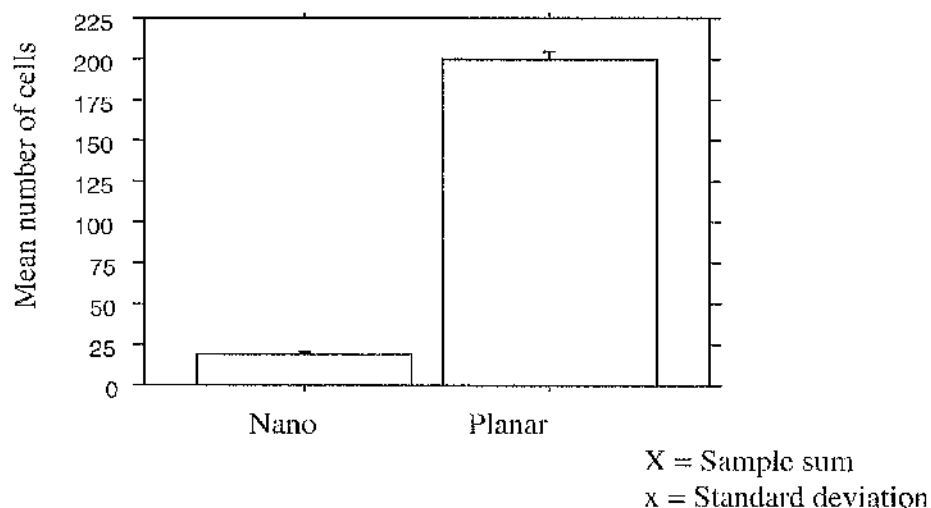


\bar{X} = Sample sum
 s = Standard deviation

	Nano	Planar		Nano	Planar
Mean	16	79	Max	25	93
Std Dev	4	8	Min	10	62
Std Error	1	1	ΣX^2	12038	274429
Count	45	44	Σx^2	710	2511

Figure 3.18 Cell adhesion to nano and planar topography in serum-free media conditions after 4 hours in culture. Cell adhesion on the two types of surface was significantly different ($P < 0.0001$).

Cell adhesion to nano and planar topography in serum- free conditions after 24 hours



	Nano	Planar		Nano	Planar
Mean	19	200	Max	29	222
Std Dev	4	11	Min	11	181
Std Error	1	2	ΣX^2	12038	274429
Count	44	45	Σx^2	672	5096

Figure 3.19 Cell adhesion to nano and planar topography in serum-free media conditions after 20 hours in culture. Cell adhesion on the two types of surface was significantly different ($P < 0.000$).

Discussion

Fabricating nanotopographical structures in polycaprolactone.

In many areas of commercial manufacturing, embossing is used as a low cost, large-scale method of producing plastic shapes and patterns. The most common uses for this pattern transfer method are in the fabrication of holograms and compact disks, where metal dies are used to repeatedly stamp out patterned plastic features. The advantage of this process in producing small features is that it is cheap, allows high throughput and yields large areas of uniformity. In addition, it requires only one fabricated die to produce many identical samples (Casey et al., 1997).

These factors were all taken into account when embarking upon a method of pattern transfer. All of these factors were fulfilled in the fabrication of nanostructures, the cost per sample was low, the quantity of nanostructures produced was high, and above all else, the uniformity and accuracy of the nanostructures was true. Another problem common to the industrial pattern transfer process is the use of a mould release agent, which has a major biocompatibility problem. This was easily circumvented by the replacement of this agent with water.

Another important problem that faces many cell biologists wishing to study the cell biomaterial interaction was addressed; that of polymer opacity. The development of what is believed to be novel and cost effective method for the production of translucent nanostructured biomaterials has been achieved.

Epitenon cell adhesion to nanotopography after varying time points

At the beginning of this set of experiments a hypothesis was formulated. It was thought that the nano-topographical substrate would act as a cue and this cue would have an effect upon cell behaviour. This part of the statement was true, however, the rest of the hypothesis stated that the effect the ordered nanotopography would have upon cell behaviour would be to orient the collagen production of individual cells. From these experiments this was found not to be the case. Over a period of 4, 20, and 96 hours cell adhesion to these surfaces was significantly reduced ($p < 0.0001$). It could be seen that in some cases, cell adhesion was being drastically altered. In figure 3.7, a culture of epitenon cells was stained with Coomassie brilliant blue total protein stain to reveal that cell adhesion on large regions on the nanopitted topography was almost non-existent.

These experiments became pivotal in determining the thrust of this thesis, what was happening at the cell-biomaterial interface and why?

BHK 21, B10D2, and HGTFN adhesion to nanopitted topography after 4, 20, and 96 hours

In this set experiments the question being asked was; is the significant reduction in adhesion of epitenon cells by the nanopitted topography cell specific? This was addressed by the use of 3 different cell types. The results of the experiments demonstrated that over varying time points the three cell types; BHK 21, HGTFN and B10D2 all showed a significant reduction in adhesion to the nanotopography when directly compared to a control surface

of planar topography. In regards to the question of the mean number of cells in relation to time cells on planar topography proliferated with time, however proliferation of cells on nanopits was not observed.

From these experiments it was possible to postulate that the effect of nano-adhesion of Rat epitenon fibroblasts, could be widened to incorporate the reduction in adhesion of the aforementioned cell types. It could therefore be argued that this effect was not a cell specific phenomenon. It was also clear that the nanopitted topography embossed into PCL was having a direct effect upon cell behaviour by presenting some form of cue. This prevented a normal cell-biomaterial interaction, occurring on the nanotopography whereas a normal reaction was observed on the planar topography.

Cell adhesion to Polystyrene, Polyurethane and Polycarbonate fabricated structures

The next question to be addressed in this chapter was whether or not this effect was a polymer specific phenomenon? By fabricating the pitted nanotopography into different types of polymer, and conducting cell adhesion experiments upon their surfaces, the results of the cell adhesion experiments involving rat epitenon fibroblasts were given greater credibility. They showed that the cell adhesion to the identical nanopitted topographies were significantly reduced ($P < 0.0001$) in each of the polymers, namely, polystyrene, polyurethane and polycarbonate.

This set of experiments finally confirmed that the observed reduction in cell adhesion was neither cell specific nor polymer specific. It was now quite clear that this influence on cell behaviour was due to a topographical cue and not some intrinsic property of the polymer being altered in some way by the nano-

fabrication process. The fact that the nanotopographic pattern could be transferred into a variety of polymers gave scope for a possible expansion of polymer types that could be utilised in the future, for possible cell devices.

Cell adhesion to nanotopography in serum-free culture conditions

The question of whether or not protein adsorption was having a direct affect on the adhesion of cells to the nanotopographic pattern was addressed. With the support of the data in figures 3.18 and 3.19, it was shown that cells grown in the absence of serum proteins showed a significant difference ($P < 0.0001$) in adhesion to the two different types of embossed topography. This showed that the proteins present in the serum were not involved in the reduction in adhesion shown in the previous experiments. Therefore the reduction in adhesion is more likely to be a direct result of the cell-material interaction as opposed to any interaction resulting from a possible change in serum-protein conformation.

It is also shown from these experiments that cells in serum-free conditions are not able to divide and their cell numbers have not increased in 24 hours in culture. This was however a direct result of the lack of serum, which is shown to depress protein synthesis and cell growth (Alberts et al., 1994).

Chapter 4

Spatial control over cells

Introduction

Surface-microfabrication techniques have been widely utilized for the spatial control of cells in culture. Many strategies have employed variations in surface charge, hydrophilicity, and topology to regulate cell functions such as attachment. Chemical surface modification of a substrate is one key to long term interaction with biological systems. Control over biomaterial surface chemistry and atomic microstructure can result in a regulated cell response (Ito, 1999). In general, surface modifications fall into two categories: (1) chemically or physically altering the molecules in the existing surface (treatment, etching, chemical modification), or (2) coating the existing surface with a material which possess a different composition (coating, grafting, thin film deposition) (Ito, 1999; Ratner, 1996).

The chemical patterning of adhesive and non-adhesive regions on a substrate at the resolution of single cells (i.e., sub-micrometer) has relied on a variety of techniques, photolithographic patterning of surface chemistries with either covalent linking or chemical adsorption of the protein, (Ratner et al., 1996; Drumheller and Hubbel, 1995) microcontact printing of self-assembled monolayers of different chemistries or proteins (Healy et al., 1994; Seebriest, 2000; Mrksich et al., 1996; Bhatia et al., 1993; Bhatia et al., 1997) and solution

coating of microfabricated surfaces (Zhang et al., 1998) are other examples. Using these approaches, substrates (typically planar) can be designed to promote cell attachment or cell repulsion, provided that the appropriate cell-specific ligands are used. Ultimately, these approaches may provide clues about chemical cues that direct tissue assembly and regeneration.

Recent advances in cell biology have highlighted the importance of the ligand-receptor interaction for controlling cellular adhesion. In particular, approaches have been developed to coat surfaces with extracellular matrix proteins to create adhesive regions (Hubbell, 1995; Folch and Toner, 1998) or to covalently link integrin ligands to the surface (James et al., 1998). The well-known integrin binding RGD (Arg-Gly-Asp) cell adhesion ligand provides a simple mechanism of modifying surfaces on the microscale to mimic the extracellular matrix. Peptides that contain the RGD attachment site, together with the integrins that serve as receptors for them, constitute a major recognition system for cell adhesion and cell-substrate interaction (Ruoslahti, 1996). The RGD sequence is the cell attachment site of a large number of adhesive extracellular matrix, blood and cell surface proteins. This integrin binding activity can be reproduced by short synthetic peptides containing the RGD sequence attached to a given surface (Pierschbacher and Ruoslahti, 1984) and small peptides with RGD, e.g. 20 peptides long, are frequently used to prevent adhesion by application in media. Since integrin-mediated cell attachment influences and regulates processes such as cell migration, growth, differentiation, and apoptosis, the RGD peptides can be used to camouflage synthetic materials and mimic actual physiological systems. Substratum

adhesiveness can be micropatterned using peptides to create a model for morphogenetic cues controlling cell behavior (Britland et al., 1992a; Britland et al., 1992b).

The previous chapter established that varying cell types had dramatically reduced adhesion on a nanopitted region fabricated into a number of different polymers. Therefore the possibility of using this surface to spatially control and pattern cells was investigated. As detailed above, many research groups have tackled this subject matter to try to control the spatial arrangement of cells in culture conditions in a predetermined fashion. A notable feature of previous methods developed for the spatial control of cells is the one-dimensional approach of chemical patterning. More precisely, micro contact printing is used as the driving force to encourage selective adhesion. This approach of utilising chemistry has a several major drawbacks when considering its potential use *in vivo*. For instance, how will the chemistry react to whole blood or the whole plethora of body fluids and environments? Another potential drawback could be the reaction of the body to the material when transferred from an *in vitro* setting, potentially activating the complement pathway. Using topography as the controlling factor of cell behaviour could possibly circumvent this problem and provide a viable alternative to surface chemistry. In theory, topography should not be affected by chemistry and thus will have the major advantage of relying on surface shape alone as its major controlling mechanism.

Results

It was postulated that with the use of a nanopitted structure it would be possible to have a more precise and accurately defined spatial control over cells in culture. A dramatic demonstration of this was to have the word "CELL" written in planar topography surrounded by nanopitted topography. The width of planar lettering was 500 μm in width with a height of 3 μm . The nanopitted and planar interface is revealed via atomic force microscopy. This shows the simplistic nature of the design with two types of topography side by side (Figure 4.1).

Epitenon cells were then cultured upon the nano-embossed PCL substrates for 48 hours under normal culture conditions. After the culture period, the cells were fixed and then stained with Coomassie brilliant blue cell stain.

The results of this experiment were quite striking (Figure 4.2). The cells demonstrated an obvious preference to adhere to the planar topography over the nano-embossed regions. It was possible to observe with the naked eye that the epitenon cells were preferentially attached to the planar region and hence were spatially arranged to make up the word 'CELL'. The framing of the nanopitted area by a further region of planar topography populated with epitenon cells was a reinforcement of this phenomenon. These results demonstrated that it was possible to use the nanotopography to control the spatial arrangement of cells grown in culture. Some epitenon cells were found to adhere to the nanopitted topography, however this was an unusual

occurrence demonstrating a significant preference to attach to the planar topography.

When the images are examined at a higher magnification (Figure 4.3 and Figure 4.4), the accuracy of the spatial control can be better appreciated. As previously mentioned, some cells do attach to the nanopitted topography but are not fully spread and do not appear to proliferate; this is emphasised by the lack of confluent areas of cell in the patterned areas.

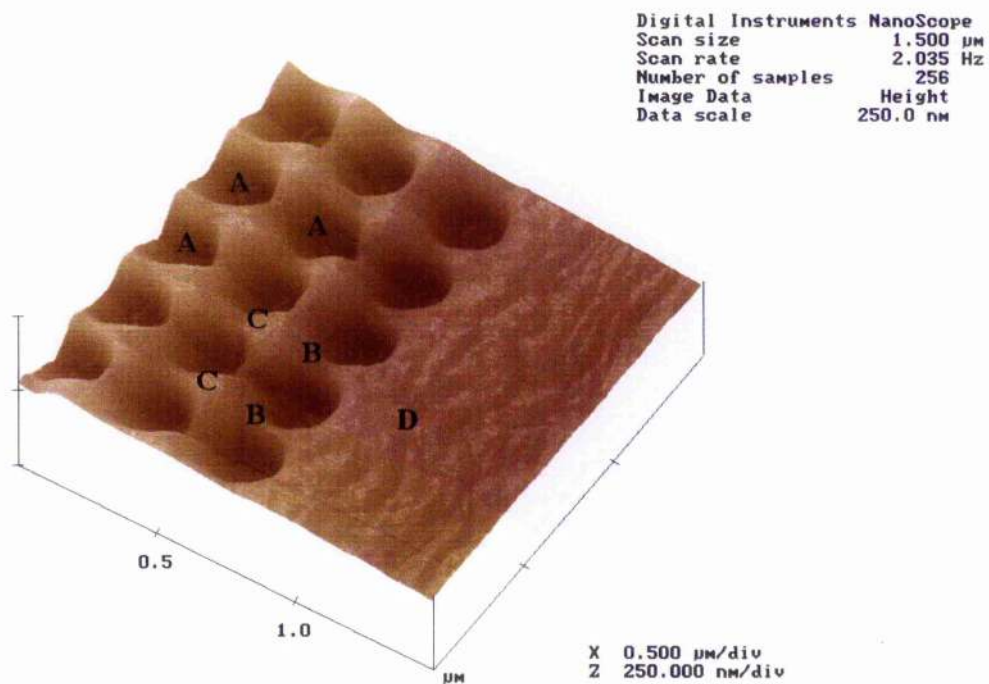


Figure 4.1 Atomic force microscopy scan of pit planar interface of a hot embossed PCL template used for the spatial control of epitenon cells and nanotopography. The nanopit area of the surface A is embossed from a pillar master. Note that in sections at B there is a certain curvature, perhaps it is this curvature, rather than a sharp edge, which prevents adhesions. C shows a domed crown at the diagonal between pits that are curved. D is a section of planar topography.

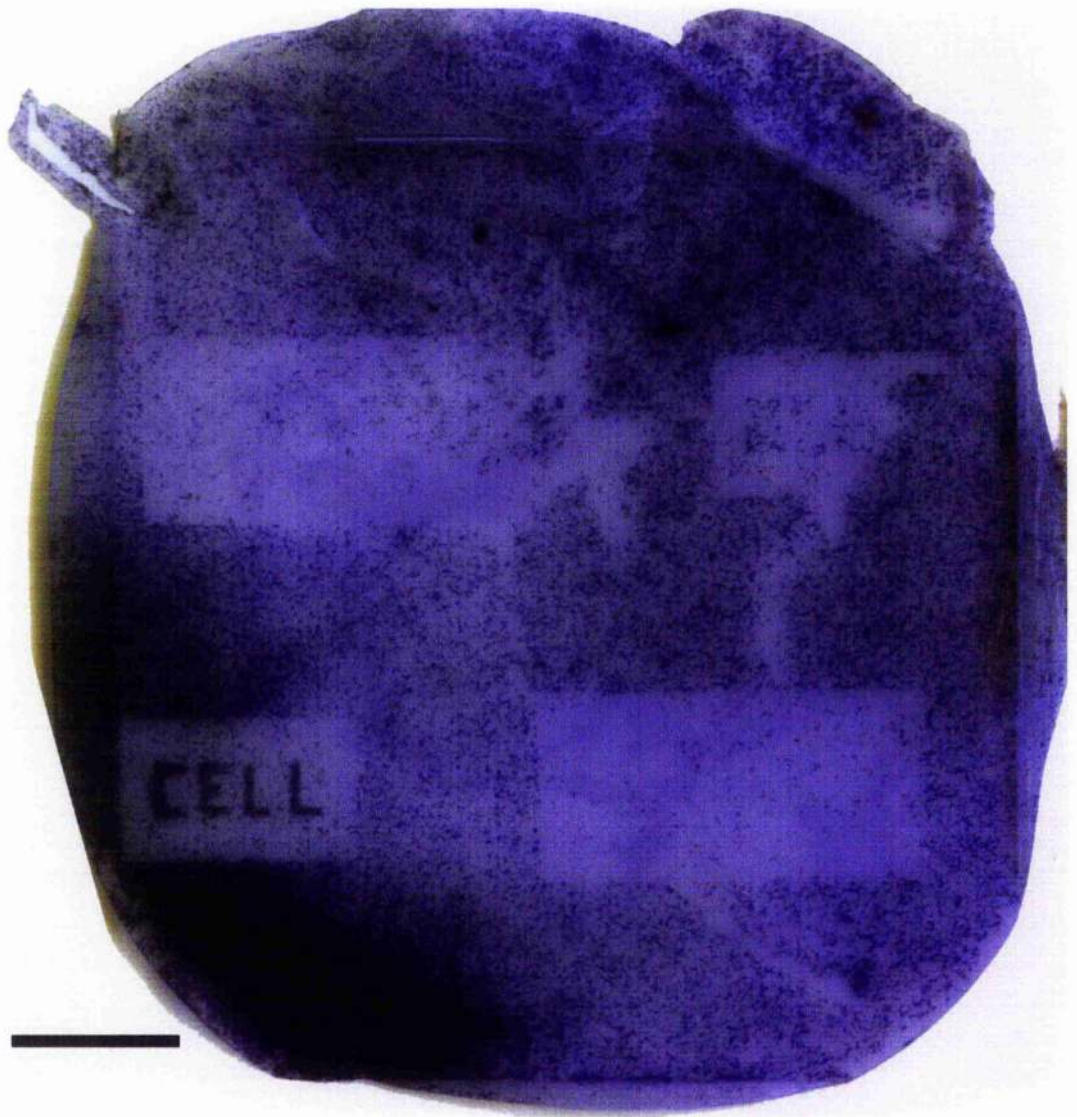


Figure 4.2 PCL sample of spatial arranged topography. Epitenon cells are stained after 48 hours in culture with Coomassie brilliant blue. The cells in the image are preferentially arranged in regions of planar topography. In the bottom right of the image, the word "cell" written in planar topography, is made visible by the staining of the sample. (Scale bar = 5000 μm).

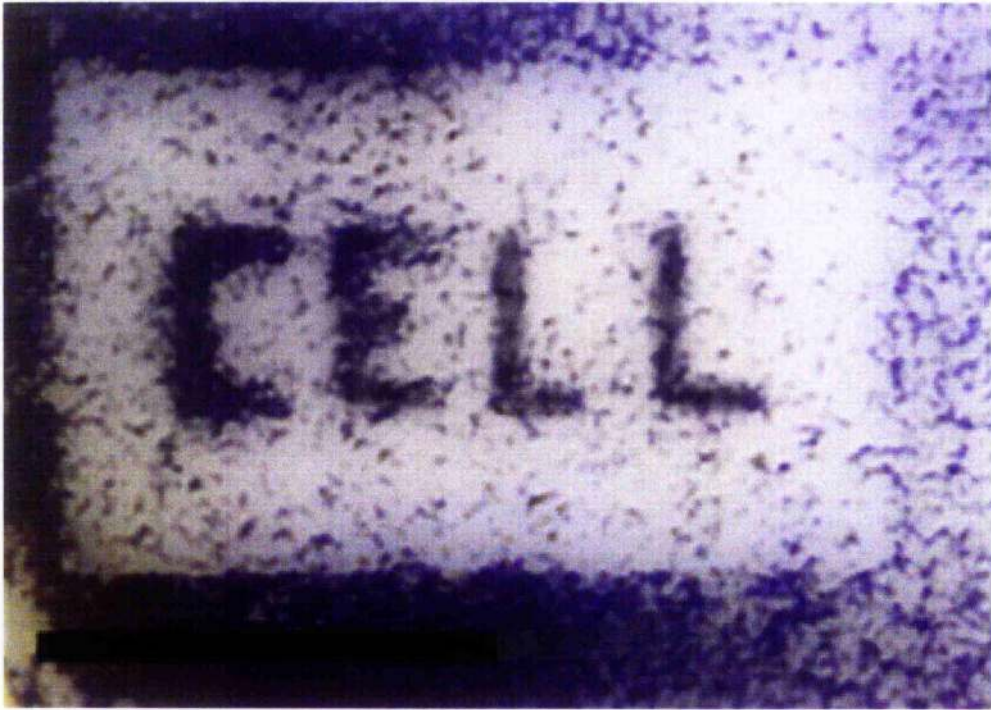


Figure 4.3 Enlarged image of epitenon cells stained with Coomassie blue after a culture period of 48 hours. This image shows the preference for cells to take up the available planar topography that has been fabricated to make the word cell. (Scale bar = 2500 μ m).

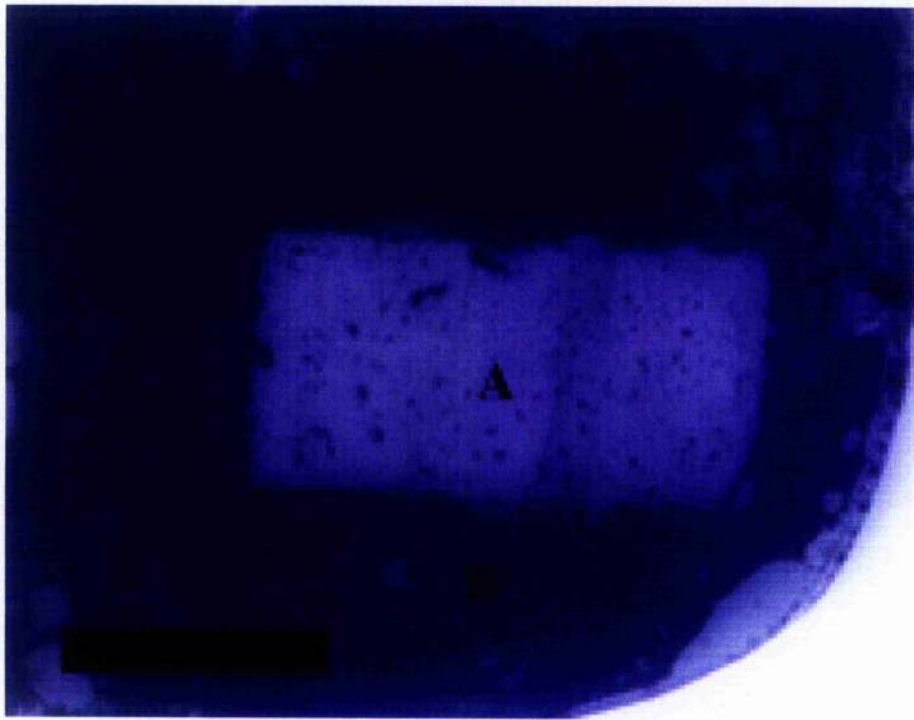


Figure 4.4 Embossed PCL sample cultured with epitenon cells (stained with Coomassie blue) for 96 hours. Epitenon cells in the image are demonstrating their propensity to adhere to the planar topography as seen in B with reduced adhesion in region A. It can be seen that cells have a propensity to form confluent sheets in the space surrounding the nanopitted region (Scale bar = 5000 μm).

Discussion

The results from these experiments demonstrate the possible uses of controlling the patterning of the nanopitted regions. PCI samples of predefined areas of nanopits linked with regions of planar topography produced a spectacular display of spatially arranged epitenon cells. The outcome of these experiments highlighted that it is possible to orient the spatial arrangement of cells in a very precise and deliberate manner. It was shown that it is feasible to isolate cells growing in culture on planar regions of topography completely surrounded by nanopitted topography. The organisation of cells on planar topography spelling the word "CELL" surrounded by the nano-pitted regions was such that when they were stained with Coomassie blue, the pattern was then visible to the naked eye, further illustrating the simplicity of the method to yield a tangible result.

The results also showed that in the longer term cultures (96 hours), it was possible to culture the cells to confluence and in the middle of this region have a non-confluent area made up of a 20 mm x 5 mm rectangle of ordered nanopits, exerting a direct influence of drastically reducing the adhesion of cells to the area. This demonstrated that at even higher densities of cells, nanopits will exclude cells proliferating upon them.

The fabrication approach used in this thesis has several distinct advantages over that used by other groups. The use of microcontact printing has yielded similar results in regard to selective cell attachment, however the employment of micro contact printing has the major disadvantage that the driving force is chemical in nature and this raises potential doubts as to its possible transfer to

an *in-vivo* setting, due to the possible immune rejection that could occur. This would be potentially overcome by the use of nanotopography for the selective attachment of cells. Yet another significant advantage of the topographical fabrication method is the high degree of control over the precise dimensions of the surface pattern where it can be fabricated at the nanometer scale.

Chapter 5

Cell Migration

Introduction

Cell migration plays a central role in many biological processes, including embryonic development, wound healing and the immune response. During development, many different cell types travel long distances through changing environments to reach their final destination. Intrinsic to this process are decisions made by cells about when to migrate, the paths to be taken, and when to stop (Huttenlocher et al., 1995).

Cell migration requires a dynamic interaction between the cell, its substrate, and the cytoskeletal-associated motile apparatus. Initiation of cell locomotion involves a directional protrusion of the leading edge, presumably via actin polymerisation, to form a lamellipodium, with its subsequent attachment to the substratum (Stossel, 1993; Lee et al. 1993b). Cell adhesion receptors then serve to connect the substratum with the cytoskeleton. After the formation and stabilisation of the lamellipodium, cells use these adhesive interactions to generate the traction and the force required for cell movement. The final step in the migratory cycle is the release of adhesions at the rear of the cell, with its subsequent detachment and retraction. This model for cell migration, although based on a few cell types such as fibroblasts, appears to apply to many diverse cell types, including those from lower eukaryotes (Sheetz, 1994; Cramer et al., 1994).

Rapid cell migration requires not only regulation of the adhesive interaction between cell surface adhesion receptors and the substratum, but also between these receptors and the cytoskeleton. In addition, the adhesive interactions between the cell and its substratum must be dynamic and require rapid rates of formation and dissolution to allow a cell to progress over its substratum. The adhesive strength at the cell front must be sufficient to generate force and traction to pull the cell forward. In contrast, the adhesive strength at the rear of the cell must be weaker to allow the cell to release from its surface (Di Milla et al., 1991). This suggests an asymmetry in adhesive strength between the cell front and the rear. Therefore, an understanding of cell migration requires not only identification of the factors controlling this adhesion and de-adhesion process, but also an appreciation of their spatial and temporal relationships.

Cell migration also requires the complex integration of motility-promoting and motility-inhibiting signals. Vast literature has accumulated describing the effects of many agents on cell migration. These include growth factors, cytokines and ECM components (Manske and Bade, 1994, Stoker and Gherardi, 1991). One class of motility-promoting molecules are the anti-adhesive ECM-components, such as SPARC, reascin and thrombospondin (Murphy-Ulrich and Hook, 1989). These factors may be present at increased concentrations in areas of inflammation, and probably enhance cell migration both by their anti-adhesive effects and by stimulation of the expression of genes encoding matrix-metalloproteinases, as seen in some cell types (Tremble et al., 1994). These anti-adhesive ECM components promote focal adhesion disassembly, which may be a mechanism by which to stimulate migration (Murphy-Ulrich and Hook, 1989; Murphy-Ulrich, 1995). It is clear

that many other migration promoting-factors also affect the organisation of focal adhesions. Certain growth factors and cytokines, including hepatocyte growth factor/scatter factor and interleukin-8, also destabilise focal adhesions and promote cell migration (Matsumoto et al., 1994, Dunlevy and Couchman, 1993).

An increasing body of literature points to the concentrations of substrate, receptor, and adhesion-related cytoskeletal components as critical determinants of migration rates. Indeed variations in substrate concentration produce a clear optimum that correlates well with migration rate. Maximal migration is observed on ECM components at intermediate substrate concentration (Koo et al., 2002). Smooth muscle cells adhere weakly and do not migrate on fibronectin, whereas high fibronectin concentrations increase cell spreading, focal adhesion formation and inhibition of cell movement (DiMilla et al., 1993). Maximal migration is also seen at intermediate cell surface integrin concentrations. Cells with low or high levels of cell surface $\alpha 5 \beta 1$ or $\alpha 2 \beta 1$ expression have lower migration rates than do intermediate levels of receptor expression (Bauer et al., 1992; Giancotti and Rushlahti, 1990; Keely et al., 1995). Thus, both substrate concentration and cell surface integrin expression levels play an important role in regulating cell motility; however, their inter-relationship has not been fully explored.

Integrin-cytoskeleton linkages are also important for regulating cell migration. Alteration in levels of cytoskeletal associated proteins modulate the migration rate. For example, decreases in levels of vinculin or α -actinin, achieved by antisense techniques, increase the rate of cell migration (Fernandez et al.,

1993) (Gluck and Benzeev, 1994). The expression of antisense α -actinin message also increases migration and tumor metastasis *in vitro*.

Results

Time lapse video microscopy

It was vital to observe what was occurring when cells encountered a nanopitted substrate. To investigate this, epitenon cells were cultured upon a hot embossed polycarbonate substrate for 96 hours. The resulting video showed quite clearly what was happening to the cells when they were cultured upon the nanotopography. The main video described below is the description of cell behaviour of epitenon cells cultured for 70 hours under normal culture conditions. The complete footage of this time-lapse footage accompanies this sequence on CD-ROM format at the back of this thesis.

Cells appear to encounter the surface in three different ways, on their own, physically attached to other groups of cells and in groups attached to a planar topography probing the nanotopography. Each of the behaviours are discussed below.

Single cell attachment

As single cells approach and make contact with the nanotopography, they settle and begin to spread as they begin to attach. After approximately 3 hours, cells would "ping" off or retract from the surface in one quick movement and immediately revert to the rounded morphology that they had when they first encountered the nano-surface (The effect could be likened to what would be expected to befall a spread cell during trypsinisation). Rounded cells would then seek to reattach to the surface and the same cycle of detachment and reattachment would occur. When single cells did attempt to adhere to the surface, they would become highly motile and would appear to probe the

surface before inevitably disengaging from the surface and rounding up. This process continued repeatedly throughout the 70 hours of the experiment. This attachment and detachment would frequently be coupled with increased motility as illustrated with the aid of video stills in Figure 5.1.

Cell clustering

One rather striking feature of the cell behaviour that was observed when cells of a rounded morphology would make a valiant attempt to adhere to the surface, would be the propensity of the cells to aggregate with other cells of a partially spread or rounded morphology. It became apparent that when two or more cells would collide in an attempt to adhere to the surface they would aggregate, developing cell-cell adhesion and form a cluster of cells (Figure 5.2). This is shown in Figure 5.3, where two groups of cells can be seen migrating in clumps towards each other. When these clusters of cells come into contact with each other they combine to form one larger cluster of cells. It is then observed that the newly formed larger cluster of cells continues to migrate in what appears to be a random fashion, continuing to pick up other cells on the way to create an increasingly larger cluster. Closer examination of this cluster of cells reveals that only some of the cells are in contact with the surface, and these are the cells that are driving the locomotion of the cluster around the nanopitted polycarbonate. Other cells in the cluster have no direct contact with the nanopitted topography only forming adhesions with other cells within the cluster.

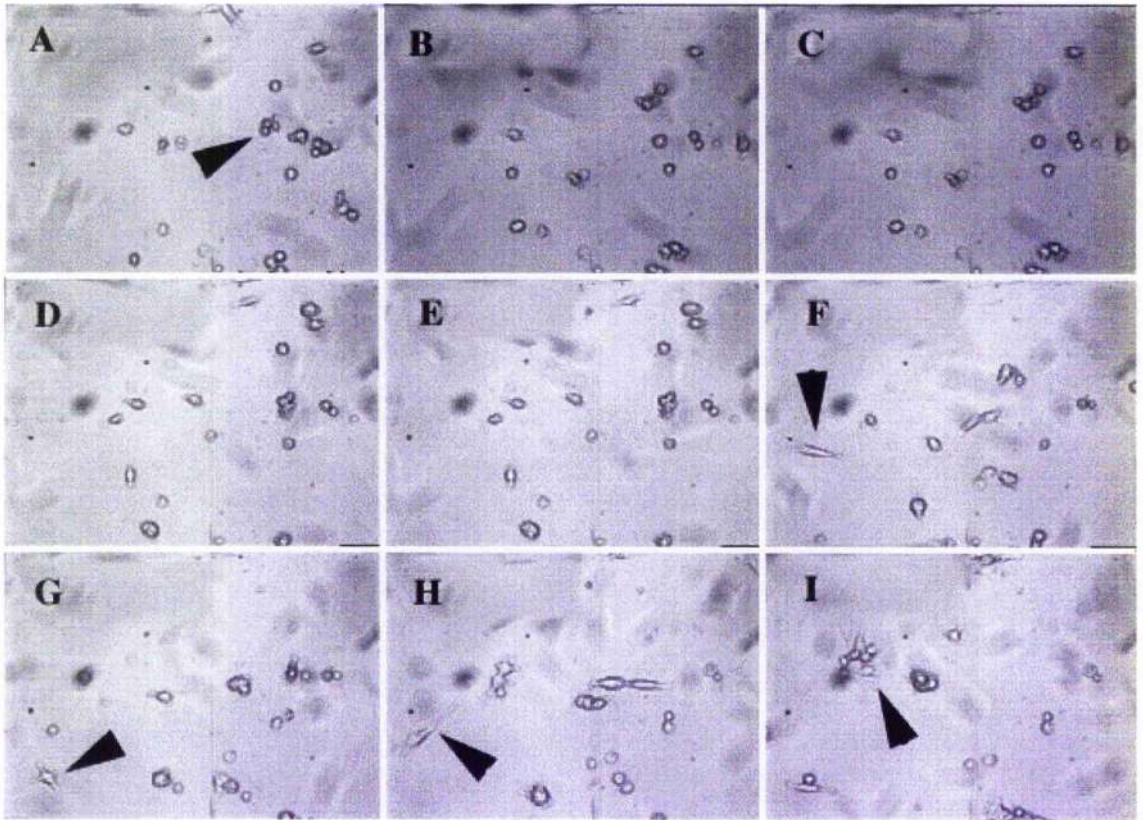


Figure 5.1 Time lapse footage of epitenon cells adhering to nanopitted topography. In part A the arrow points to general rounded morphology assumed by all cells at the start of the sequence. In frames B to F it can be seen that an epitenon cell starts to spread and then in frames G and H it is starting to lose its grip and then finally in frame I the cell resumes the rounded morphology it was exhibiting at the start of the sequence.

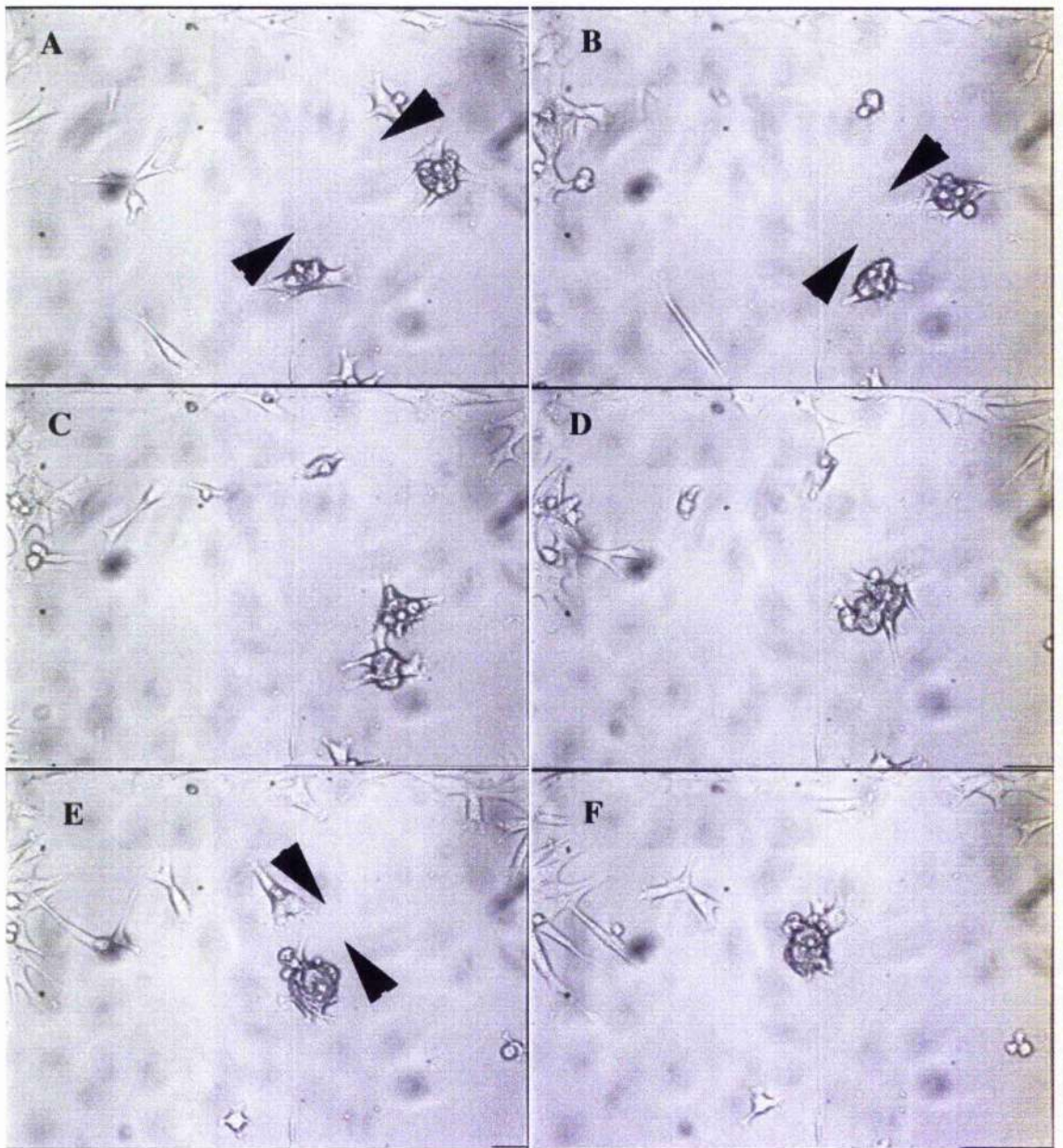


Figure 5.2 In Frame A two clusters of cells are visible upon a nanopitted surface. In frame B they can be seen to migrate towards each other, making contact and forming a larger cluster in frames C and D. In frame E another cell is migrating towards the cluster this cell becomes part of the main cluster in frame F.

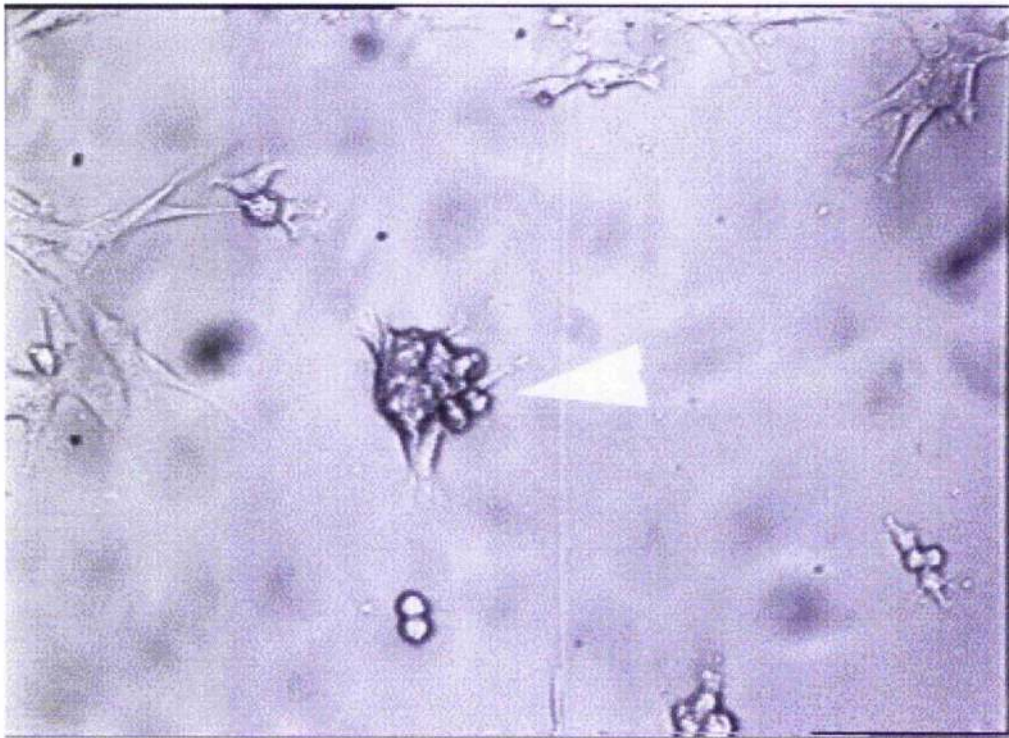


Figure 5.3 A large cluster of approximately 10 cells has formed upon the nanopitted surface. It should be noted that some cells are in contact with the substrate, these cells are the driving force of the cluster migration. Others cells within the cluster are only exhibiting cell-cell contacts within the cluster and not making any attempt to make contact with the underlying topography.

The planar/ pit boundary

In Figure 5.4 both nano and planar topography are visible. It can be observed that the cells in the planar region are behaving in a predictable manner i.e. their primary behaviour is that of proliferation, and keeping migration to a minimum. From this Figure (and more clearly in Movie 2) it can be seen that a group of cells is straddling both nano and planar topographies. The cells anchored on the planar region probe the nanopitted topography attempting adhesion for around two hours, after which time the failure to adhere causes them to completely retract preferring the more stable planar region for adhesion and proliferation upon the planar topography. It has also been observed that a spread cell would leave the planar topography and enter the nanopitted area where it adheres to a stationary rounded cell and then returns with the cell attached to the planar topography. The previously rounded cell that was picked up from the pitted topography would then resume a "normal" cell biomaterial interaction of adhering to and spreading upon the topography.

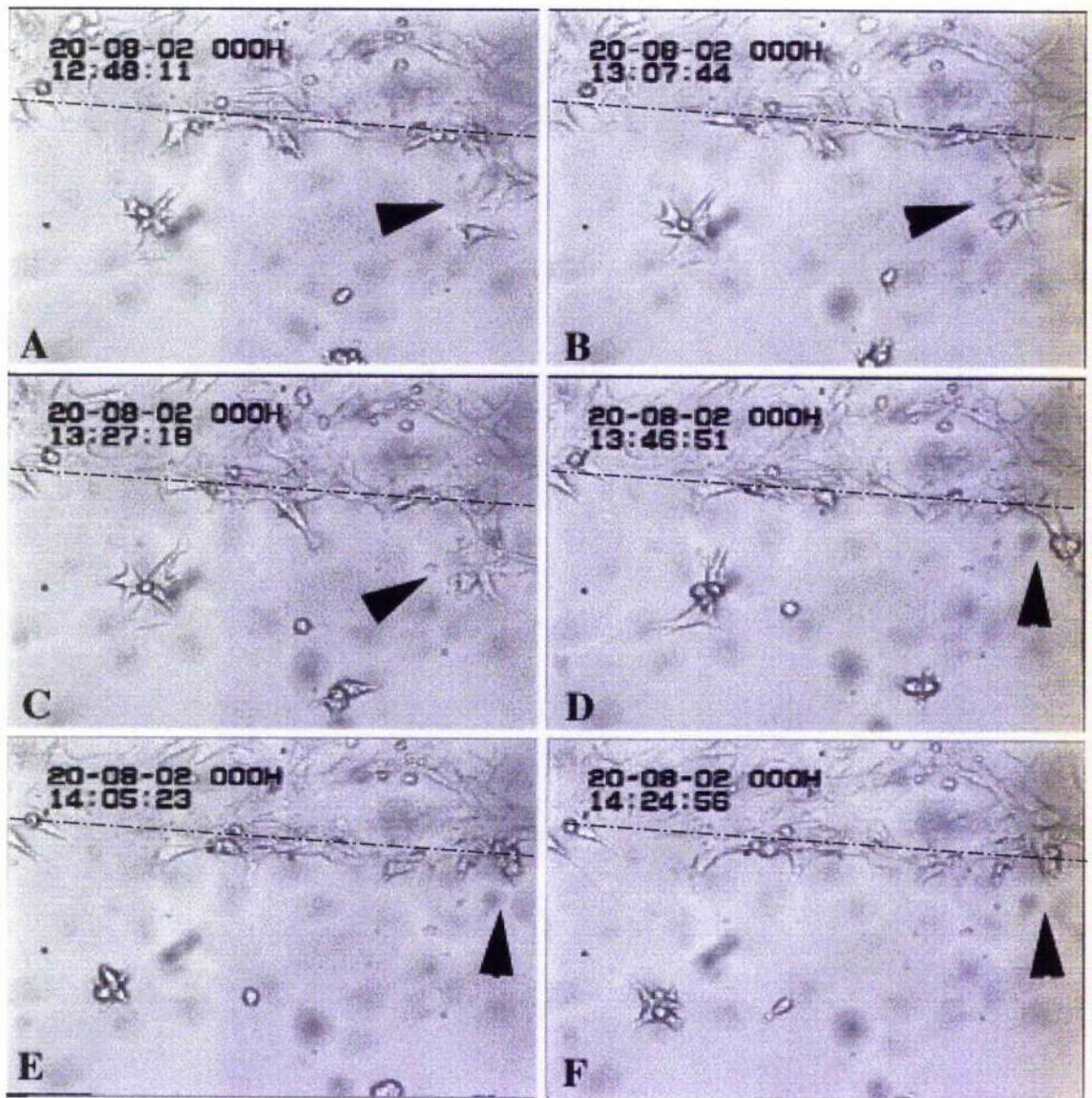


Figure 5.4 In this sequence the boundary between the planar and a broken line illustrates the nanopitted topography. The planar region is at the top of the frame where the majority cells have congregated. In this sequence it can be seen that a cluster of cells aggregated in the planar portion are probing the nanopitted region. These cells attach to a cell “struggling” on the planar topography and then pull backward to the planar topography taking the new recruited cell with it to the relative stability of the planar topography

Scanning electron microscopy investigation of cellular reaction to nanotopography

To gain a better insight into the direct interaction between the cell and the nanotopography, scanning electron microscopy (SEM) was carried out. Standard in-house protocols for SEM preparations require the use of a solvent (HMDS) which degraded the polycaprolactone, leading to the destruction of the topography. Here a technique of freeze-drying was employed to allow the PCL sample to be viewed and scanned. Epitenon cells were cultured upon the nanotopographical surface for 48 hours, freeze dried, sputter coated and scanned using a Hitachi S900 SEM (detailed in chapter 2).

In Figure 5.5, a typical epitenon cell reacting to nanotopography can be seen in the micrograph. The cell appears to be probing the surrounding environment, in this case a nanopitted topography via its filopodia. A noticeable feature is that the diameter of a pit is approximately the same width as the filopodia that the cell has sent out to probe the underlying substrate.

Analysis of SEM micrographs revealed several features of the cellular interaction with the nanotopography not visible by conventional light microscopy. The most noticeable of these was the probing of the nanotopographical surface by the cell's filopodia.

It could be seen quite clearly, that the filopodia would not, in general, enter the pits (Figure 5.6). Through the analysis of the micrographs, it was established that the cells prefer filopodia not to enter the pit directly but they appeared to prefer to sit upon the ridges of the pits. In Figure 5.7 it can be seen using post hoc statistical testing that this difference was statistically

significant in respect to a preference of the filopodia to attach to the top ridge versus the pits directly.

The micrograph shown in Figure 5.8 shows a region of planar topography surrounded by nanopits. It can be clearly seen from this image the obvious preference cells have for the planar topography over that of the nanopitted region. The vast majority of the cells in the image are spread and demonstrating their preference to the planar topography by congregating and adhering within this region. This is a demonstration of what is happening in general with regards to the cell behaviour upon the surface topography.

Another noteworthy feature of the micrographs relates to the diameter of the filopodia, which are of a similar size to that of the pit diameter (Figure 5.5). This illustrates that the e-beam fabricated features of the structure in the nanometre range, have a great biological relevance, due to the similar sizing of this particular cellular feature. This is made all the more relevant as filopodia have been directly implicated in a several morphogenetic processes (Wood et al., 2002). This suggests it is possible that fabricating structures in the nanometre range could have a direct effect upon cell features and thus cell behaviour.

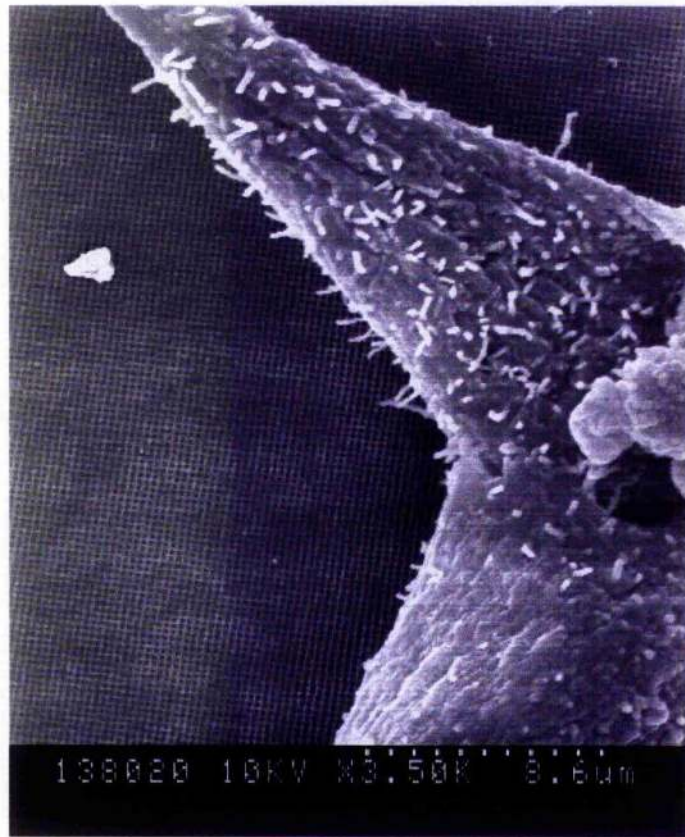
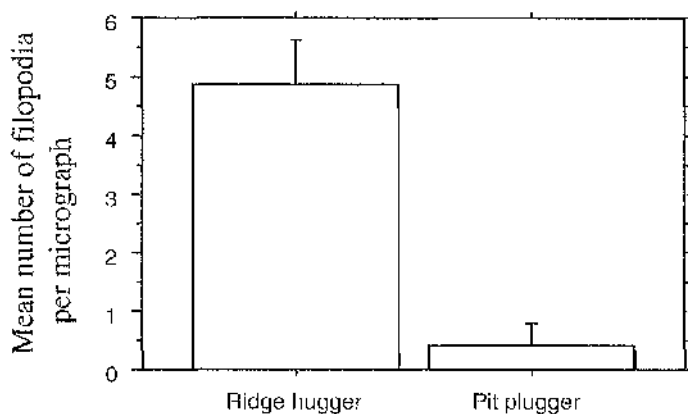


Figure 5.5 A SEM micrograph of an epitenon cell cultured on a nano topography for 48 hours. The cell in this micrograph has many filopodia emanating from the cell. These cell processes are thought to be one way in which a cell senses a substrate.

Filopodia positioning of epitenon cells on nanopitted PCL



	Ridge hugger	Pit Plugger		Ridge hugger	Pit plugger
Mean	4.9	.4	Max	7	2
Std Dev	1	1	Min	2	0
Std Error	.3	.1	ΣX^2	692	17
Count	27	27	Σx^2	47	22

Figure 5.6 Graphical representation of filopodia behaviour; ridge hugging or pit plugging. Filopodia deemed to be either adhering to the ridge of the nanotopographic pattern were classified as ridge huggers. Other configurations of filopodia of either partially or completely covering a pit are denoted as pit pluggers.

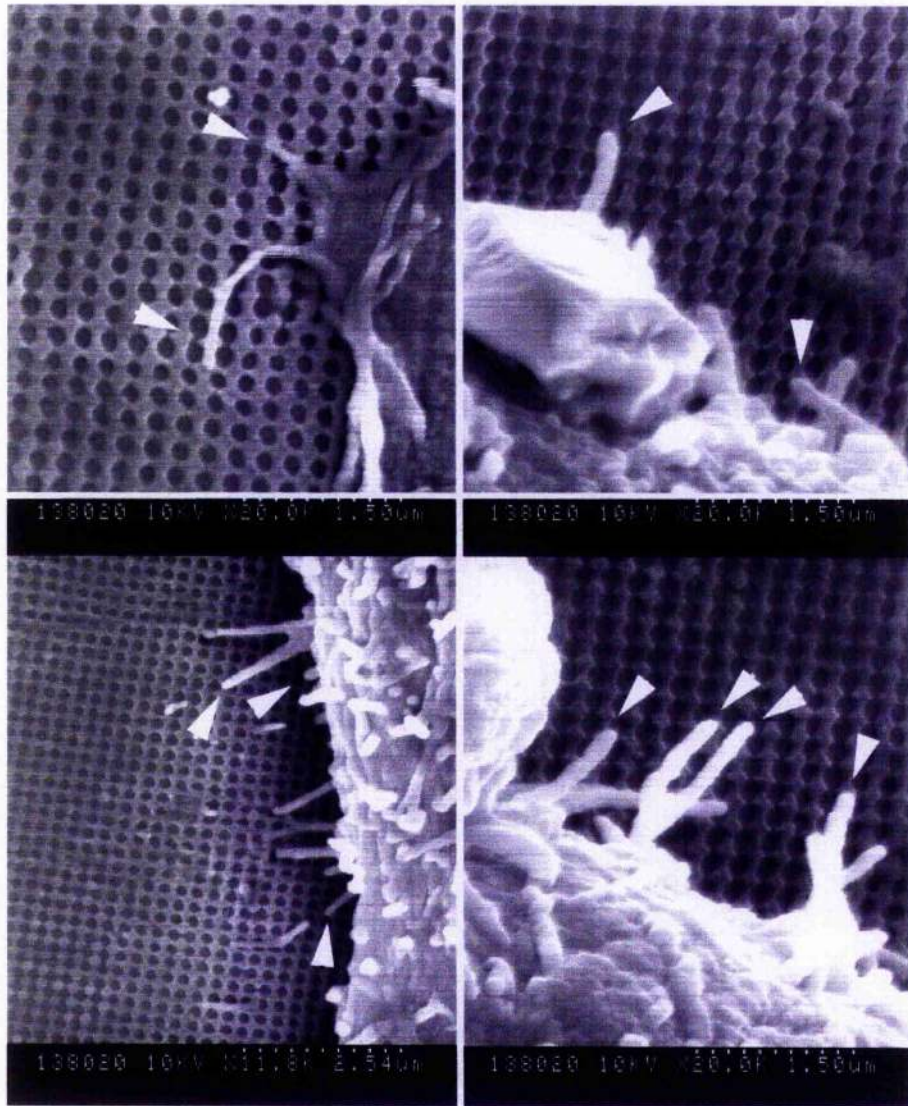


Figure 5.7 Epitenon cells probing the nanotopography with their filopodia. The filopodia highlighted in these micrographs are displaying a preference to attach to the top of the ridges formed by the nanopits as opposed to entering the pits or indeed sitting on top of or plugging the pits.

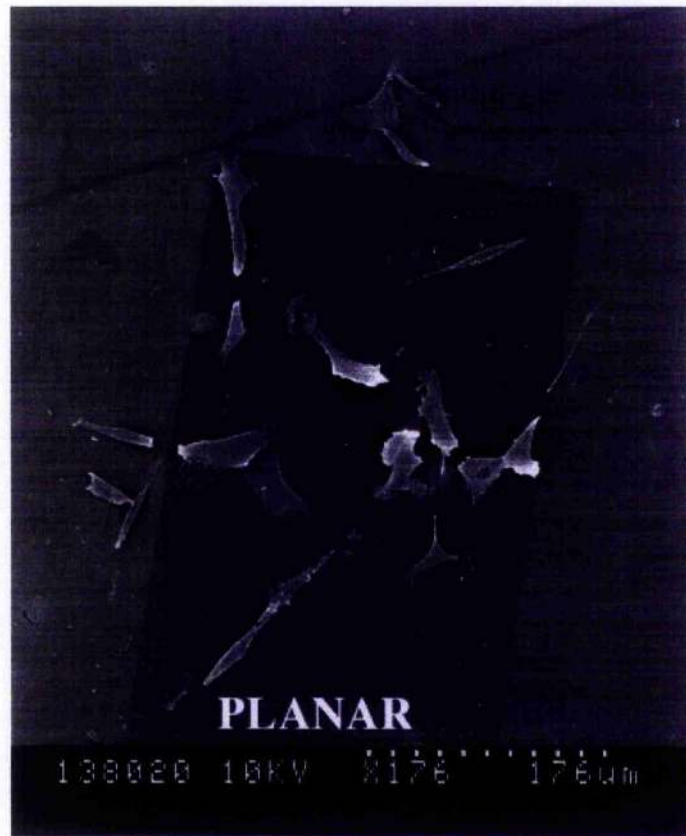


Figure 5.8 A micrograph of epitenon cells cultured on planar and nanopitted topography. The planar region (the darker grey rectangle) denoted in the figure, demonstrates the general preference for cell adhesion on planar topography.

AFM investigation of cell interaction

With the advent of atomic force microscopy by Binnig and colleagues in 1986 (Binnig et al., 1986) the world of scanning probe microscopy has enabled scientists to utilise this technology to investigate surfaces in a new and exciting way. One key advantage of this technology for the cell engineer is to examine cells and their interactions with their surroundings, in their live state. This permits investigations into the cell substrate interactions, circumventing the need for fixation of biological samples and building up a more detailed and a truer picture of the cell-biomaterial interaction.

Epitenon cells were cultured upon nanopitted polycaprolactone for a period of 40 days. The sample was kept in carbon dioxide buffered culture media and imaged via contact mode atomic force microscopy. The resulting images obtained from scanning the surface revealed some surprising features of the cell-material interaction. In Figure 5.9 it can be seen from the resulting scan that the epitenon cells appear to have deformed the surface quite considerably. This was apparent via the micron-sized craters, which appeared to have been pulled from the surface. Scans of the pitted surfaces, which had been kept in identical experimental conditions except for the addition of cells, showed that the polymer surface, which is biodegradable in nature, did have visible wear but was not damaged. This was embodied by pit widening after 40 days of culture (Figure 5.10). However, the surfaces, which were scanned, did not show any evidence of the micron sized craters that were apparent in the samples where cells were cultured for a 40 day period.

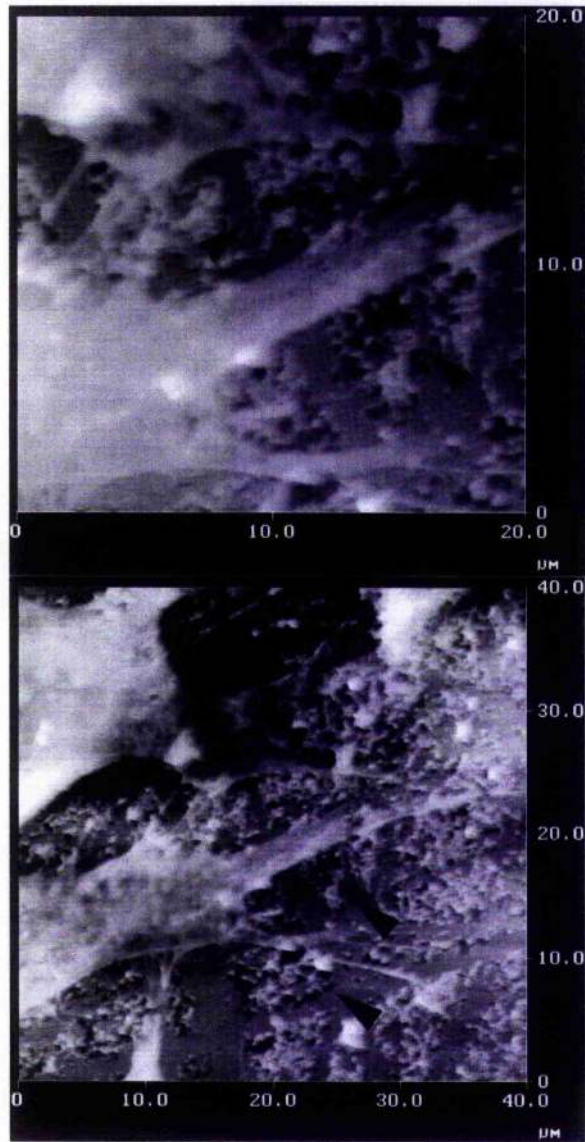


Figure 5.9 AFM scans in tissue culture media of epitenon cells upon nanopitted topography cultured for 40 days. In these images the arrows indicate the apparent degradation of the structure. It is speculated that this deformation is caused directly by the cells pulling portions of the polycaprolactone from the surface or it could possibly also be due to the enzymatic degradation of the polymer surface.

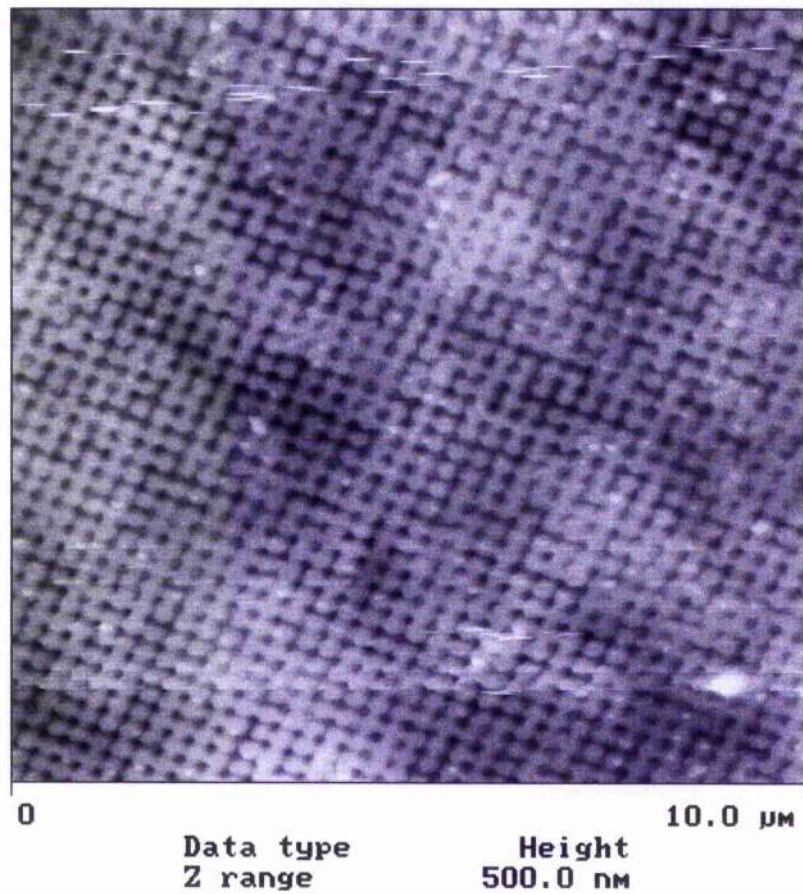
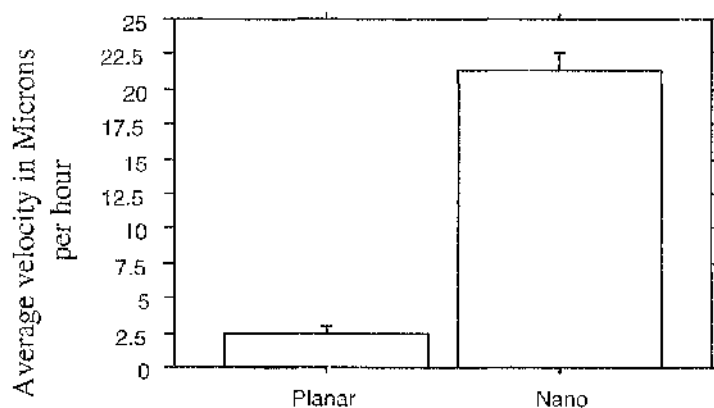


Figure 5.10 AFM scan of a nanopitted surface kept in culture conditions without cells for 40 days. The surface is showing signs of biodegradation which is highlighted by the widening of the pits. However, in comparison to surfaces cultured with cells in the previous Figure (5.9), the surface has remained relatively intact.

Cell motility speeds

The motility of cells encountering the nanotopography was directly compared with that of the motility of epitenon cells measured on the planar topography. The motility of cells encountering a planar topography is significantly slower ($P < 0.0001$) when compared with that of the highly motile behaviour exhibited by the epitenon cells on the nanopitted topography (Figure 5.11). The locomotory velocity of cells encountering a nanotopographic substrate was 21 μm per hour, which was found to be 8 fold quicker than that of the locomotory velocity of a cell encountering a planar topography of 2.5 μm per hour.

Cell migration rates of cells on Planar and nanotopography



	Nano	Planar		Nano	Planar
Mean	2.5	21.3	Max	5	27
Std Dev	1	2.8	Min	1	15
Std Error	.2	.5	ΣX^2	267	16575
Count	36	36	Σx^2	37	28

Figure 5.11 Average migration rates for cell cultured on nanopitted and planar embossed polycarbonate surfaces. (Statistical analysis carried out via ANOVA post-hoc testing, N=36) The migration rates of cells on nanopitted topography are significantly higher than the rate of migration of cells $P < 0.0001$.

Discussion

Time lapse video microscopy

From the analysis of the video microscopy, an unconventional cell-material interaction was revealed. It was shown that the cell interaction to the nanotopography was previously unknown and highly unusual. The findings of this work demonstrated that cell behaviour was directly influenced by topography.

In terms of a single cell's reaction to the nanotopography the cell employed one of two modes. The cells would either attempt to remain stationary and maintain a rounded morphology or alternatively, the cell may attempt adhesion resulting in repeated failures. When cells made repeated attempts to adhere to the nanotopography the time between partially adhering and becoming unstuck was approximately 3 hours. Cells had a propensity to become highly motile. The motility of these cells attempting adhesion was elevated, to the extent that it was significantly higher ($P < 0.0001$) than that of cells adhering to the neighbouring planar topography.

Another facet of the cell behaviour upon the nanotopography was the propensity for cells to form clusters with each other, requiring the formation of rapid cell-cell adhesions. These clusters were also highly motile and displayed a similar behaviour to that of a single cell on the topography e.g. attempting to adhere repeatedly but failing to make stable contacts. Another

feature of these clusters was that only a few cells were actually in direct contact with the underlying topography. Other cells within the cluster could be clearly seen to attach only to other cells within the cluster.

It was observed that cells seem to show a direct preference for a planar topography over a nano one, in the fact that cells could be seen to probe the nanopits from the planar topography, but would rarely be seen migrating onto the nanopitted surface from the planar topography. It was also observed that cells in clusters attached to the nanotopography would probe the surface and occasionally adhere to cells upon the nanotopography and pull them back to the planar surface.

SEM investigation

It was established in preliminary attempts to prepare PCL samples for SEM viewing, that traditional SEM protocols are detrimental to polymer integrity. The necessary use of HMDS for dehydrating the sample damaged the polymer and rendered samples unviewable. However the freeze drying of samples was shown to be a quicker method for SEM preparation of PCL samples. This is an integral feature of looking at the effects of nanotopography and the interaction of cells, being able to view intact topographical features and the effect, if any, they have with cells and their processes.

This probing mechanism of cells is demonstrated by the presence of filopodia emanating from the cell. The interaction of these cell processes with the topography was shown to be predictable. In no instance were filopodia seen to enter the pits that they were probing. Filopodia were shown to prefer the top

of the ridges as opposed to being placed directly on top of a pit entrance. This preference for filopodia to reside upon a ridge as opposed to within a pit was deemed to be statistically significant ($P < 0.0001$).

Atomic force microscopy investigation of cell interaction

Epitenon cells were imaged in culture conditions. Atomic force microscopy scans revealed what was happening to the polymer surface after 40 days of continuous culture. The surfaces, which had epitenon cells trying to adhere to the surface, had large micron sized craters missing from the polymer surface. To determine whether it was the cells which caused micron sized degradation of the polymer, surfaces were cultured without cells. These surfaces showed some signs of degradation manifesting as some pit widening, however, crater formation was not present on these surface samples. This suggests that it was the epitenon cells in the cultures that were creating the increased degradation of the polymer surfaces due to their repeated attempts to adhere to the nanopitted topography.

Chapter 6

The cytoskeleton and its response to nanotopography

Introduction

Control of cell shape and cytoskeleton

The extracellular matrix is critical in determining whether cells will grow, differentiate, or undergo apoptosis (Galbraith and Sheetz, 1999). The ECM regulates cell morphogenesis through focal adhesions by altering the shape of the intracellular cytoskeleton, which in turn orients much of the cell's metabolic machinery. So far much attention has been paid to the molecular basis of the cytoskeletal polymerisation and assembly, but little is known about how cells geometrically control cytoskeleton mechanics and mechanical tension (Chen et al., 1997c)

To demonstrate the importance of cell shape a technique was used that allows spontaneous assembly of monolayers of alkanethiols to create micropatterned surfaces, producing chemically identical adhesive islands of arbitrary size and geometry at micrometer level (Singhvi et al., 1994a). Goldmann et al., (2000) describe in detail the various stages involved in generating patterned substrates to create islands of ECM surrounded by nonadhesive regions for cells to attach and spread only in adhesive regions. Using this technique has shown that ECM appears to be the dominant regulator that dictates whether cells proliferate, differentiate or die. Studies with living and membrane permeabilised cells confirm that changes in cell shape result from the action of

mechanical tension, which is generated from within microfilaments, and balanced by resistance sites within the underlying ECM. Analysis of the molecular basis of these effects reveals that ECM molecules alter cell growth via both biochemical and biomechanical signalling mechanisms (Sheetz et al., 1999).

In relation to the atomic force microscopy scans of nanopitted PCL surfaces used in this thesis, there was no evidence of ECM deposition upon the nanopitted surface after varied culture periods.

Focal adhesions

During recent years knowledge about focal adhesions and their role in spreading, migration and survival has increased vastly. The ever increasing number of proteins being found to participate in focal adhesions makes them one of the most complex protein aggregates formed in a cell (Zamir and Geiger, 2001b). Focal adhesions fulfil mechanical and sensing functions that involve reversible anchorage of the actin cytoskeleton to the ECM during migration and monitoring intracellular or extracellular tension.

The use of chimeric molecules, comprising green fluorescent protein (GFP) attached to various focal adhesion proteins has made important contributions to our understanding of focal adhesions. Owing to the stoichiometric fusion of GFP to focal adhesion proteins, such GFP chimeras can be used not only as markers for cellular attachment sites but also to provide dynamic and quantitative information about the composition of a focal adhesion (Zamir et

al., 2000; Balaban, 2001; Beningo and Dembo, 2001; Ballestrem, 2001). In parallel, progress has also been made in measuring the mechanical traction forces exerted by cells when they interact with elastic surfaces, (Balaban 2001; Beningo and Dembo, 2001; Dembo et al., 1996; Dembo and Wang, 1999). One of the emerging ideas from this work is that focal adhesions are mechanical transducing devices with a mechanical sensor function. Hence, they relay changes of intra- and extracellular tension into signaling paths that in turn modify the composition and behavior of the focal adhesion, directly influencing the migratory and contractile state of the cell (Geiger and Bershadsky, 2001; Benigo and Wang, 2002)

Focal contacts as mechanosensors

One of the intriguing features of focal contact formation and stability is their strict dependence on myosin-II-driven contractility. Chemical inhibitors of myosin light chain phosphorylation and actin dependent myosin ATPase activity suppress focal contact and stress fibre formation (Volberg et al., 1994; Chrzanowaska-Wodnicka and Burridge, 1996). Similar effects can be obtained by over expression of non-muscle caldesmon, a protein that restrains the interactions of myosin heads with actin filaments (Helfman, et al., 1999). Moreover, expression of a dominant negative deletion mutant of myosin IIA heavy chain blocks cell contractility and consequently suppresses the formation of matrix adhesion (Wei and Adelstein, 2000). It is noteworthy that both chemical inhibitors and caldesmon inhibit focal contact formation even when the cells express constitutively active Rho (Chrzanowaska-Wodnicka

and Burridge, 1996; Helfman et al., 1999). Thus, myosin II acts downstream of rho-dependent formation of focal contacts. It is also important to state that the sensitivity to myosin II inhibition is a characteristic feature of focal contacts discriminating them from other types of actin-integrin adhesion complexes, including focal complexes and fibrillar adhesions, although in some studies high doses of inhibitors induced disruption of focal complexes (Rotner et al., 1999).

The nature of the mechanical switch that triggers focal adhesion and stress fibre formation is not known. However, it is known that force applied to focal contacts can be either endogenous (i.e. actomyosin driven) or exogenous. Specifically, when local mechanical force is applied from the outside, growth of focal contacts is achieved even if actomyosin contractility is blocked and rho activity suppressed by specific inhibitors (Riveline et al., 2001). Experiments with force application by micropipette showed that tension-dependent regulation of focal contact assembly is a local process (Riveline et al., 2001). In another experimental system, centripetally moving beads attached to the cell surface via integrin were restrained by laser tweezers, thereby inducing a mechanical force applied to the integrin receptor complex (Chouquet et al., 1997). This led to a local increase in the force exerted on the bead by the cell (reinforcement), a process that can be explained by the force-dependent local recruitment of new components into primary adhesions (Galbraith et al., 1999; Chouquet et al., 1997).

Results

F-actin

Previous chapters have investigated the interaction between the cell and the nanotopography to which it was exposed. In this chapter the intracellular interactions of cells encountering nanotopography were analysed. The F-actin component of epitenon cells cultured on nanopits and a planar topography was investigated. Epitenon cells were incubated at 37°C for 48 hours and then stained via indirect immunofluorescence with fluorescent Phalloidin for 48 Hours. F-actin was probed to visualise what effect if any, the topography was having on the cytoskeleton of cells when confronted with nanopitted topography versus planar.

The results of these experiments describe reactions of specific cytoskeletal components when they are challenged by this nanopitted topographic cue. Scanning confocal microscopy revealed that the organisation and development of the cytoskeleton was distorted. The F-actin cytoskeleton appears less defined, probably due to the reduced spreading of the cells on the nanopitted topography. The normal development of stress fibres of cells adhering to planar surface (Figure 6.1) was absent from the cells on the nanopits. The F-actin of the cells attached to the nanotopography is visibly disorganised in comparison to cells cultured on a planar topography and is illustrated in Figure 6.2 by its lack of order and contains small areas of branching. This is in direct contrast to the F-actin of cells on planar topography, which takes on a linear organised appearance (Figure 6.1).

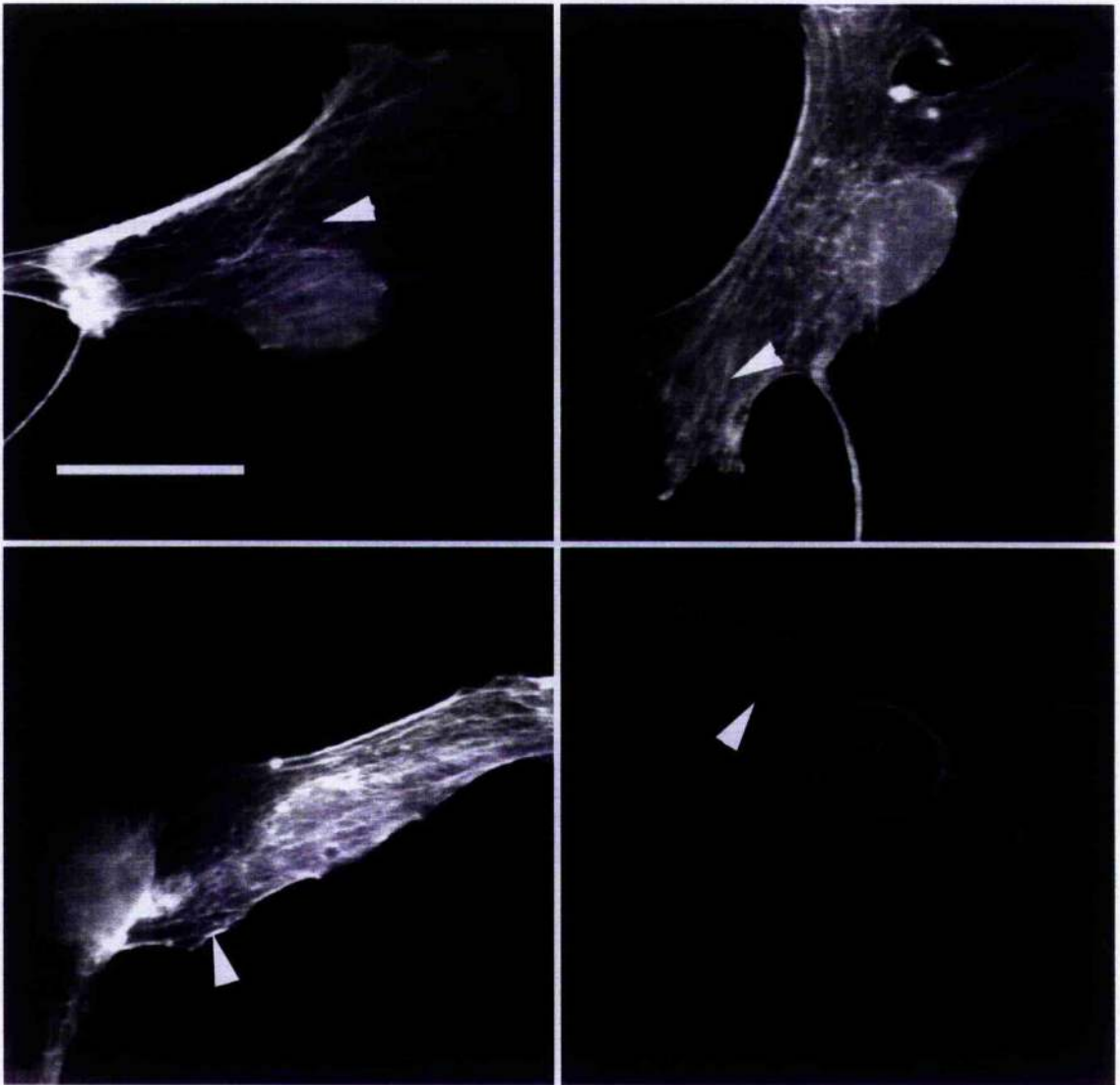


Figure 6.1 F-actin staining of the cytoskeleton in epithelial cells cultured on a planar topography for 48 hours. The F-actin within these cells is of a classic morphology, highly organised and visible as defined strands of the actin cytoskeleton (indicated by the arrows). (Scale bar = 10 μ m).

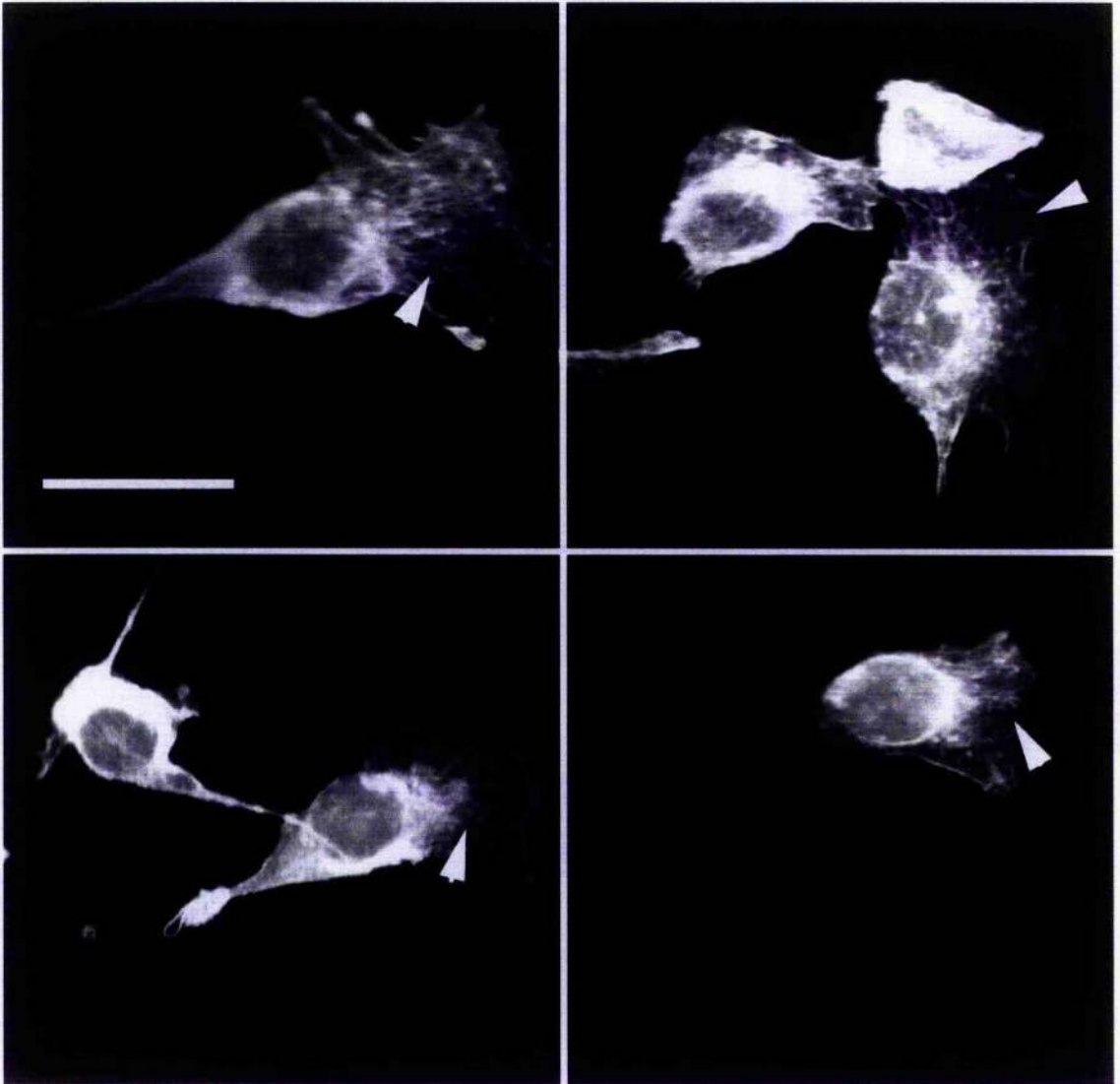


Figure 6.2 F-actin cytoskeleton of epitenon cells cultured on nanopitted topography for 48 hours. The F-actin cytoskeleton within these cells is abnormal when compared to the morphology of the F-actin displayed of the epitenon cells cultured upon a planar topography (Figure 6.1). The cytoskeleton is on the whole undefined, (as indicated by the arrows) and where it is visible the branches of actin are small and lack the typical patterning that would be expected of a cell cultured for this time period (Scale bar = $10\mu\text{m}$).

Vinculin containing Focal contacts

Vinculin-containing focal contacts of epitenon cells were probed to visualise the localisation, quantity and size of these components. Vinculin is a component of focal adhesions and was chosen to be stained due to its noted abundance within focal contacts (Chrzanowaska-Wodnicka and Burridge, 1996).

In figure 6.3 it is shown quite clearly how a typical cell will attach to a planar biomaterial surface. These adhesions are well defined and appear to be evenly spaced out throughout the cell. Figure 6.4 demonstrates vinculin staining for cells cultured on nanotopography and quite the opposite of normal staining can be seen. The focal adhesions are not well defined, they are also clumped together in regions and not evenly spatially arranged. (The reason for the clumping of focal adhesions is most likely due to scratches on the master surface, which are then directly transferred into the polymer replica during the embossing process).

The size and number of the focal adhesions were also investigated. The overall number of cells adhering to the nanotopography was significantly reduced ($P < 0.0001$). This was also coupled with the fact that the overall sizes of individual adhesions were significantly smaller ($P < 0.0001$) when they were directly compared with the size of individual focal adhesions on a planar surface (Figure 6.5).

Another feature of the vinculin distribution in cells on nanopitted topography is the speckled appearance of vinculin in these images. These appear to be representative of very small patches of vinculin. These adhesions appear retarded and are either in their infancy or transitory in nature.



Figure 6.3 Vinculin containing focal contacts of epithelial cells cultured on a planar PCL topography. The patterning of these focal adhesion is deemed to be classic in morphology and distribution is well spaced and ordered, illustrating a normal cell-biomaterial interaction (scale bar = 10 μm).

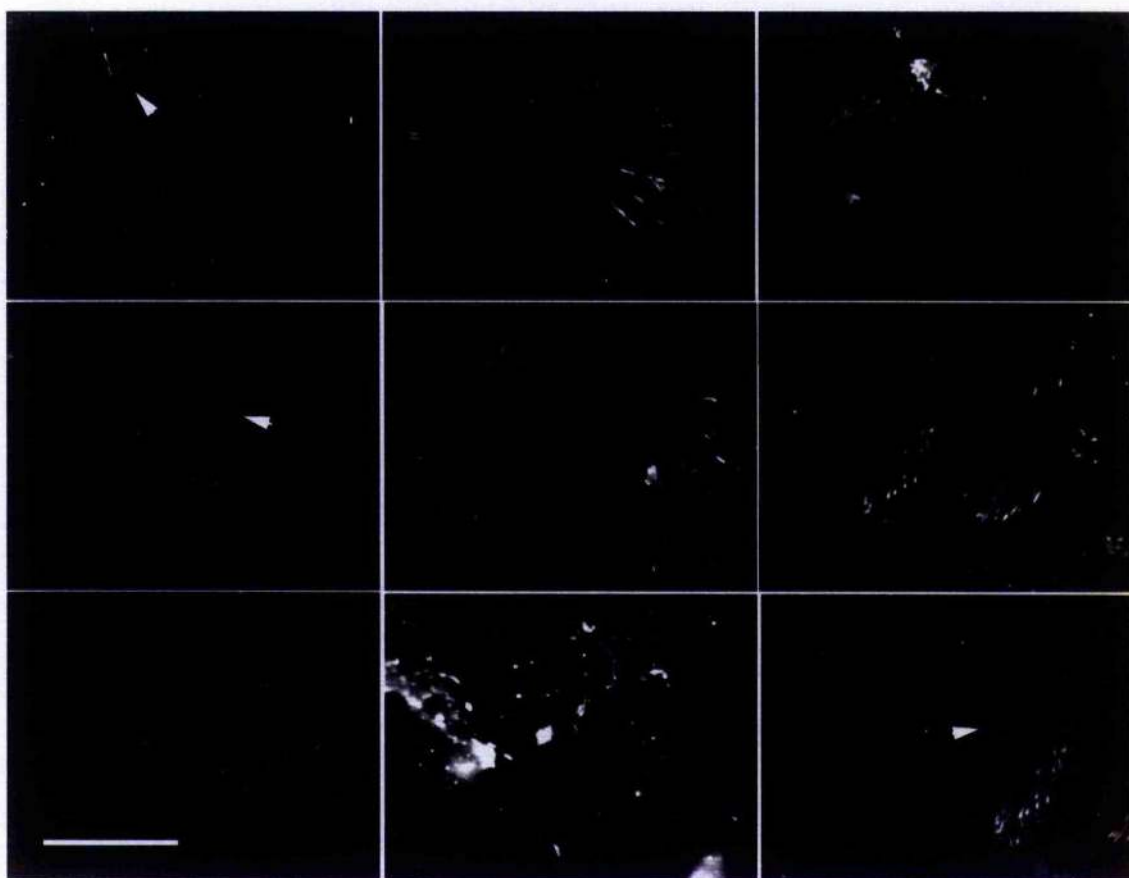
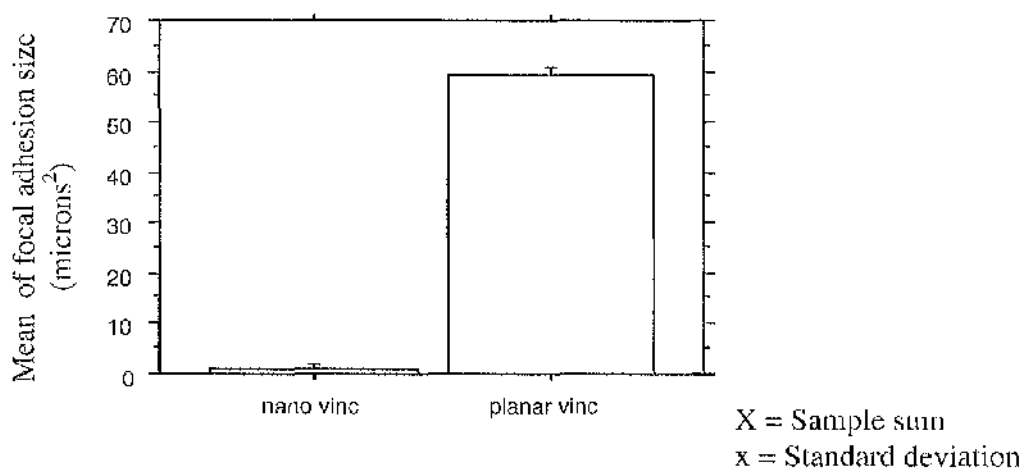


Figure 6.4 Vinculin containing focal contacts of epithelial cells cultured on nanopitted PCL topography. The focal adhesions seen in these populations of cells are visibly disrupted. These are fewer in number and the focal adhesions appear smaller. It is also important to note the speckling of vinculin throughout the cell displaying an abnormal sparse dispersal of vinculin in these cell populations (Scale bar = 10 μm).

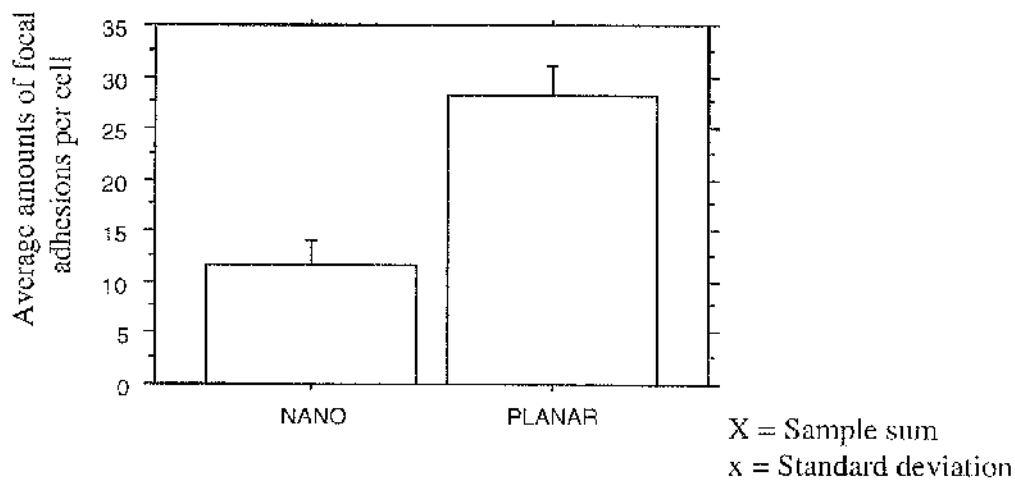
Focal adhesion sizes on nano and planar topography



	Nano	Planar		Nano	Planar
Mean	1.2	59.2	Max	34.6	46.8
Std Dev	3.7	6.0	Min	.1	54.0
Std Error	0.3	0.5	ΣX^2	1755	421303
Count	119	119	Σx^2	1595	4141

Figure 6.5 Average size of individual vinculin containing focal adhesions. The size of focal adhesions for cells cultured on a nanopitted are smaller than that of those cultured on a planar substrate. From the graph it can be clearly seen that the size difference of the focal adhesions are significantly different ($P < 0.0001$).

Amount of focal adhesions per cell



	Nano	Planar		Nano	Planar
Mean	12	28	Max	22	38
Std Dev	5	6	Min	2	3
Std Error	1	1	ΣX^2	5837	30009
Count	36	36	Σx^2	1013	1505

Figure 6.6 Average amount of focal adhesions present per cell. The number of focal adhesions associated to cells on nanopitted topography was significantly less than those of the control planar topography cell populations ($P < 0.0001$).

β -tubulin distribution

The β -tubulin distributions were also examined in epitenon cells cultured on nanotopography and a control planar topography after a period of 48 hours. From the images obtained from the confocal microscopy, clear differences between the arrangement of β -tubulin in the cells on the two types of topography were visible. In Figure 6.7 the cells on the control planar surface are seen to exhibit a normal patterning of β -tubulin. It is also notable that the cells on these surfaces have started to proliferate, with groups of cells being imaged as opposed to the single cells present in figure 6.8. This is in stark contrast to the patterning shown by epitenon cells cultured upon nanotopography. It can be seen that the β -tubulin formation was disrupted upon the nanopitted topography. In general the β -tubulin staining was undefined, and quite often was dispersed throughout the cell. This indicates that the β -tubulin has not formed in its usual way. β -tubulin normally would be found to combine to form long continuous structures within the cell. The development of the cytoskeleton of cells appeared severely impaired as a direct result of those cells coming into direct contact with the ordered nanotopography.

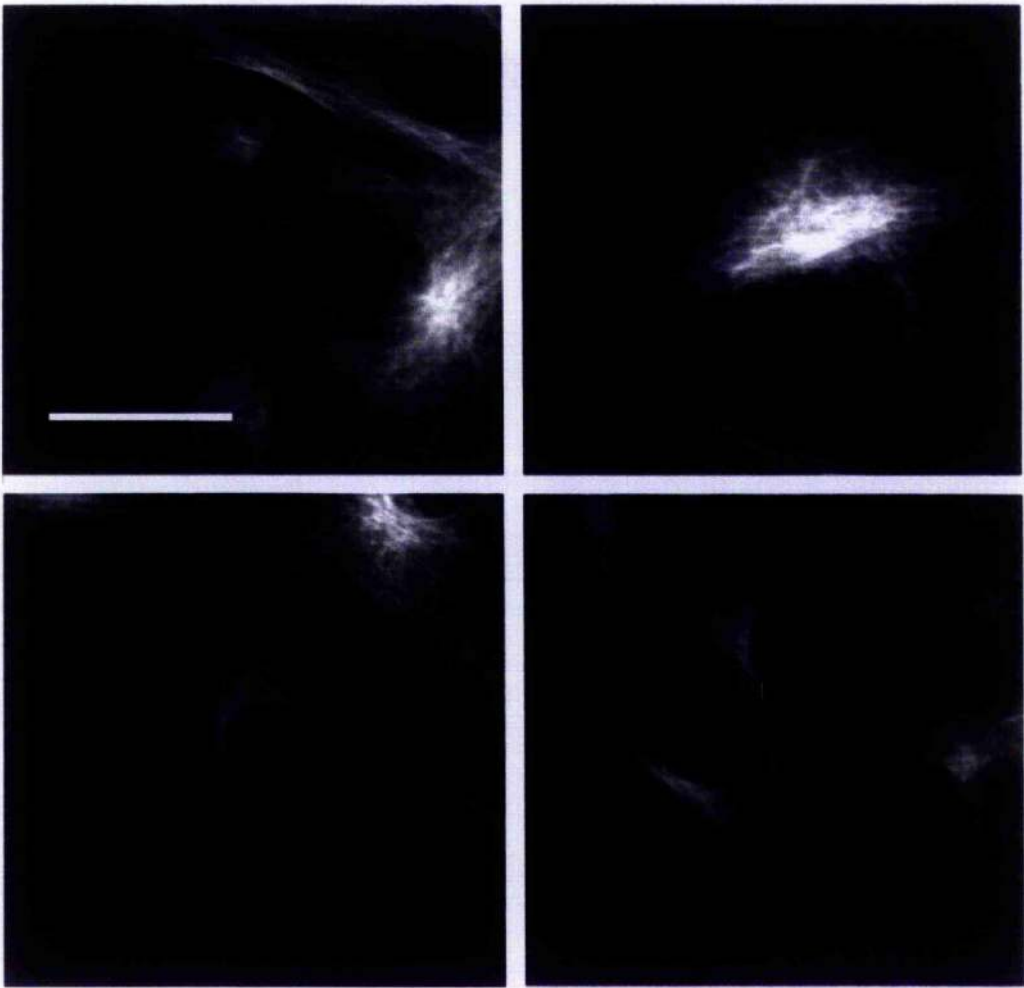


Figure 6.7 β tubulin staining of HGTFN cells cultured on a control planar topography for 48 hours. The β -tubulin configuration in these arrays of cells are classic in nature forming individual continuous branching structures (scale bar = 10 μm).

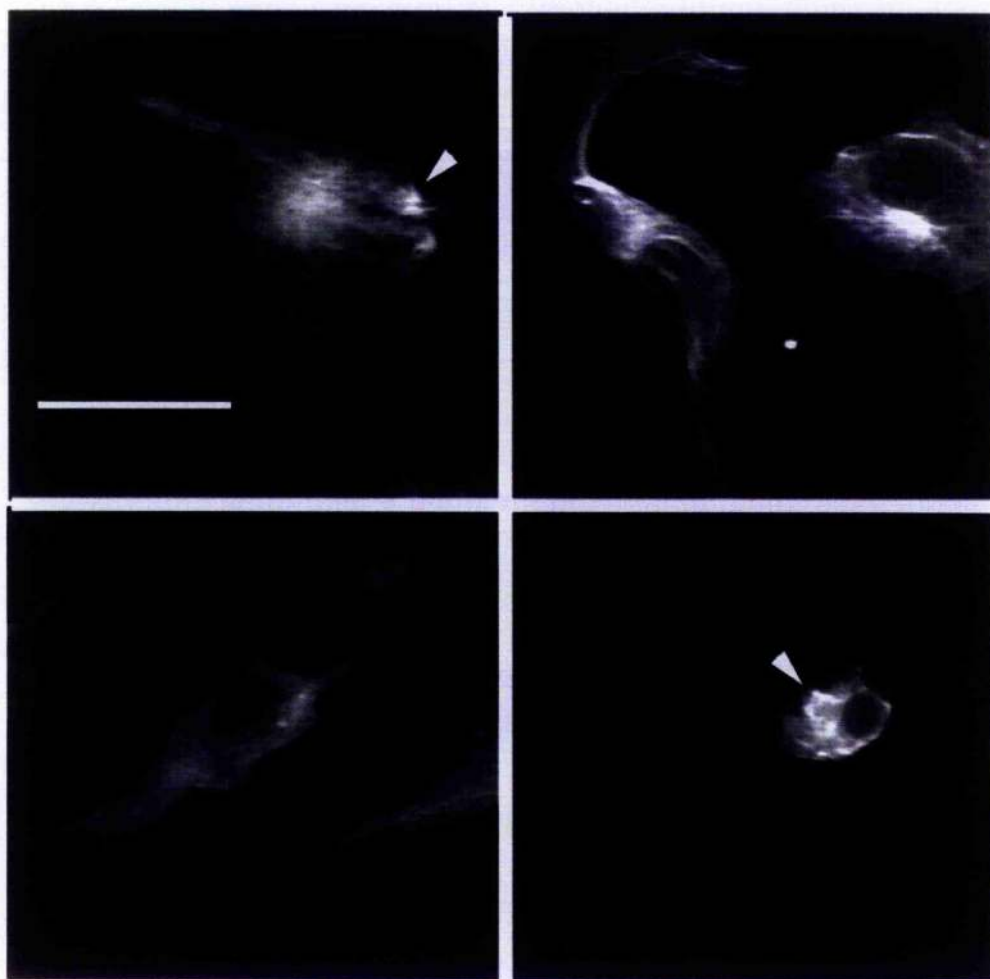


Figure 6.8 β tubulin staining of HGTFN cells cultured on nanopitted topography for 48 hours. The β -tubulin arrangements within these cell populations appears markedly different to that displayed by the control samples (Figure 6.7). The β -tubulin arrangement has clumped together and appears undefined pointing towards an obvious curtailment in formation by the underlying nanotopography (scale bar = 10 μm).

Discussion

The effect of the nanopitted surface upon the components of the cell cytoskeleton was investigated. These studies demonstrate that cells cultured on nanopitted topography have disrupted and undeveloped cytoskeletal components. The examination of the cytoskeleton was tackled by the fluorescent probing of three integral components; F-actin, β -tubulin and vinculin containing focal adhesions, which combine to form what is generally, termed the cytoskeleton.

F-actin cytoskeleton

The visual examination of confocal images of the F-actin cytoskeleton highlighted critical differences in the formation of the cytoskeleton of cells cultured on nanopitted topography versus those cultured on the control planar surface. The formations of long interconnected strands of F-actin were notably absent from cells cultured on nanopitted topography. Instead of a defined structure, a disrupted one was present in cells cultured upon nanopitted topography. The condensing of these F-actin components embodied the malformation of the F-actin cytoskeleton. The signature branching of the F-actin cytoskeleton found in the control planar cultured cells was replaced by small regions of disorganised F-actin in cells in contact with the nanopitted topography.

Vinculin containing Focal adhesions

The visualisation of vinculin containing focal contacts reveals notable difference between cells on the two types of topography. The focal contacts that are formed between the cell and the planar topography are deemed to be normal in nature, being well organised and well developed. However, the focal contacts of cells cultured on a nanotopography are notably different in several respects, the first of which is that these focal contacts are far fewer in number than their counterparts on a planar topography. The focal contacts on the nanopitted surface have been shown to be significantly less in number, ($P < 0.0001$) than those on the planar surface. Moreover these focal contacts are smaller in size. It was noted from the confocal images that there is a substantial amount of speckling of vinculin through the cell, pointing towards undeveloped and immature adhesions being formed. This observation is backed up by statistical analysis of the individual focal adhesion sizes on the nanopitted surface being significantly smaller ($P < 0.0001$) than the adhesions associated with the planar topography.

β -tubulin distribution

The confocal analysis of β -tubulin distributions of cells attached to the experimental nanotopography and control planar topography revealed differences in the patterning and overall development of tubulin. In the cells that were cultured upon the planar topography the formation of long tubulin strands emanating from microtubule organising centres was apparent. This was indicative of the expected tubulin morphology in a normal cell-

biomaterial interaction. Tubulin patterning within cells cultured on the nanotopography was noticeably different. The tubulin was disorganised and could be seen to be largely condensed into undefined regions in the cells.

Chapter 7

Topography or chemistry?

Introduction

A question that is repeatedly asked when dealing with the reaction of cells to substrate topography is whether cells are reacting to the topography or the chemistry of the substrate in these interactions. The only experimental work in this field which has taken a direct approach to solving this dilemma, was work detailed by Britland et al., (1996). They combined topography and chemical patterning of poly-L-lysine bound to the surface and examined the orientation of neurites to these devices. Britland and his co-workers aligned the chemical patterns, which were 25 μm wide, to the bottom of the grooves. They printed the laminin tracks at 90° to the grooves, which were all of varying depths. The results from devices with chemical tracks orientated at right angles to the topographic cue showed that when the grooves were 500 nm deep or less, the cells reacted chiefly to the chemical cue. On deeper grooves the topographic cue over-rode the chemical one and at 5 μm depth the topographic effect oriented about 80% of the cells and the laminin only 7%.

These interesting results however have raised further questions Curtis et al., (1998) had suggested that the reaction of cells to tracks of laminin and other proteins were in actual fact a reaction of the cells to the nanometric topography at the edge of the track. This is in effect reversing the viewpoint we have from chemistry to topography. It was also noted when examining the reaction of the neurones to the chemically patterned tracks, that cells often

align to the edges of the tracks. This observation suggested that it was not cells reacting to the topography of the groove, but instead it was the topographic cue created by the shape of the chemical cue.

The hypothesis that the protein tract were creating a topographical cue was tested by Pritchard et al., (1995) who designed a system where the chemical tracts did not have nanometric edges. They achieved this by filling the grooves made between the protein ridges with an alkane thiol. The cells in this relatively featureless environment still aligned to the tracts. These results appear at first sight to be a convincing demonstration that cells react to chemical patterning. However the Au-alkane thiol system used was discredited by Wang et al., (1997) who showed that protein slumping, dislocation and perhaps even denaturation takes place at the edge of the tract due to the presence of the short chain alkane thiols.

The aim of this chapter is to add further fuel to the debate over what has a greater effect over cell behaviour; chemistry or topography. It was demonstrated in Chapter 3 that the spreading area of a cell coming into contact and successfully adhering to the nanotopographic cue is significantly smaller than the spreading area of cells adhering to a planar topography ($P < 0.0001$). Here the question being asked is what the effect would be of introducing poly-L-lysine (PLL) directly to the surface to increase cell adhesion and spreading. The principle behind the method is that the polycationic polylysine molecules adsorb strongly to various solid surfaces, leaving cationic sites, which combine with the anionic sites on cell surfaces (Mazia et al., 1975). This experiment would be a direct comparison of two diametrically opposed cues; a topographical cue that decreases cell spreading

and adhesion against a chemical cue. This should have the effect of actively increasing cell adhesion and spreading.

Results

Cells were cultured upon nanotopographic and planar PCL surfaces for 48 hours and incubated at 37 °C. The area of cell spreading on nanotopographic surface features was compared directly with spreading on a planar topography. This experiment demonstrated that the overall spreading size of cells cultured on the nanotopography was significantly smaller when compared with cells spreading on a planar topography ($P < 0.0001$). Cells cultured on the planar topography were in the region of 300 μm^2 larger than their counterparts cultured on the nanotopography (1600% larger). The different morphology of epitenon cells on two surface types visible in figures 7.1 and 7.2. It can be clearly seen that the cells cultured on a planar larger spreading area than cells cultured upon nanopitted topography. It can be observed from the images that cells cultured on the planar topography have large lamelapodia, which are on the whole absent from cells cultured upon the nanotopography. In figure 7.3 the outlines of cells spread on nanotopography have been overlaid on to the planar image to further emphasise this disparity.

Both planar and nanopitted surface types were treated with poly-l-lysine and cultured with epitenon cells for 48 hours in parallel with un-coated samples with the identical topography. The results in figure 7.4 and figure 7.5 show that surfaces coated with PLL increased the area of cell spreading on these treated surfaces in comparison to the spreading of cells on similar surfaces

without coating ($P < 0.0001$). Thus demonstrating that the poly-L-lysine was having the desired effect of increasing overall adhesion.

However, analysis of the data generated by cell adhesion counts, showed that the PLL does not cancel out the effect of the regular nanopitted surface on the numbers of cells attaching (Figure 7.6). The overall amount of cells attaching to the surface was not elevated by the presence of PLL ($P = 0.1369$).

With respect to the PLL coating of the nanopitted surface, the PLL treatment crucially did not increase the area of cell spreading on the nanopitted area significantly ($P = 0.894$) when compared with a non-coated surface. When the PLL-coated nano surfaces are compared with the planar surface there are still significant differences between the indicators of how well the cells are adhering (Figure 7.5). It is apparent that the PLL has had the direct effect of increasing cell spreading yet the underlying effect of the nanometric surface to diminish cell spreading is still significant. The amount of cell spreading between the nanotopographic surface types was not significantly different (Figure 7.5). Thus demonstrating that the repulsive cue present at the nano surface had not been affected significantly by the addition of PLL to the surface.

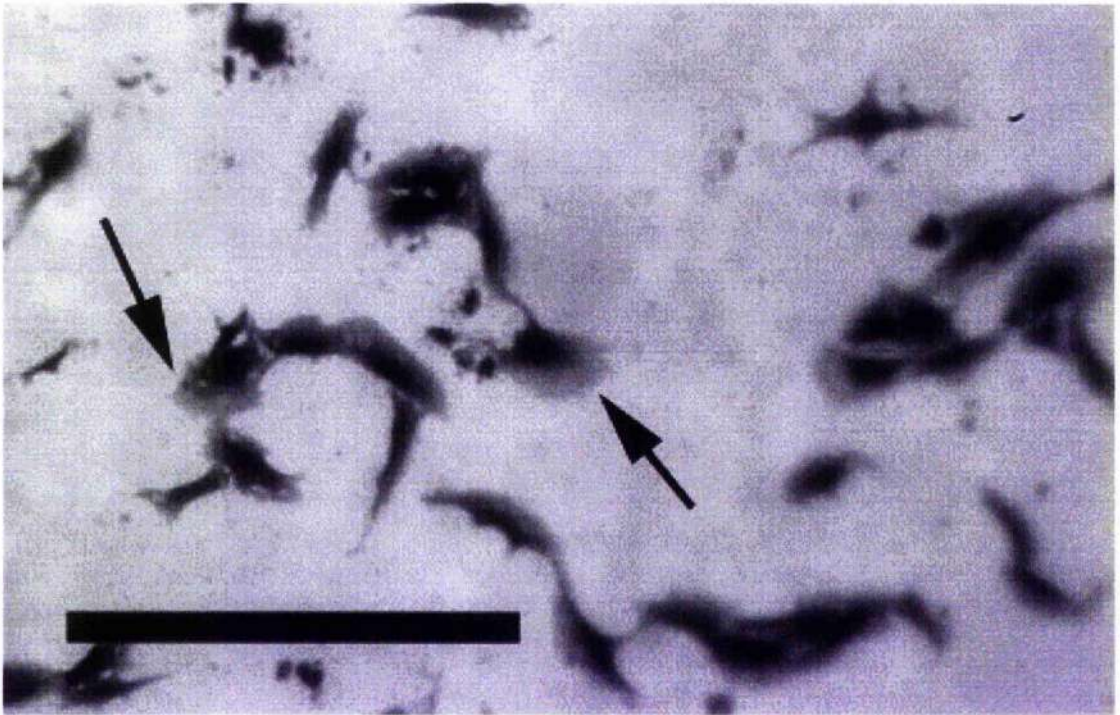


Figure 7.1 Morphology of epitenon cells cultured on planar topography for 48 hours (cells stained with Coomassie brilliant blue). The arrows highlights the presence of lamellapodia emanating from the leading edge of the cells in this image. Scale bar = 40 μm

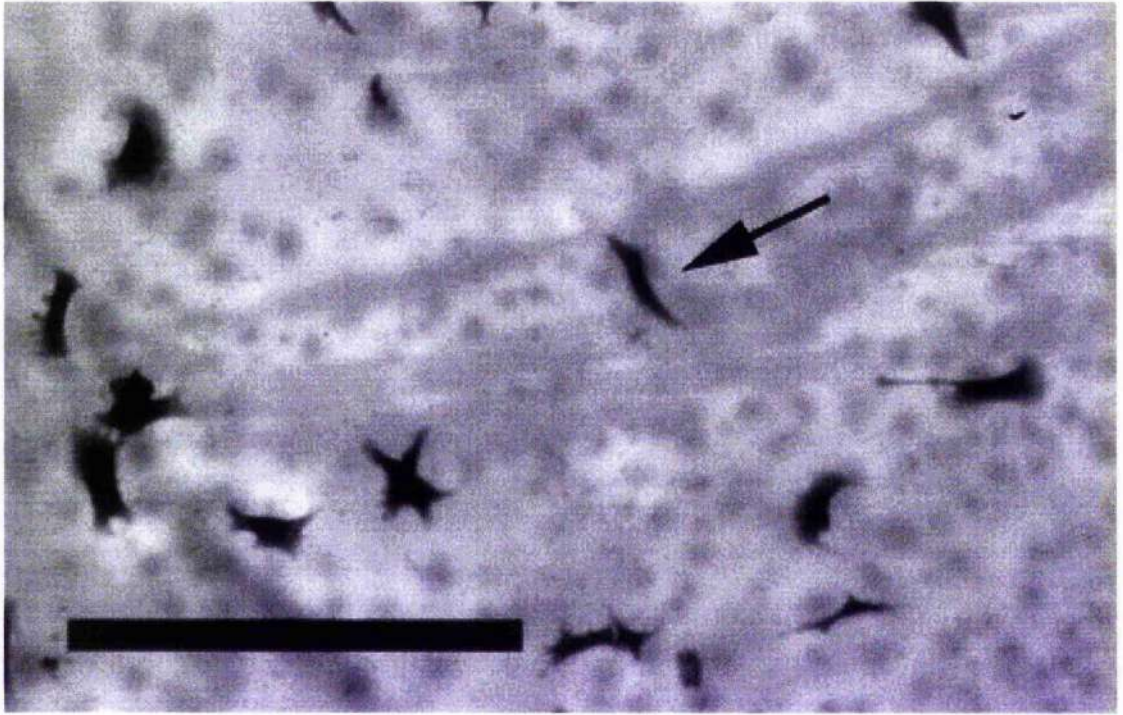


Figure 7.2 Morphology of epitenon cells cultured on nanopitted PCL topography for 48 hours (cells stained with Coomassie brilliant blue). The cell highlighted in this image is much smaller than its planar counterparts and lacks a developed lamellapodia. Scale bar = 40 μm

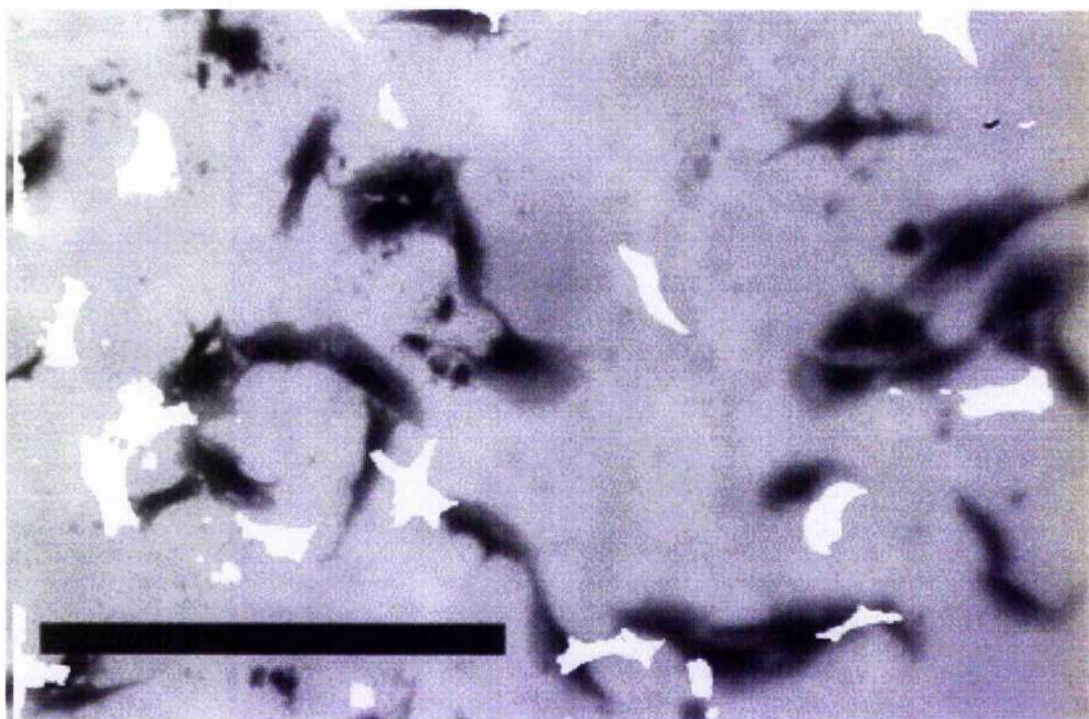


Figure 7.3 Direct comparison of cell morphology between cells cultured upon two types of topography. Cells highlighted in white are cells cultured on nano-pitted PCL. It is visible in this overlay of images that the overall size of cells cultured on nano-pits is noticeably smaller and lacks a developed lamellapodia.

(Scale bar = 40 μm).

Cell spreading area on 4 different surface types

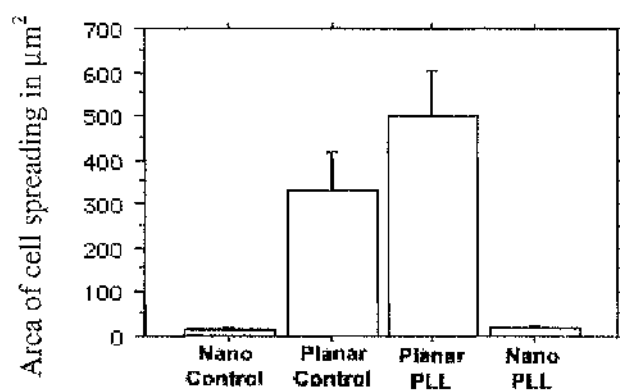


Figure 7.4 Graphical representation of epitenon cell spreading area for cells cultured on nano- and planar substrata. Control surfaces were untreated ϵ -PCL; the PLL surfaces were incubated with poly-L-lysine for 15 minutes prior to culturing of cells (for statistical test results consult Table 1).

Means of cell adhesion to four different surface types after 48 hours

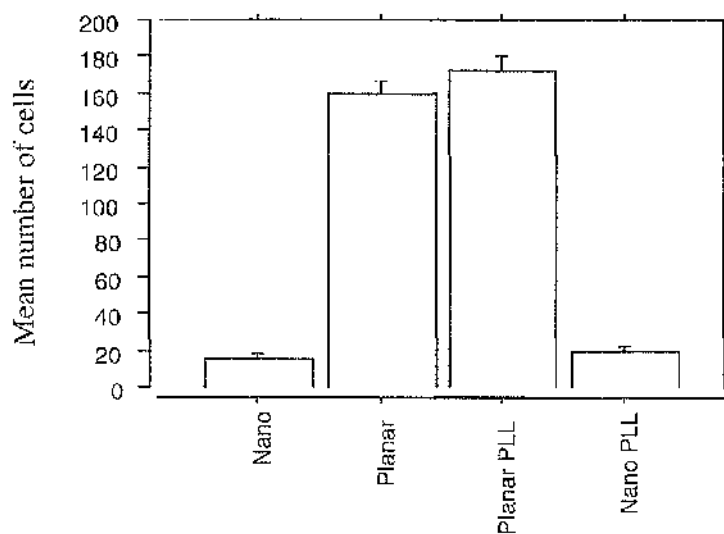


Figure 7.5 Graphical representation of epitenon cell adhesion. Cells were cultured on nano- and planar substrata; control surfaces were untreated PCL; the PLL surfaces were incubated with poly-L-lysine for 15 minutes prior to culturing of cells (for statistical test results consult Table 2).

TABLE 1
**P-VALUES OF STATISTICAL
 COMPARISONS OF CELL SPREADING ON 4
 DIFFERENT SURFACE TYPES.**

Surface comparison	P-VALUE
Nano control Versus Planar control	< 0.0001
Nano control Versus Planar PLL	< 0.0001
Nano control Versus Nano PLL	0.8948
Planar control Versus Planar PLL	< 0.0001
Planar control Versus Nano PLL	< 0.0001
Planar PLL Versus Nano PLL	< 0.0001

TABLE 2
**P-VALUES OF STATISTICAL
 COMPARISONS OF NUMBERS OF CELLS
 ON 4 DIFFERENT SURFACE TYPES.**

Surface comparison	P-VALUE
Nano control Versus Planar control	< 0.0001
Nano control Versus Planar PLL	< 0.0001
Nano control Versus Nano PLL	0.1369
Planar control Versus Planar PLL	< 0.0001
Planar control Versus Nano PLL	< 0.0001
Planar PLL Versus Nano PLL	< 0.0001

Discussion

The results in this chapter demonstrate that the effect of surface chemistry upon cell behaviour is complex and interesting. These experiments have been able to circumvent concerns raised by Curtis and Wilkinson (1998) regarding the possible topographical effect generated by chemical patterning in Britland's experiments (Britland et al., 1996). This was due to the PLL upon the topographic cue completely covering the nanosurface without the possibility of exerting edge effects caused by laying a chemical cue in stripes as in the Britland study. It was also demonstrated that the chemical cue chosen did indeed increase cell spreading of cell in contact with a planar topography ($P < 0.0001$).

Results here demonstrate that cell spreading in populations cultured on unmodified planar and nanopitted PCL showed that spreading area of cells cultured upon nanopits was significantly smaller ($P < 0.0001$) when directly compared to the area of spreading on a control planar topography.

The key finding of these experiments was that there was no statistical difference between the spreading of a cell encountering a nanotopographic substrate with or without the PLL coating. This result demonstrated that it was possible for the underlying topography to be dominant over a competing chemical cue. It was then possible to state that the repellent cue generated by the nanotopography was greater than that of the opposite attractive cue generated by the PLL (Gallagher et al., 2002).

This demonstrates for the first time that nanotopography is capable of overcoming a chemical cue and that the effect generated by the topography is dominant over the chemical one.

Chapter 8

General Discussion

The interactions of cells with topographic features have been investigated since the late nineteenth century. Loeb (1898) was the first scientist to conduct research in the field of the stereotropism of cells, which was further developed by Harrison (Harrison, 1912). His research led to the invention of tissue culture. Harrison's observations that a solid support was necessary in order for a nerve cell to extend through the medium began the study of tissue engineering as we know it today. However, it was not until the last third of the century that defined topography on a micrometric scale became available to the cell biologist. Only then did detailed studies of contact guidance with respect to well defined substrata become a widely researched field. The natural progression was to reach further down the metric scale to the realm of the nanometre and investigate nano-scaled structures and their effects upon cultured cells.

The major advances in nanofabrication techniques only truly began in the 1990s. The main basis of this thesis is to investigate the effect of a defined nanotopography, manufactured by electron beam lithography, upon the behaviour of cells. This study is influenced by and is important to the manufacture and production of biomaterials for clinical use, *in vivo*. The hypothesis that surface texture of a biomaterial can exert influence upon cells that come in contact with it was central to this study. The purpose of research on the nanometre scale is to observe the effects of controlled surface

patterning and then in turn apply this knowledge to the design of surface coatings for biomaterials and cell devices of the future.

Such investigations of cell interactions with regular nanotopographies is believed to be entirely novel. However studies have been carried out on the cell reaction to defined random nanotopography. Turner et al., (1997) investigated the effects of random silicon columnar structures upon cells, the columnar structures referred to as silicon grass. They found that transformed astrocytes from a continuous cell line showed a preference for wet-etched regions of the surface over grassy regions. In contrast, primary cortical astrocytes from neonatal rats showed a preference for silicon grass over the wet-etched surface. This seminal work acted as springboard for the work carried out in this thesis. In this study, we take this investigation a step further, where regularity and symmetry of the topography were introduced to the experimental approach of studying the effect of ordered nanotopography upon cell behaviour.

With respect to the question of what the role of ordered nanotopography is in regards to the reaction of cells to topography, work carried out by Sutherland et al., (2001) lead to the fabrication of random nanometric surfaces by the adsorption of polydisperse nanoparticles onto solid surface to create random nanostructured surface. They adsorbed negatively charged polystyrene particles with a diameter of 110 nm, onto positively charged titanium, giving rise to a randomly distributed nanotopographic surface for *in vitro* cell studies. The results of work carried out to investigate the role of cell adhesion with these random nanotopographies showed no marked change in cell adhesion.

Reduction of cell adhesion as a result of ordered nanotopography

In chapter 3 the adhesion of cells to nanopitted topography embossed into a PCL substrate was investigated. The results of these cell adhesion studies demonstrated that epitenon cell adhesion to the nanopitted region of topography over varying time points of 4, 20, and 96 hours was significantly reduced. This was then reinforced by subsequent experiments involving epitenon cells cultured for a substantially longer time period of 37 days. It can be seen in figure 3.5 that the epitenon cells were cultured to confluence upon the planar topography but failed to proliferate to any notable degree on the nanopitted topography. These adhesion experiments established that the adhesion of epitenon cells appeared to be directly influenced by the topography cue or some other derivative feature.

The significant reduction in adhesion was also displayed by other cell types namely, BHK 21, HGTFN, and B10D2; all of which all showed a significant reduction in cellular adhesion to nanopitted topography. These results indicated that the effect was not cell type specific. This was in direct contrast to the work carried out by Turner et al., (1997), where they found a reduction in adhesion of transformed astrocytes from a continuous cell line upon random nanometric projections. Adhesion of primary cortical astrocytes showed a reversal in behavior, eliciting a preference for the random topography.

Cellular response to nanotopography

The focal adhesion response of cells to random nanotopography was investigated by Kononen and colleagues (Kononen et al., 1992) who studied the effect of surface processing on the attachment and proliferation of fibroblasts on titanium. Their findings in relation to sandblasted titanium are echoed by the results in this thesis. The topography of note was sandblasted titanium, which had a nanometrically rough random topography. They showed that the gingival fibroblasts cultured on sandblasted surfaces lacked vinculin-containing focal adhesions. This was coupled with a reduction in the spreading of the fibroblasts and an absence of a developed cytoskeleton.

These results are similar to the findings in this thesis with regards to an ordered nanotopography. They point towards the electrostatic theory in which sharp points and edges give rise to locally high charge densities. Thus, on the sandblasted titanium surface there may exist locally relatively high electric fields, whereas the planar does not possess such local differences in electron density. It should be noted that such mechanical states are related mainly to bulk material, and are therefore largely absent from thin titanium foils evaporated, for example, onto plastic or glass substrata (Kononen et al., 1992). The findings and hypothesis of Kononen et al., (1992) can be related to the type of nanostructure used in this thesis. At sharp points or ridges in a structure, a high build up of charge would be present, not electrons as they describe it. Indeed in the context of an ordered nanopitted structure you would have a uniform build up of charge across the entirety of the ordered nanotopography.

This is further supported and expanded by the observations of Curtis et al., (2001) with regards to nanopitted surface topography and its symmetrical nature. They claim it is this symmetrical nature that plays a pivotal role in reducing adhesion markedly. It is noted that the adhesion of cells to discontinuities such as vertical cliffs results in high adhesion at the cliff. The difference in the adhesive properties is proposed to be a result of the symmetry or its converse, because the cliffs are anti-symmetrical, namely the top edge is 'convex' and the bottom is 'concave'. The cliffs, which promote adhesion (Wojciak-Stothard et al., 1996b), are ordered in one dimension, but are anti-symmetrical. Curtis et al., (2001) also noted that non-living particles of approximately the same size as cells show a similar low adhesion to regular topography (Figure 8.1).

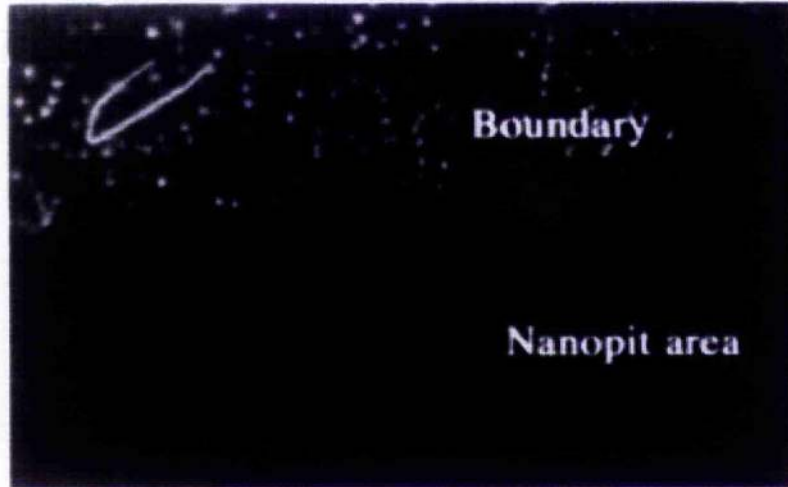


Figure 8.1 Attachment of fluorescent carboxylate 20 μm diameter beads to a nanopitted surface in polycaprolactone. The medium used was protein-free saline. Note the failure of attachment over the pitted area and extra accumulation just outside the nanopitted area. The horseshoe-shaped object is a piece of cellulose lint that fell into the sample. (Image taken from Curtis et al., 2001).

It has been observed by Gleiche et al., (2000) that at a glass-water interface there was a non-linear behaviour of interfacial forces on phospholipid strips which had a distance of around 100 nm between them. In this and other studies (Fraudin et al., 2000; Higgins et al., 2000), there appears to be a scale limitation to these phenomena, in that non-linear effects appear below certain scale limits (Curtis et al., 2001). These limits were identified as being in or around the 100 nm region which is close to the nanometric scale used in this thesis. It was suggested by Curtis et al., (2001) that this limit was possibly that of the maximum effective range of van der Waals (dispersion) forces, and that the van der Waals attractions between pockets of water formed on top of nanopits might prevent full wetting of a surface, but this would only occur if the forces were balanced in a array of pits or pillars.

This dispersion hypothesis is now furthered by the experiments in Chapter 5, in which the filopodia of cells probing the nanometric features indicated that there was a preference for the filopodia, (which are of a similar diameter to the nanopits) to become what is termed as 'ridge huggers' as opposed to 'pit pluggers'. These observations add weight to role of van der Waals forces generating a non-wettable surface, in that the forces being generated by the close proximity of the other pits are preventing the pits being probed by filopodia. Regarding the lack of probing by filopodia relate to findings regarding a nanoporous polymer 'Versapore' which had pores ranging from 400 nm to 3 μm in width (Campbell and Craig, 1989). It was found that fibroblasts adhere preferably to pores of sizes between 1 and 3 μm , whilst pore sizes of between 200 and 300 nm reduced adhesion. It was also noted from SEM micrographs that filopodia do not enter into surface openings of the

200 nm and 300 nm pores allowing the cells no mechanical foothold or anchorage.

Previously detailed experiments involving the repulsion of polystyrene beads when introduced to the quartz master (see figure 8.1) add further weight to the probability that the effects of the nanopitted topography on cell behaviour detailed in this thesis are due to physical forces. It should be noted that the beads are between 25 and 35% of cell diameter, which places them in the general size class of cells (Curtis et al., 2001).

The role of the cytoskeleton

In Chapter 6 the reaction of the components, which make up the cytoskeleton were examined with the aid of immuno-cytochemistry and confocal microscopy. From the resulting images generated, the β -tubulin, F-actin, and vinculin containing focal adhesions were shown to be directly influenced by the underlying nanopitted topography. In the case of β -tubulin and F-actin the development of these cytoskeletal components were visibly malformed showing a lack of defined structure that was present in the cytoskeleton of the cells cultured on the control sample. These findings are an echo of O'Hara and Buck (1979) whom observed that the cellular reaction to topography is influenced by the cytoskeletal organisation, the adhesion receptors involved, and the mobility of the cell.

It is thought possible that this lack of a defined structure could possibly due to the cell taking on the shape and dimensions of the nanopitted topography. There are suggestions (Curtis and Wilkinson, 1999) that cells compare

mechanical stresses within different regions of themselves, both those produced by the internal contractile mechanisms of the cell and those imposed by other cells and events outside the tissue. Thus if a cell attempts to bend round a sharp corner, stress distributions within the cell will be altered. This explanation of a possible mechanism of cell sensing and reacting directly to the topographic environment is further added to by the finding of Dunn and Heath (1976), who noted that cells will not cross ridges though they will migrate along them. Dunn and Heath suggested that the cause of this was that the cytoskeleton of protein fibres within the cell, especially those made of the protein actin, are relatively rigid and unbendable (Dunn and Heath 1976). These fibres are usually oriented and to impinge on and effect would have a knock on effect on their propensity to orientate, which would cause a stress concentration within parts of the cytoskeleton. In work by Bell et al., (1979) it was noted that fibroblasts exert considerable forces to their substratum and contract collagen gels. Meyle et al., (1995) concluded that the intracellular fibres must be straight and not bent. They implied that the reason cells align to grooved substrate topography is to avoid distortion of their cytoskeleton.

In light of the findings of poor cell adhesion and the distortion of the cytoskeleton, it is feasible that the cellular reaction is indeed affected directly by the cytoskeleton. The cytoskeleton is trying to take on the shape of the underlying topography and hence is having to bend repeatedly. This in turn causes a build up of stress which can be likened to the coiling of a spring where the more undulations that it is put under increases the amount of stress that is localised at specific point.

Focal adhesion spacing

Thus far, possible mechanisms for the reduced adhesion of cells have been suggested. Another possible mechanism for the lack of adhesion could be due to the reduction of vinculin-containing focal adhesion size and number observed in chapter 6. It is also conceivable to attribute the lowered long-term adhesion to the disruption of the maturation of focal contacts. Massia and Hubbell (1991) have shown that the density of RGD peptides is crucial to cellular attachment. At very low densities cells will attach but not form focal adhesions (440 nm), but at slightly higher density (144 nm) cells will spread and form focal adhesions. This requirement for a high density of integrin ligands suggests that integrin clustering is necessary in order for focal contacts to mature. The nanopitted surface could thus disrupt integrin clustering by allowing only a limited number of integrins to interact at any one point with the surface; this may account for the small vinculin patches forming over nanostructured areas (Gallagher et al., 2002).

It is suggested that the influence that the nanopitted region has on the arrangement could be the same phenomenon seen in Chapter 5. It was noted that the filopodia of cells cultured on nanopitted topography had a preference for their filopodia to attach to the ridge (i.e. 'ridge hugger') as opposed to covering over the pits ('pit pluggers'). With this in mind it is reasonable to assume that the focal adhesions are also following a similar formation and being allowed to adhere to the top of the ridges and thus being expelled from the region above the pits reducing the overall area of attachment. In addition, the spacing of the cell-surface interaction could be inhibiting the internal interaction between integrins, which is necessary for cross-phosphorylation

and the establishment, as well as maintenance of, mature focal contacts (Chrzanowaska-Wodnicka and Burridge, 1996).

Cell migration

The increase in cell migration of epitenon cells cultured on a polycarbonate nanopitted topography observed in Chapter 5 can be directly related to the reduction in size and numbers of vinculin-containing focal adhesions observed in Chapter 6. The correlation between the lack of actin stress fibres and vinculin-containing focal adhesions is thus associated with a lack of motility and a strong adhesion to the growth substratum. This is observed within the cells cultured on planar topography, which have developed stress fibres. Vinculin-containing focal adhesions have a reduced motility, which is in direct contrast to the finding of cells cultured on nanotopography in this thesis. Cells, which are rapidly moving, such as those on a nanopitted topography, lack all of these structures (Chrzanowaska-Wodnicka and Burridge, 1996). This is a cause and effect relationship with the nanopitted topography influencing cell behaviour directly as it has an effect upon focal adhesion formation which then has a knock on effect upon the cytoskeleton which leads to an increase in cell motility.

Chemistry versus topography

The experiments regarding the influence of topography upon cell behaviour whilst a competing chemical cue is present gave a further insight into which cue has a dominant effect over the other. This study followed on in a similar

vein to the Britland et al., (1996b) work in which chemical stripes align cells at right angles to the competing grooved topography. The results from the experiments in Chapter 7, in which an adhesion-promoting cue of poly-L-lysine covered the entire adhesion-reducing cue of nanopitted topography, demonstrated that a concentration of 1 mg of Poly-L-lysine per ml of PBS was enough to increase cell adhesion and hence cell spreading area. Nevertheless the increase in adhesion and spreading size of cells on nanopitted topography was not enough to impinge on the outcome of reduced adhesion and spreading area. It can therefore be deduced from these experiments that the lowering of the adhesive properties generated by the nanotopographical surface is greater than the adhesion-promoting effect generated by PLL.

Spatial control

The results of using defined areas of non-adhesive nanotopography coupled with adhesion compatible planar topography to predetermine the positioning of cells in Chapter 4 yielded promising results. It demonstrated that it is possible to pattern a surface with areas of planar topography where cells adhered and spread normally within these confines and in general avoided the nanopitted topography. These results are of great importance to the tissue engineer, paving the way for a surface topography to be used to pattern cells with a high degree of accuracy onto a biomaterial scaffold. In theory, it is possible that this could be utilised as a guide for extending neurones into repairing tissues and aid the endothelial cells of the blood vessels to penetrate, as they must, into nearly all repairing tissues. Equally importantly we must be

able to position all cells and make them hold that position (Curtis and Riehle, 2001).

Future work

Different nanometric surface topographies

In this thesis only one size of nanometric surface pattern was investigated, that of pits 80 nm deep with a centre-to-centre spacing of 300 nm. It would be of great interest to study other depths and spacing on a nanometric scale. The preference for filopodia to attach to the planar regions of topography within the nanopattern could be furthered by investigating the reaction of cells with an increased centre-to-centre spacing. This could allow cells a greater area for attachment giving rise to the possibility of cells laying down more focal contacts with the surface and hence a possible knock on effect upon levels of cell adhesion. Yet another parameter that could be altered would be the pit widths to see what effects if any this has on the reaction of the cells to the topography. To address the question of symmetry and its role in reducing the adhesion of cells (Curtis et al., 2002) it would be interesting to design and fabricate structures that were regular but made up of offset rows of pits (Figure 8.2).

Ideas for future structure fabrication



Figure 8.2 This is a pattern that could be used to test what the role of symmetry plays in regards to the reduced adhesion of cells, this hypothesis was proposed in Curtis et al., (2001). Part A is a representation of the symmetrical properties of the pattern used in this thesis. In part B is a new design for a nanopitted substrate, this pattern could help solve issues regarding the role of symmetry and cellular reaction

Protein adsorption

The effects of protein adsorption upon the ordered nanotopography used in this thesis would be another interesting experiment to assay whether or not there are any changes when introduced to a topographic cue. This could be achieved by incubating proteins (possibly ECM components) with the surface and then assaying the levels of protein present on the surface by staining with Coomassie blue and measuring the optical density of the protein content on a nanopitted surface with a planar surface as a control. The surface area of the nanopitted region would be larger than that of a planar surface, and this would have to be taken into account when measuring the optical density.

Contact angle measurements

Contact angle measurement should be conducted on the nanopitted structures to obtain a precise value. Surfaces with a water contact angle above 150° (superhydrophobic surfaces) have recently been attracting a great deal of attention. Because of its small contact area with water, both chemical reactions and bonding formation through water are limited on a superhydrophobic surface.

Surface treatments

Rather interesting experiments could be carried out to further test the effects of a topographical cue against that of a chemical cue. It would be ideal to conduct similar experiments to those in Chapter 7 involving other chemical

cues known to increase cellular adhesion. Nanometric surfaces could be coated with fibronectin, laminin and RGD peptides, to further stretch the topography versus chemistry debate. These experiments would demonstrate conclusively whether or not the non-adhesive effect of the nanotopography was greater than a variety of competing chemical cues. It would also be of interest to find out what concentration of adhesion promoting cue if any can overcome the non-adhesive effects of the ordered nanotopography.

References

Abercrombie, M. and Dunn, G.A. (1975). "Adhesion of fibroblasts to substratum during contact inhibition observed by interference reflection microscopy." *Experimental Cell Research* 92: 57-62.

Abrams, J. (1997). "Role of endothelial dysfunction in coronary artery disease." *American Journal of Cardiology* 79(12B): 2-9.

Abrams, L. and Presser, F. D. (1998). ""The view and the canine connection: an atlas of mandibular anterior tooth Aesthetics." *Journal of Aesthetic Dentistry* 10(3): 104-20.

Affrossman, S., Henn, G., Oneill, S. A., Pethrick, R. A. and Stamm, M. (1996): "Surface topography and composition of deuterated polystyrene-poly(bromostyrene) blends". *Macromolecules* 29:5010-5016.

Alberts, B., Bray, D., Lewis, J., Raff, M., Roberts, K. & Watson, J. D. (1994) *Molecular Biology of the Cell* (Garland, New York).

Balaban, N. Q. (2001): "Force and focal adhesion assembly: a close relationship studied using elastic micropatterned substrates. *Nature Cell Biology*" 3:466-472.

Ballestrem, C. (2001): "Marching at the front and dragging behind: differential $\alpha V\beta 3$ integrin turnover regulates focal adhesion behavior". *Journal of Cell Biology* 155:1319-1332

Bauer, J. S. S., Giancotti, F.G., Ruoslahti E. and Juliano, R.L. (1992): "Motility of fibronectin receptor-deficient cells on fibronectin and vitronectin: collaborative interactions among integrins. *Journal of Cell biology*" 116:477-487.

Bayliss, M. T., Osborne, D., Woodhouse, S. and Davidson, C. (1999) "Sulfation of chondroitin sulfate in human articular cartilage. The effect of age, topographical position, and zone of cartilage on tissue composition". *Journal of Biological Chemistry* 274 (22) 15892-15900.

Bell, E., Ivarsson, B. and Merrill, C. (1979) " Production of a tissue-like structure by contraction of collagen lattices by human fibroblasts of different proliferative potential *in vitro*" *Proceedng of the National Academy of Sciences U S A* 76 (3) 1274-1278.

Beningo, K. A. and Dembo, M. (2001). "Nascent focal adhesions are responsible for the generation of strong propulsive forces in migrating fibroblasts." *Journal Cell Biology* 153(4): 881-888.

Benigo, K. A. and Wang Y. L. (2002). "Flexible substrata for the detection of cellular traction forces." *Trends in Cell Biology* 12: 79-84.

Bershadsky, A. and Chausovsky, A. (1996). "Involvement of microtubules in the control of adhesion-dependent signal transduction." *Current opinion in cell Biology* 6(10): 1279-1289.

Bhatia S.K., Texeria, J., Anderson, M., Shriver-Lake, L.C., Calvert, J.M., Georger, J.H., Hickman, J.J., Dulcey, C.S., Schoen, P.E. and Ligler, F.S. (1993): "Fabrication of surfaces resistant to protein adsorption and application to two-dimensional protein patterning." *Annals of Biochemistry* 208(1): 197-205.

Bhatia, S. K., Yarmush, M.L. and Tonner, M. (1997). "Controlling cell interactions by micropatterning in co-cultures: hepatocytes and 3T3 fibroblasts." *Journal of Biomedical Material Research* 34: 189-199.

Binnig, G., Quate, C.F., and Gerber, C. (1986) *Physics Review Letters*, 56: 930-933.

Blanquaert, F., Barritault, D. and Caruelle, J.P. (1999). "Effects of heparin-like polymers associated with growth factors on osteoblast proliferation and phenotype expression." *Journal of Biomedical Material Research* 44(63-72).

Boeck, M. S., Baas, T. and Hubert, F.T. (1998). "Template-assisted nanopatterning of solid surfaces." *Biopolymers* 47(2): 185-193.

Bohanon, T., Elender, G., Knoll, W., Koberle, P., Lee, J.S., Olfenhausser, A., Ringsdorf, H., Sackmann, E., Simon, J., Tovar, G. and Winnik, F.M. (1996). "Neural pattern formation on glass and oxidized silicon surfaces modified with poly(N-isopropylacrylamide)." *Journal Biomaterial Science* 8: 19-39.

Bos, G. W., Scharenborg, N.M., Poot, A.A., Engbers, G.H.M., Beugeling, T., van Aken, W.G. and Feijen, J. (1999). "Proliferation of endothelial cells on surface-immobilized albumin-heparin conjugate loaded with basic fibroblast growth factor." *Journal of Biomedical Material Research* 44: 330-340.

Bowers, R. R., Harmon, J. and Peterson, J.D. (1992). "Fowl model for vitiligo genetic regulation on the fate of the melanocytes." *Pigment Cell Research: Suppl* 2:242-8

Branch, D. W., Wheeler, B. C. and Genepay, R.T. (2000). "Long-term maintenance of patterns of hippocampal pyramidal cells on substrates of polyethylene glycol and microstamped polylysine." *IEEE Transactions On Biomedical Engineering* 47(3): 290-300.

Britland, S., Clark, P., Connolly, P., and Moores, G. (1992a). "Micropatterned sub-stratum adhesiveness: a model for morphogenetic cues controlling cell behaviour." *Experimental Cell Research* 198: 124-129.

Britland, S., Perez-Arnaud, E., Clark, P., McGinn, B., Connolly, P. and Moores, G. (1992b). "Micropatterning proteins and synthetic peptides on solid

supports: a novel application for microelectronics fabrication technology." *Biotechnology in Progress* 8: 155-160.

Britland, S., Morgan, H., Wojciak-Stothard, B., Riehle, M., Curtis, A. and Wilkinson, C. (1996): "Synergistic and hierarchical adhesive and topographic guidance of BHK cells." *Experimental Cell Research*. 228: 313-325.

Brunette, D. M., Kenner, G.S. and Gould, T.R. (1983). "Grooved titanium surfaces orient growth and migration of cells from human gingival explants." *Journal of Dental Research* 62(10): 1045-1048.

Brunette, D. M. and Chou., B. (1999). "The effects of the surface topography of micromachined titanium substrata on cell behavior *in vitro* and *in vivo*." *Journal of Biomechanical Engineering*. 51: 178-185

Burrows, M. T. (1911). "The growth of tissues of the chick embryo outside the animal body, with special reference to the nervous system." *Journal of Experimental Zoology* 10: 63-84.

Buser, D., Schenk, R. K., Steinemann, S., Fiorellini, J. P., Fox, C. H. and Stich, H. (1991) "Influence of surface characteristics on bone integration of titanium implants. A histomorphometric study in miniature pigs" *Journal Biomedical Materials Research* 25 (7) 889-902.

Campbell, C. E. and von Recum, A.F. (1989). "Microtopography and soft tissue response." *Journal of Investigative Surgery* 2: 51-74.

Carrel, A. and Burrows, M.T. (1911). "An addition to the technique of the cultivation of tissues in vitro." *Journal of Experimental medicine* 14: 244-247.

Casey, B. G., Monaghan, W. and Wilkinson, C.D.W.. (1997). "Embossing of nanoscale features and environments." *Microelectronic Engineering* 35(1-4): 393-396.

Chen, G., Ito, Y. and Imanishi, Y. (1997a). "Regulation of growth and adhesion of cultured cells by insulin conjugated with thermoresponsive polymers." *Bitechnology and Bioengineering*. 15: 174-182

Chen, G., Ito, Y., Imanishi, Y., Magnani, A., Lamponi, S. and Barbucci, R. (1997b). "Photoimmobilization of sulphated hyaluronic acid for antithrombogenicity." *Bioconjugate Chemistry* 8: 730-734.

Chen, G., Mirshk, M. Haung, S., Whitesides, G.M.. and Ingber, D.E. (1997c). "Geometric Control of Cell Life and Death." *Science* 276: 1425-1428.

Chou, L., Firth, J.D., Uitto, V.J. and Brunette, D.M. (1995). "Substratum surface topography alters cell shape and regulates fibronectin mRNA level, mRNA stability, secretion and assembly in human fibroblasts." *Journal of Cell Science* 108(4): 1563-1573.

Chouquet, D., Felsenfeld, D.P. and Sheetz, M.O. (1997). "ECM rigidity causes strengthening of integrin-cytoskeleton linkages." *Cell* 88: 39-48.

Chrzanowaska-Wodnicka, M. and Burridge, K. (1996). "Rho-stimulated contractility drives the formation of stress fibres and focal adhesions." *Journal of Cell Biology* 133: 1403-1451.

Clark, P., Connolly, P., Curtis, A.S.G., Dow, J.A.T. and Wilkinson, C.D.W. (1991). "Cell guidance by ultrafine topography *in vitro*." *Journal of Cell Science* 99: 73-77.

Clark, P., Britland, S. and Connolly, P. (1993). "Growth cone guidance and neuron morphology on micropatterned laminin." *Journal of Cell Science* 50: 385-97.

Clemence, J. F., Ranieri, J.P., Aebischer, P. and Sigrist, H. (1995). "Photoimmobilization of a bioactive laminin fragment and pattern-guided selective neuronal cell attachment." *Bioconjugate Chemistry* 6: 411-7.

Cochran, B., Capaldi, R. A. and Ackrell, B. A. (1994) "The cDNA sequence of beef heart CII-3, a membrane-intrinsic subunit of succinate-ubiquinone oxidoreductase" *Biochimica et Biophysica Acta* 1188 (1-2) 162-6.

Craighead, H. G. (2000). "Nanoelectromechanical systems." *Science* 290(5496): 1532-1535.

Craighead, H. G., James, C. D. and Turner, A.M.P. (2001). "Chemical and topographical patterning for directed cell attachment." *Current Opinion in Solid State and Materials Science* 5(2-3): 177-184.

Cramer, L. P., Mitchison, T.J. and Thierot, J.A. (1994). "Actin-dependent motile forces and cell motility." *Current Opinion in Cell Biology* 6: 82-86.

Cramer, L. P. and Mitchison, T.J. (1995). "Myosin is involved in post-mitotic cell spreading." *Journal of Cell Biology*. 131: 179-189.

Curtis, A. S. G. and Varde, M. (1964). "Control of cell behaviour: topological factors." *Journal of the National Cancer Institute* 33: 15-36.

Curtis, A. S. G. and Clark, P. (1990). "The effects of topographic and mechanical properties of materials on cell behavior." *Critical Reviews in Biocompatibility* 5(4): 343-362.

Curtis, A. S. G. and Wilkinson, C.D.W. (1997). "Topographical control of cells." *Biomaterials* 18(24): 1573-1583.

Curtis, A. S. G., Casey, B., Gallagher, J.O., Pasqui, D., Wood, M.A. and Wilkinson, C.D.W. (2001). "Substratum nanotopography and the adhesion of

- biological cells. Are symmetry or regularity of nanotopography important?"
Biophysical Chemistry 94: 275-283.
- Curtis, A. and Riehl, M. (2001) "Tissue engineering: the biophysical background" Physical and Medical Biology 46 (4)R47-65
- Dembo, M. (1989). "Mechanics and control of the cytoskeleton in *Amoeba proteus*." Biophysical Journal 55(6): 1053-1080.
- DeFife, K. M., Colton, E., Nakayama, Y., Matsuda, T. and Anderson, J.M. (1999). "Spatial regulation and surface chemistry control of monocyte/macrophage adhesion and foreign body giant cell formation by photochemically micropatterned surfaces." Journal of Biomedical Material Research 45: 148-154.
- Dembo, M. and Harris A. K. (1981). "Motion of particles adhering to the leading lamella of crawling cells." Journal of Cell Biology 91(2 Pt 1): 528-536.
- Dembo, M., Oliver, T., Ishihara, A, and Jacobson, K. (1996). "Imaging the traction stresses exerted by locomoting cells with the elastic substratum method." Biophysical Journal 70(4): 2008-2022.
- Dembo, M. and Wang, Y. L. (1999). "Stress at the cell-to-substrate interface during locomotion of fibroblasts." Biophysical Journal 76: 2307-2316.

Den Braber, E. T., de Ruijter, J.E., Smits, H.T., Ginsel, L.A., von Recum, A.F. and Jansen J.A. (1995). "Effect of parallel surface microgrooves and surface energy on cell growth." *Journal of Biomedical Material Research* 29: 511-518.

Den Braber, E. T., de Ruijter, J.E., Smits, H.T., Ginsel, L.A., von Recum, A.F. and Jansen, J.A. (1996). "Quantitative analysis of cell proliferation on substrata with micro-grooves." *Biomaterials* 17(11): 1093-1099.

Den Braber, E. T., de Ruijter, J.E., Ginsel, L.A., von Recum, A.F. and Jansen, J.A. (1998). "Orientation of ECM protein deposition, fibroblasts cytoskeleton, and attachment complex components on silicone micro-grooved surfaces." *Journal of Biomedical Material Research* 40(2): 291-300.

Desai, T. A. (2000a). "Microfabricated interfaces: new approaches in tissue engineering and biomolecular separation." *Biomolecular Engineering* 17(1): 23-26.

Desai, T. A. (2000b). "Micro- and nanoscale structures for tissue engineering constructs." *Medical Engineering and Physics* 22: 595-606.

Deutsch, J. M., Russell, B. and Desai, T.A. (2000). "Fabrication of microtextured membranes for cardiac myocyte attachment and orientation." *Journal Biomedical Materials Research (Applied Biomaterials)*: 53 452-459

Dewez, J. L., Lhoest, J.B., Detrait, E., Berger, V., Dupont-Gillain, C.C., Vincent, L.M., Schneider, Y.J., Bertrand, P. and Rouxhet, P.G. (1998). "Adhesion of mammalian cells to polymer surfaces: from physical chemistry of surfaces to selective adhesion on defined patterns." *Biomaterials* 19: 1441-1445.

DiMilla, P. A., Barbee, K., and Lauffenburger, D.A. (1991). "Mathematical model for the effects of adhesion and mechanics on cell migration speed." *Biophysical Journal* 60: 15-37.

DiMilla, P. A., Stone, J.A., Quinn, J.A., Albedella, S.M. and Lauffenburger, D.A. (1993). "Maximal migration of human smooth muscle cells on fibronectin and type IV collagen occurs at an intermediate attachment strength." *Journal of Cell Biology* 122: 729-737.

Drumheller, P. D. and Hubbell, J. A. (1994). "Polymer networks with grafted cell adhesion peptides for highly biospecific cell adhesive substrates." *Analytical Biochemistry* 222(2): 380-388.

Drumheller, P. and Hubbell, J.A. (1995). "Surface immobilization of adhesion ligands for investigations of cell-substrate interactions." In: Bronzino, J. (editor). *The Biomedical Engineering Handbook*. Boca Raton, FL: CRC Press.

Dunlevy, J. R. and Couchman J. R. (1993). "Controlled induction of focal adhesion disassembly and migration in primary fibroblasts." *Journal of Cell Science* 105 (Pt 2): 489-500.

Dunlevy, J. R. and Couchman, J.R (1995). "Interleukin-8 induces motile behaviour and loss of focal adhesion in primary fibroblasts." *Journal of Cell Science* 108: 311-321.

Dunn, G. A. and Heath, J.P. (1976). "A new hypothesis of contact guidance in tissue cells." *Experimental Cell Research* 101: 1-14.

Elvenspock, M. and Jansen, H. *Silicon Micromachining*, Cambridge University Press, Cambridge (1998) pp. xiv and 406 .

Feighan, J. E., Goldberg, V. M., Davy, D., Parr, J. A. and Stevenson, S. (1995) "The influence of surface-blasting on the incorporation of titanium-alloy implants in a rabbit intramedullary mode" *Journal of Bone and Joint Surgery* 77 (9) 1380-1395

Fernandez, J. L. R., Geiger, B., Salomon, D. and Benzeev, A. (1993). "Suppression of vinculin expression by antisense transfection confers changes in cell morphology, motility, and anchorage dependent growth of 3T3 cells." *Journal of Cell Biology* 122: 1285-1294.

Flemming, R. G., Murphy, C.J., Abrams, G.A., Goodman, S.L. and Nealey, P.F. (1999). "Effects of synthetic micro- and nano-structured surfaces on cell behavior." *Biomaterials* 20(6): 573-588.

Folch, A. and Toner, M. (1998). "Cellular micropatterns on biocompatible materials." *Biotechnology in Progress* 14: 388-392.

Folch, A., Hurtado, O. Schmidt, M.A. and Toner, M. (1999). "Moulding of deep polydimethylsiloxane microstructures for microfluidics and biological applications." *Journal of Biomechanical Engineering* 12(1): 28-34.

Fraudin, C., Braslau, A. and Luzet, D., (2000) "Reduction in the surface energy of liquid interfaces at short length scales" 403: 871-874.

Fromherz, P., Schaden, H. and Vetter, T. (1991). "Guided outgrowth of leech neurons in culture." *Neuroscience Letters*. 129: 77-80.

Galbraith, C. G., Elbaum, M., Riveline, D., Bershadsky, A.D., Geiger, B. and Sheetz, M.P. (1999). "Concentration of vinculin at small fibronectin beads requires force." *Molecular Cell Biology* 10 (Supplement: 65a) 11-16.

Galbraith, C. G. and Sheetz M. P. (1999). "Keratocytes pull with similar forces on their dorsal and ventral surfaces." *Journal of Cell Biology* 147(6): 1313-1324.

Gallagher, J. O., Mc Ghee, K.F., Wilkinson, C.D.W. and Riehle, M.O. (2003). "Interactions of cells with ordered nanotopography." *IEEE Nanobioscience In Press*.

Geiger, B. and S. J. Singer (1979). "The participation of alpha-actinin in the capping of cell membrane components." *Cell* 16(1): 213-222.

Geiger, B. and Bershadsky, A. (2001). "Assembly and mechanotransductory function of focal contacts." *Current opinion in Cell Biology* 13: 584-592.

Giancotti, F. G. and Roushalti, E. (1990). "Elevated levels of the $\alpha 5 \beta 1$ fibronectin receptor suppresses the transformed phenotype of CHO cells." *Cell* 60: 849-859.

Gleiche, L., Chi, F. and Fuchs, H. (2000) Nanoscopic channel lattices with controlled anisotropic wetting. *Nature* 403: 173-175.

Gluck, U. and Benzeev A. (1994). "Modulation of alpha-actinin levels affects cell motility and confers tumorigenicity on 3T3 cells." *Journal of Cell Science*. 107: 1773-1782.

Goldmann, W. H. (2000). "Kinetic determination of focal adhesion protein formation." *Biochemical Biophysical Research Communication* 271(2): 553-537.

Goodman, S. L., Sims P. A. and Albrecht R. M. (1996). "Three dimensional bio-mimetic extracellular matrix textured materials." *Biomaterials* 17: 2087-2095.

Halliday, H. L. (1997). "Synthetic or natural surfactants." *Acta Paediatr* 86(3): 233-237.

Hanarp, P., Sutherland, D., Gold, J. and Kasemo, B. (1999). "Nanostructured model biomaterial surfaces prepared by colloidal lithography." *Nanostructured Materials* 12: 429-432.

Harrison, R. G. (1910). "The outgrowth of the nerve fibre as a mode of protoplasmic movement." *Journal of Experimental Zoology*. 9: 787-846.

Harrison, R. G. (1911). "On the stereotropism of embryonic cells." *Science* 34: 279-381.

Harrison, R. G. (1912). "The cultivation of tissues in extraneous media as a method of morphogenic study." *Anatomical Record* 6: 181-63.

Healy, K. E., Lom, B. and Hockberger, P.E. (1994). "Spatial distribution of mam-malian cells dictated by material surface chemistry." *Biotechnology and Bioengineering*. 43(8): 792-800.

Heath, J. P. and G. A. Dunn (1978). "Cell to substratum contacts of chick fibroblasts and their relation to the microfilament system. A correlated

interference-reflexion and high-voltage electron-microscope study." *Journal of Cell Science*. 29: 197-212.

Helfman, D. M., Levy, E.T., Berthier, C., Shututman, M., Riveline, D., Grosheva, I., Lachish-Zalait, A., Elbaum, M. and Bershadsky, A.D. (1999). "Caldesmon inhibits non muscle contractility and interferes with the formation of focal adhesion." *Molecular Cell Biology* 10: 3097-3112.

Higgins, J. M., Cernadas, M. and Purcell, F.G. (2000). "The role of alpha and beta chains in ligand recognition by beta 7 integrins." *Journal of Biological Chemistry* 275(33): 25652-25664.

Hironaka, K., H. Makino, and Yamamoto, A. (1993). "Renal basement membranes by ultrahigh resolution scanning electron microscopy." *Kidney International* 43(2): 334-345.

Horbert, C. B., McLernon, T.L., Hypolite, C.L., Adams, D.N., Pikus, L., Huang, C.C., Fields, G.B., Letourneau, P.C., Distefano, M.D. and Hu, W.S. (1997). "Micropatterning gradients and controlling surface densities of photoactivatable biomolecules on self-assembled monolayers of oligo(ethylene glycol) alkanethiolates." *Chemical Biology* 4: 731-737.

Hubbell, J. A., Massia, S.P. and Drumheller, P.D. (1992). "Surface-grafted cell-binding peptides in tissue engineering of the vascular graft." *Annals Of The New York Academy Of Sciences* 665: 253-258.

Hubbell, J. A. (1995). "Biomaterials in tissue engineering." *Biotechnology* 13(6): 565-576.

Hubbell, J. A. (1996). "Hydrogel systems for barriers and local delivery in the control of wound healing." *Journal of controlled release* 39(2-3).

Huber, M., Heiduschka, P., Kienle, S., Pavlidis, C., Mack, J., Walk, T., Jung, G. and Thanos, S. (1998). "Modification of glassy carbon surfaces with synthetic laminin-derived peptides for nerve cell attachment and neurocyte growth." *Journal of Biomedical Material Research* 41: 278-88.

Huttenlocher, A., Sandborg, R. R. and Horwitz A.F. (1995). "Adhesion in cell migration." *Curr Opin Cell Biol* 7(5): 697-706.

Hynes, R. O. (1992). "Cell movement." *Cell* 69(1) 11-25.

Hynes, R. O. (1999). "Cell adhesion: old and new questions." *Cell* 9(12): M33-37.

Ingber, D. E. (1997). "Tensegrity- The architectural basis of cellular mechanotransduction." *Annual Review Of Physiology* 59: 575-599.

Inoue, T., Cox, J. E., Pilliar, R. M. and Melcher, A. H. (1987) "Effect of the surface geometry of smooth and porous-coated titanium alloy on the

orientation of fibroblasts *in vitro*" Journal of Biomedical Material Research 21 (1) 107-126.

Ito, Y., Chen, G., Guan, Y. and Imanishi, Y. (1997). "Patterned immobilization of thermoresponsive polymer." Langmuir 13: 2756-2759.

Ito, Y. (1999). "Surface micropatterning to regulate cell functions." Biomaterials 20: 2333-2342.

James, C. D., Davis, R.C., Kam, L., Craighead, H.G., Isaacson, M., Turner, and Whitesides, J.N. (1998). "Patterned protein layers on solid substrates by thin stamp microcontact printing." Langmuir 14(4): 741-744.

Jockusch, B. M., Bubeck, P. and Enkleman, D.T. (1995). "The molecular architecture of focal adhesions." Annual Review of Cell and Developmental Biology 11: 379-416.

Kapur, R., Spargo, B.J., Chen, M.S., Calvert, J.M. and Rudolph, A.S. (1996). "Fabrication and selective surface modification of 3-dimensionally textured biomedical polymers from etched silicon substrates." Journal of Biomedical Material Research. 33(4): 205-216.

Kapur, R., Calvert, J.M., and Rudolph, A.S. (1999). "Electrical, chemical, and topological addressing of mammalian cells with microfabricated systems." Journal of Biomechanical Engineering. 121(1): 65-72.

Keely, P. J., Fong, A.M., Zutter, M.M. and Santoro, S.A. (1995). "Alteration of collagen-dependent adhesion, motility, and morphogenesis by the expression of antisense $\alpha 2\beta 1$ integrin mRNA in mammary cells." *Journal of Cell Science* 108: 595-607.

Keller, R. F. and J. Spieth (1984). "Neural crest cell behavior in white and dark larvae of *Ambystoma mexicanum* - time-lapse cinemicrographic analysis of pigment cell-movement *in-vivo* and in culture." *Journal Of Experimental Zoology* 229: 109- 126.

Kononen, M., Hormia, M., Kivisahti, J., Hautaniemi, J. and Thesleff, I.(1992). "Effect of surface processing on the attachment, orientation, and proliferation of human gingival fibroblasts on titanium." *Journal of Biomedical Materials Research* 26(10): 1325-1341.

Koo, L. Y., Irvine, D. J. and Graham, M. (2002). "Co-regulation of cell adhesion by nanoscale RGD organization and mechanical stimulus." *Journal of Cell Science* 115(Pt 7): 1423-1433.

Lee, G. M., Zhang, F., Ishihara, A., McNeil, C. L. and Jacobson, K. A. (1993a): "Unconfined lateral diffusion and an estimate of pericellular matrix viscosity revealed by measuring the mobility of gold-tagged lipids." *Journal of Cell Biology* 120(1): 25-35.

Lee, J., Ishihara, A. and Jacobson, K (1993b). "How do cells move along surfaces." *Trends in Cell Biology* 3: 366-70.

Lee, J. H. and Lee, H. B. (1993). "A wettability gradient as a tool to study protein adsorption and cell adhesion on polymer surfaces." *Journal of Biomaterials Science, Polymer Edition* 4(5): 467-481.

Leob, L. (1898). "Über transplantation von Weisser Haut auf eine Defekt in Schwarzer Haut und umgekehrt am Ohr des Meerschwienchens." *Archive für Entwicklungsmechanik der Organismen* 6: 1-44.

Lin, J. G., Ma, Y. S., Chao, A. C., Huang, C. I. (1999): "BMP test on chemically pretreated sludge." *Biosensor Technology*. 68(2): 187-192.

Lin, J. G. and Wu, L. T. 1999 "Effects of berberine on arylamine N-acetyltransferase activity in human colon tumor cells" *American Journal of Medicine* 27 (2) 265-275.

Lo, H., Ponticello, M. and Leong, K. (1995). "Fabrication of controlled release biodegradable foams by phase separation." *Tissue Engineering*. 1: 15-28.

Lo, H., Kadiyala, S. and Wantabe P.(1996). "Poly(L-lactic acid) foams with cell seeding and controlled-release capacity." *Journal Of Biomedical Materials Research* 30(4): 475-84.

Lom, B., Healy, K.E. and Hockberger, P.E. (1993). "A versatile technique for patterning biomolecules onto glass coverslips." *Journal of Neuroscience Methods* 50: 385-397.

Manske, M. and Bade, E.G. (1994). "Growth factor-induced cell migration: biology and methods of analysis." *International Review of the Cytoskeleton* 155: 49-96.

Manske, M. and Lesker, P. A. (1985). "Flexor tendon nutrition." *Hand Clinics* 1(1): 13-24.

Marouds, N. G. (1972). "Anchorage dependence: Correlation between amount of growth and diameter of bead, for single cells grown on individual glass beads." *Experimental Cell Research* 74: 337-342.

Martin, J. Y., Z. Schwartz, and Jenson, F.O. (1995). "Effect of titanium surface-roughness on proliferation, differentiation, and protein-synthesis of human osteoblast-like cells (mg63)." *Journal Of Biomedical Materials Research* 29: 389-401.

Massia, S. P. and J. A. Hubbell (1991). "An RGD spacing of 440 nm is sufficient for integrin $\alpha_v \beta_3$ -mediated fibroblast spreading and 140 nm for focal contact and stress fibre formation." *Journal of Biological Sciences* 114(5): 1089-100.

Matsuda, T., Inoue, K. and Sugawara, T. (1990). "Development of micropatterning technology for cultured cells." *Transactions of the American Society for Artificial Internal Organs* 36: M559-563.

Matsuda, T. and Inoue, K. (1990). "Photoreactive surface modification technology for fabricated devices." *Transactions of the American Society for Artificial Internal Organs* 36: 161-164.

Matsuda, T. Inoue, K. and Sugawara, T. (1994). "Microfabricated surface designs for cell culture and diagnosis." *Transactions of the American Society for Artificial Internal Organs* 40(3): M594-597.

Matsuda, T. and Sugawara, T. (1995). "Development of surface photochemical modification method for micropatterning of cultured cells." *Journal of Biomedical Material Research* 29: 749-756.

Matsumoto, K. and Kramer, R.H. (1994). "Scatter factor induces tyrosine phosphorylation of FAK and promotes migration and invasion by oral squamous carcinoma cells." *Journal of Biological Chemistry* 269: 31807-31813.

Matsumoto, N., Matsue, T. and Uchida, I. (1994). "Paired cell alignment using a jagged microarray electrode." *Bioelectrochemistry and Bioenergetics* 34(2): 199-202.

Mattsson, J., Berleth, T. and Sung, Z. R. (2000) Biology in pictures. Grow with the flow *Current Biology* 10 (3) R91.

Mazia, D., Schatten, G. and Procter, R.G.(1975). "Adhesion of cells to surfaces coated with polylysine. Applications to electron microscopy." *J Cell Biology* 66(1): 198-200.

McCaig, C. D. and Zhao, M. (1997). "Physiological electrical fields modify cell behaviour." *Bioessays* 19(9): 819-826.

Meyle, J., K., Wolfburg, H. and von Recum, A.F. (1993). "Surface micromorphology and cellular interactions." *Journal of Biomaterial Applications* 7(4): 362-374.

Meyle, J., Gultig, K. and Nisch, W. (1995). "Variation in contact guidance by human cells on a microstructured surface." *Journal of Biomedical Materials Research*. 28(1): 81-88.

Mikos, A. G., Sarakinos, G., Leite, S.M., Vacanti, J.P. and Langer, R. (1993). "Laminated three-dimensional biodegradable foams for use in tissue engineering." *Biomaterials* 14(5): 323-330.

Mooney, D., Organ, G., Vacanti, J.P., and Langer, R. (1994). "Design and fabrication of biodegradable polymer devices to engineer tubular tissues." *Cell Transplantation*. 3(2): 203-210.

Mrksich, M., Chen, C.S., Xia, Y., Dike, L.E., Ingber, D.E. and Whitesides, G.M. (1996). "Controlling cell attachment on contoured surfaces with self-assembled monolayers of alkanethiolates on gold." *Proceedings of the National Academy of Science USA* 93: 10775-10778.

Mrksich, M. and Whitesides, G.M. (1996). "Using self-assembled monolayers to understand the interactions of man-made surfaces with proteins and cells." *Annual Review of Biophysical and Biomolecular Structure*: 26:155-178.

Murphy-Ulrich, J. E., and Hook, M (1989). "Thrombospondin modulates focal adhesions in endothelial cells." *Journal of Cell Biology* 109: 1309-1319.

Murphy-Ulrich, J. E. (1995). "Anti-adhesive proteins of the extracellular matrix: thrombospondin, tenascin, and SPARC." *Trends Glycoscience and Glycotechnology* 7: 89-100.

Murphy-Ulrich, J., Pallero, M.P. and Sage, E.H. (1995). "SPARC mediates focal adhesion disassembly in endothelial cells through a fostatin-like region and Calcium binding EF hand." *Journal of Cell Biochemistry* 57: 341-350.

Nimni, M. E. (1997). "Review: polypeptide growth factors: targeted delivery systems." *Biomaterials* 18: 1201-25.

O'Hara, P. T. and Buck, R.C. (1979). "Contact guidance in vitro. A light transmission, and scanning electron microscope study." *Experimental Cell Research*. 121: 235-249.

Okano, T., Yamada, N., Okuhara, M., Sakai, H. and Sakurai, Y. (1995). "Mechanism of cell detachment from temperature-modulated, hydrophilic/hydrophobic polymer surfaces." *Biomaterials* 16: 297-303.

Parsons, J. T., Slack, J.K. Taylor, J.M. and Weed, S.A. (2000). "Focal adhesion kinase: a regulator of focal adhesion dynamics and cell movement." *Oncogene* 19: 5606-5613.

Patel, N., Padera, R., Sanders, G.H.W., Cannizzaro, S.M., Davies, M.C., Langer, R., Roberts, C.J., Tendler, S.J.B., Williams, P.M. and Shakesheff, K.M. (1998). "Spatially controlled engineering on biodegradable polymer surfaces." *Journal of American Society for Experimental Biology* 12: 1447-99.

Pelham, R. J., Jr. and Wang, Y. (1997). "Cell locomotion and focal adhesions are regulated by substrate flexibility." *Proceedings of the National Academy of Sciences, U.S.A.* 94(25): 13661-5.

Petit, C. and Pileni, M. P. (2000). "Physical properties of self-assembled nanosized cobalt particles." *Applied Surface Science* 162: 519-528.

Petit, V. and J. P. Thiery (2000). "Focal adhesions: structure and dynamics." *Biol Cell* 92(7): 477-494.

Pierschbacher, M. D. and Ruoslahti, E. (1984). "Cell attachment activity of fibronectin can be duplicated by small synthetic fragments of the molecule." *Nature* 309(3): 953-960.

Pritchard, D. J., Morgan, H. and Cooper, J. M. (1995) "Patterning and regeneration of surfaces with antibodies" *Analytical Chemistry* 67 (19) 3605-3607.

Qiu, Q., Sayer, M., Kawaja, M., Shen, X. and Davies, J. (1998). "Attachment, morphology, and protein expression of rat marrow stromal cells cultured on charged substrate surfaces." *Journal of Biomedical Material Research* 42: 117-127.

Rajnicek, A. M., Britland, S. and McCaig, C.D. (1997). "Contact guidance of CNS neurites on grooved quartz: influence of groove dimensions, neuronal age and cell type." *Journal of Cell Science* 110(Pt23): 2905-2913.

Ranieri, J. P., Bellamkonda, R., Jacob, J., Vargo, T.G., Gardella, J.A. and Aebischer, P. (1993). "Selective neuronal cell attachment to a covalently

patterned monoamine on fluorinated ethylene propylene films." *Journal of Biomedical Material Research* 27: 971-925.

Ratner, B. D. (1996). "The engineering of biomaterials exhibiting recognition and specificity." *Journal of Molecular Recognition* 9(5-6): 617-25.

Ratner, B. D., and Castner, D.G. (1997). "Surface modification of polymeric biomaterials." New York: Plenum Press. Edition(2)

Riehle, M., Dalby, M., Johnstone, H., Gallagher, J., Wood, M. A., Casey, B., McGhee, K., Affrossman, S., Wilkinson, C. D. W. and Curtis, A. S. G.(2002): *Nanometric Surface Patterns For Tissue Engineering: Fabrication And Biocompatibility In Vitro. Materials Research Society Proceedings; Nanopatterning: From Ultralarge-Scale Integration to Biotechnology. Boston, MA, USA, Materials Research Society. 15(2): 87-96*

Riveline, D., Zamir, E., Balaban, N.Q., Schwarz, U., Ishizaki, T., Narumiya, S., Kam, Z., Geiger, B. and Bershadsky, A.D. (2001). "Focal contacts as mechanosensors: externaly applied local mechanical force induces growth of focal contacts by a mDia-1-dependent and ROCK-independent mechanism." *Journal of Cell Biology* 153: 324-328

Rosenberg, M.D. (1962a) Long range interactions between cell and substratum *Nature* 48 1343:1349.

Rosengerg, M.D. (1962b) "layering of Behinic acid" *Nature* 52:1478-1480.

Rotner, K., Hall, A. and Small, J.V. (1999). "Interplay between rac and rho in the control of substrate dynamics." *Current Biology* 9: 640-648.

Rovensky, Y., Bershadsky, A., Givargizov, E., Obolenskaya, L. and Vasiliev, J. (1991): "Spreading of mouse fibroblasts on the substrate with multiple spikes." *Experimental Cell Research* 197(1): 107-12.

Ruoslahti, E. (1996). "RGD and other recognition sequences for integrins." *Annual Review of Cell and Develpmental Biology* 12: 697-715.

Salthouse, T. N. (1984) "Some aspects of macrophage behavior at the implant interface" *Journal of Biomedical Material Research* 18 (4) 395-401.

Schmidt, J. A. and von Recum, A.F. (1991). "Texturing of polymer surfaces at the cellular level." *Biomaterials* 12: 385-9.

Scotchford, C. A., Cooper, E., Leggett, G.J. and Downes, S. (1998). "Growth of human osteoblast-like cells on alkanethiol on gold self-assembled monolayers: the effect of surface chemistry." 6: 112-117

Sechriest, V. F. (2000). "GAG-augmented polysaccharide hydrogel: a novel biocompatible and biodegradable material to support chondrogenesis." *Journal of Biomedical Material Research* 49: 534-541.

Sheetz, M. P., Felsenfeld, D. P. and Galbraith, C. G. (1998): "Cell migration: regulation of force on extracellular-matrix-integrin complexes." *Trends in Cell Biology* 8(2): 51-54.

Sheetz, M. (1994). "Cell migration by graded attachment to substrates and contraction." *Society for Cell Biology* 5: 149-155.

Sheetz, M. P. and Kuo, S. C. (1993). "Tracking nanometer movements of single motor molecules." *Methods In Cell Biology* 39: 129-36.

Shi, H. and Ratner, B. D. (2000). "Template recognition of protein-imprinted polymer surfaces." *Journal of Biomedical Materials Research* 49(1): 1-11.

Shingvi, R., Kumar, A., Lopez, G.P., Stephanopoulos, G.N., Wang, D.I.C., Whitesides, G.M. and Ingber, DE (1994). "Engineering cell shape and function." *Science* 264: 296-298.

Shirato, I., Tomino, Y. and Busaki, T.(1991). "Fine structure of the glomerular basement membrane of the rat kidney visualized by high-resolution scanning electron microscopy." *Cell and Tissue Research* 266(1): 1-10.

Sims, J. R., Karp, S. and Ingber, D.E.(1992). "Altering the cellular mechanical force balance results in integrated changes in cell, cytoskeletal and nuclear shape." *Jornal of Cell Science* 103 (Pt 4): 1215-1222.

Singhvi, R., Kumar, A. and Stephanopoulos, G. (1994a). "Engineering cell shape and function." *Science* 264(5159): 696-8.

Singhvi, R., Stephanopoulos, G. and Wang, D.I.C. (1994b). "Review: Effects of substratum morphology on cell physiology." *Biotechnology and Bioengineering* 43: 764-771.

Soekarno, A., Lom, B. and Hockberger, P.E. (1993). "Path finding by neuroblastoma cells in culture is directed by preferential adhesion to positively charged surfaces." *Neuroimage* 1: 129-144.

Spargo, B. J., Testof, M.A., Nielsen, T.B., Stenger, D.A., Hickman, J.J. and Rudolph, A.S. (1994). "Spatially controlled adhesion, spreading, and differentiation of endothelial cells on self-assembled molecular mono-layers." *Proceedings of the National Academy of Science USA* 91: 11070-11074.

Stahl, B., Mueller, B., von Boxberg, Y., Cox, E.C. and Bonhoeffer, F. (1990). "Biochemical characterization of a putative axonal guidance molecule of the chick visual system." *Neuron* 5: 735-43.

Stenger, D. A., Georger, J.H., Dulcey, C.S., Hickman, J.J., Rudolph, A.S., Nielsen, T.B., McCort, S.M. and Calvert, J.M. (1992). "Coplanar molecular assemblies of amino- and perfluorinated alkylsilanes: characterization and geometric definition of mammalian cell adhesion and growth." *Journal of the American Chemical Society* 114: 8435-42.

Stepien, E., Stanisz, P. and Petit, R. (1999). "Contact guidance of chick embryo neurons on single scratches in glass and on underlying aligned human skin fibroblasts." *Cell Biology International*. 23(2): 105-116.

Stoker, M. and Gherardi, E. (1991). "Regulation of cell movement: the mitogenic cytokines." *Biochemical and biophysical Acta* 1072: 81-102.

Stossel, T. (1993). "On the crawling of animal cells." *Science* 260: 1086-1094.

Taguchi, T. K., A. Sakamoto, N. and Akashi, M. (1998). "Preparation of a novel functional hydrogel consisting of sulfated glucose-bearing polymer: activation of basic fibroblast growth factor." *Journal of Biomedical Material Research* 41: 386-391.

Takezawa, T., Yamazaki, M., Mori, Y., Yonaha, T. and Yoshizato, K. (1992). "Morphological and immunocyto-chemical characterization of a hetero-spheroid composed of fibroblasts and hepatocytes." *Journal of Cell Science* 101: 495-501.

Takezawa, T., Mori, Y., Yonaha, T. and Yoshizato, K. (1993). "Characterization of morphology and cellular metabolism during the spheroid formation by Fibroblasts." *Experimental Cell Research* 208: 430-441.

Takezawa, T., Ito, A. and Mori, Y. (1994). "Histological observations of hetero-spheroid consisting of human dermal fibroblasts and human epidermal keratinocytes." *Connective Tissue* 26: 1110-1115.

Theriot, J. A. and Mitchison, J. (1992). "Actin microfilament dynamics in locomoting cells." *Journal of Cell Biology* 118:367-371.

Thomas, C. H., McFarland, C.D., Jenkins, M.L., Reznia, A., Steele, J.G. and Healy, K.E. (1997). "The role of vitronectin in the attachment and spatial distribution of bone-derived cells on materials with patterned surface chemistry." *Journal of Biomedical Material Research* 37:81-90.

Thomson, R., Yaszemski, M. and Mikos, A. (1997). "Polymer scaffold processing." *Principles of tissue engineering*: 263-72.

Tobasnick, G. and Curtis, A.S.G. (2001) "Chloride channels and the reaction of cells to topography" *Biophysical Chemistry* 2: 49-60.

Tremble, P., Lane, T., Sage, E. and Werb, Z. (1993). "SPARC:a secreted protein associated with morphogenesis and tissue remodeling, induces expression of MMP's in fibroblasts through a novel ECM-dependent pathway." *Journal of Cell Biology* 121: 451-456.

Tremble, P. Chamley, E. and Werb, Z. (1994). "The ECM ligands fibronectin and tenascin collaborate in regulating collagenase gene expression in fibroblasts." *Molecular Cell Biology* 5: 439-453.

Trinkhaus, J. (1992). "The forces that shape the embryo." *Cells into organs*. Prentice-hall, Englewood Cliffs, N.J. pp 27-46.

Turner, S., Kam, L., Isaacson, M., Craighead, H. G., Shain, W. and Turner, J. (1997): "Cell attachment on silicon nanostructures." *Journal of Vacuum Science and Technology B* 15: 2848-2854.

Ueno, K., Miyashita, A., Endoh, E., Takezawa, M., Yamazaki, M., and Mori, T. (1992). "Formation of multicellular spheroids composed of rat hepatocytes." *Research Communication in Chemical Pathology and Pharmacology* 77: 107-120.

Valentini, R. F., Vargo, T.G., Gardella, J.A. and Aebischer, P. (1993). "Patterned neuronal attachment and outgrowth on surface modified, electrically charged Fluoropolymer substrates." *Journal of Biomaterial Science (Polymer Edition)* 5: 13-36.

van Kooten, T. G., Whitesides, J.F. and Von Recum, A.F. (1998). "Influence of silicone surface texture on human skin fibroblast proliferation as determined by cell cycle analysis." *Journal of Biomedical Materials Research*. 43: 1-14.

Vicu, C., Carcenac, F., Pepin, A., Chen, Y., Mejias, M., Lebib, A., Manin-Ferlazzo, L., Couraud, L. and Launois, H. (2000): "Electron beam lithography: resolution limits and applications." *Applied Surface Science* 164: 111-117.

Volberg, T., Geiger, B., Citi, S. and Bershadsky, A.D. (1994). "Effect of protein kinase inhibitor H-7 on the contractility, integrity, and membrane anchorage of the microfilament system." *Cell Motility and the Cytoskeleton* 29: 321-338.

von Recum, A. F. and van Kooten, T. G. (1995). "The influence of microtopography on cellular-response and the implications for silicone implants." *Journal Of Biomaterials Science Polymer Edition* 7: 181-198.

von Recum, A.F., Kim, S.W., Kikuchi, A., Okuhara, M., Sakurai, Y. and Okano, T. (1998). "Novel thermally reversible hydrogel as detachable cell culture substrate." *Journal of Biomedical Material Research* 40: 631-639.

Walboomers, X. F., Groes, H.J.E., Ginsel, L.A. and Jansen, J.A. (1998). "Microgrooved subcutaneous implants in the goat." *Journal of Biomedical Material Research* 42: 634-641.

Walter, J., Kern-Veits, B., Huf, J., Stolze, B., and Bonhoeffer, F. (1987). Recognition of position-specific properties of tectal cell membranes by retinal axons *in vitro*. *Development*. 101: 685-696.

Wang, R., Stromer, M. H. and Huiatt, T. W. (1998) " Integrin expression in developing smooth muscle cells" *Journal of Histochemical Cytochemistry* 46 (1) 119-126

Wei, Q. and Adelstein, R.S. (2000): "Conditional expression of a truncated fragment of nonmuscle myosin II-A alters cell shape but not cytokinesis in HeLa cells." *Molecular Biology of the Cell* 11: 3617-3627.

Wei, L., Wang, L., Carson, J. A., Agan, J. E., Imanaka-Yoshida, K., Schwartz, R. J. (2001): "beta 1 integrin and organized actin filaments facilitate cardiomyocyte-specific RhoA-dependent activation of the skeletal alpha-actin promoter." *Journal of the American Society of Experimental Biology*. 15(3): 785-796.

Weiss, P. (1945). "Experiments on cell axon orientation *in vitro*: the role of colloidal exudates in tissue orientation." *Journal of Experimental Zoology*. 100: 353-386.

Wheeler, B. C., Corey, J. M., Brewer, G. J. and Branch, D. W. (1999): "Microcontact printing for precise control of nerve cell growth in culture." *Journal of Biomechanical Engineering* 121(1): 73-78.

Wilke, A., Schonian, U., Yager, D.T. and Maisch, B. (1990). "Morphometric analyses of the skin of dogs with atopic dermatitis and correlations with cutaneous and plasma histamine and total serum IgE." *Veterinary Pathology* 27(3): 179-86.

Wilke, A., Schonian, U., Herzum, M., Hengstenberg, C., Hufnagel, G., Brilla, C. G. and Maisch, B. (1995): "Extracellular-matrix and cytoskeleton of the myocardium in cardiac inflammation LA- German." *Herz* 20: 95-108.

Wilkinson, C. D. W., Riehle, M., Wood, M., Gallagher, J. and Curtis, A.S.G. (2002). "The use of materials patterned on a nano- and micro-metric scale in cellular engineering." *Materials Science and Engineering C* 19: 263-69.

Wojciak-Stothard, B., Madeja, Z., Korohoda, W., Curtis, A. and Wilkinson, C. (1995a): "Activation of macrophage-like cells by multiple grooved substrata - topographical control of cell behavior." *Cell Biology International*: (6) 485-490.

Wojciak-Stothard, B., Curtis, A. S. G., Monaghan, W., McGrath, M., Sommer, I. and Wilkinson, C. D. W. (1995b): "Role of the cytoskeleton in the reaction of fibroblasts to multiple grooved substrata." *Cell Motility and the Cytoskeleton* 31: 147- 158.

Wojciak-Stothard, B., Curtis, A., Monaghan, W., Macdonald, K. and Wilkinson, C. (1996): "Guidance and activation of murine macrophages by nanometric scale topography." *Experimental Cell Research*. 223: 426-435.

Wojciak-Stothard, B., Denyer, M., Mishra, M. and Brown, R. A. (1997): "Adhesion, orientation, and movement of cells cultured on ultrathin fibronectin fibers." *In Vitro Cellular and Developmental Biology*. Animal 33(2): 110-117.

Wood, M. A., Riehle, M. and Wilkinson, C. D. W. (2002): "Patterning colloidal nanotopographies." *Nanotechnology* 13(5): 605-609.

Yamato, M., Okumura, M., Karikusa, F., Kikuchi, A., Sakurai, Y. and Okano, T. (1999). "Signal transduction and cytoskeletal reorganization are required for cell detachment from cell culture surfaces grafted with a temperature-responsive polymer." *Journal of Biomedical Material Research* 44: 44-52.

Yamasaki, M., Tsuchida, K., Kobayashi, K., Takezawa, T. and Mori, Y. (1994). "A novel method to prepare size-regulated spheroids composed of human dermal fibroblasts" *Biotechnology and Bioengineering* 44: 38-44.

Zamir, F., Katz, M., Posen, Y., Erez, N., Yamada, K. M., Katz, B. Z., Lin, S., Lin, D. C., Bershadsky, A., Kam, Z. and Geiger, B. (2000): "Dynamics and segregation of cell-matrix adhesions in cultured fibroblasts." *Nature Cell Biology*. 2(4): 191-196.

Zamir, E. and Gieger, B. (2001a). "Molecular diversity of actin-integrin adhesion complexes." *Journal of Cell Science* 28: 567-574.

Zamir, E. and Gieger, B. (2001b). "Molecular complexity and dynamics of cell-matrix adhesions." *Journal of Cell Science* 114: 3583-3590.

Zhang, M., Ishihara, A., McNeil, C. I. and Jacobson, K. A. (1998). "Hemocompatible polyethylene glycol films on silicon." *Biomedical Microdevices* 1(1): 81-89.